AD-A062 156 AERONAUTICAL RESEARCH LABS MELBOURNE (AUSTRALIA) F/G 12/1
LECTURES ON MODERN FOURIER TRANSFORM METHODS.(U)
FEB 78 B C HOSKIN

UNCLASSIFIED ARL/STRUC-TM-276 NL

1 OF 3
AD
A062156

1 OF 3

AD
A062156

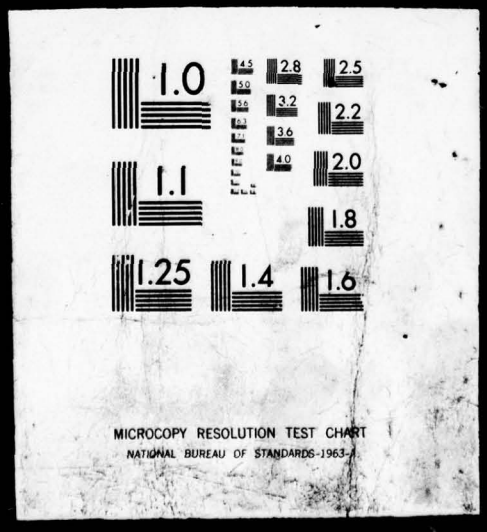

ARL-STRUC-
Tech-Memo-276

AR-001-271



# DEPARTMENT OF DEFENCE

## DEFENCE SCIENCE AND TECHNOLOGY ORGANISATION

## AERONAUTICAL RESEARCH LABORATORIES

MELBOURNE, VICTORIA



STRUCTURES TECHNICAL MEMORANDUM 276

# LECTURES ON MODERN FOURIER TRANSFORM METHODS

Edited

by

Brian C. HOSKIN

Approved for Public Release



COPY No 15

February, 1978

APPROVED

FOR PUBLIC RELEASE

AR-001-271

DEPARTMENT OF DEFENCE

DEFENCE SCIENCE AND TECHNOLOGY ORGANISATION

AERONAUTICAL RESEARCH LABORATORIES

(14) ARL/STRUC-TM-276

Structures Technical Memorandum 276

# (6) LECTURES ON MODERN FOURIER TRANSFORM METHODS.

Edited by

(10) Brian C. Hoskin

(11) Feb 78 (12) 211 p.



## SUMMARY

This memorandum is a compilation of notes prepared in connection with a series of lectures on Modern Fourier Transform Methods given at the Aeronautical Research Laboratories. The topics covered include Classical Fourier Methods, the Discrete Fourier Transform, the Fast Fourier Transform Algorithm, Time Series Analysis, Practical Computational Questions, The Retrieval of Signals from Noise, Application of Fourier Transforms to Vibration Problems, and Fourier Optics and Holography.

POSTAL ADDRESS: Chief Superintendent, Aeronautical Research Laboratories, Box 4331, P.O., Melbourne, Victoria, 3001, Australia.

## FOREWORD

These notes were prepared in connection with a series of lectures on modern Fourier transform methods that was held at the Aeronautical Research Laboratories, Melbourne, between June and August 1977. All lecturers were members of ARL staff with the exception of Dr. R. Kirsner who is the Director of the Physical Sciences, St. Vincent's Hospital, Melbourne. The names of the lecturers and the topics discussed by each are shown in the list of contents.

Whilst analytical methods based on Fourier series or integrals have been widely used in all branches of the physical sciences for many years, over the past decade or so these methods have undergone important developments especially as regards their implementation on a digital computer. The lectures were particularly concerned with these modern developments. The lectures covered both the mathematical theory behind the methods and, also, certain applications; these last were, naturally, governed by areas of interest at ARL.

The authors would like to express their best thanks to Mrs Diana Piel for her care in typing these notes.

--- o0o ---

## CONTENTS

--- oOo ---

# CHAPTER 1 : REVIEW OF CLASSICAL FOURIER METHODS

## 1.1 General

From the mathematical point of view, the key concept in Fourier methods of analysis is that a more or less arbitrary function can be expressed as a (generalised) sum of the trigonometric functions (sines and cosines) or their equivalent, the complex exponentials. The sum may take the form of an infinite series (classical Fourier series), an integral (classical Fourier transform), or a finite series (discrete Fourier transform). Classical Fourier methods concentrate on the case where the arbitrary function is given by some analytical expression whilst present interest is more with a function expressed as a discrete set of numerical values; the latter format, of course, is especially appropriate for computer applications. However, before discussing what can perhaps be best termed "numerical Fourier methods" which are based on the discrete Fourier transform it is useful to review, albeit briefly, their classical counterparts. Of the very extensive literature on the classical methods special attention is drawn to the accounts by Hsu(1), Champeney(2), Bracewell(3) and Papoulis(4); these are all oriented towards applications of current interest. Other standard texts are listed in references (5), (6), (7) and (8).

## 1.2 Physical Motivation for Fourier Series

The fact that an arbitrary function can be expressed as a sum of the trigonometric functions can hardly be deemed intuitively evident and it may be useful to describe briefly how such a result was discovered. Essentially, it came out of studies of the vibration of a tense string carried out by Daniel Bernoulli around 1750. (Truesdell(9) has described at length the "celebrated and deplorable quarrel" which arose between Bernoulli on the one hand and Euler, Lagrange and D'Alembert on the other, over the validity of this work).

The partial differential equation governing the small vibrations of a uniform string of line density, d, and under a tension, T, is

$$u_{xx} - (1/c^2)\, u_{tt} = 0 \qquad (1.2.1)$$

where u denote the lateral displacement at a distance x along the string at time t, and $c^2 = T/d$. Confining attention to the case when the string is initially at rest in some deformed configuration there will be initial conditions of the form

$$u(x,o) = g(x) \tag{1.2.2}$$

$$u_t(x,o) = 0 \tag{1.2.3}$$

As well, there will be boundary conditions at the ends x=0 and x=L of the string. First, consider the case of 'fixed ends' Fig.1.1 where

$$u(o,t) = u(L,t) = 0 \tag{1.2.4}$$

Use of the method of "normal modes" (which is here equivalent to the method of "separation of variables") shows that an expression of the form

$$u(x,t) = \sum_{n=1}^{\infty} b_n \sin(n\pi x/L) \cos(n\pi ct/L) \tag{1.2.5}$$

satisfies the conditions (1.2.1), (1.2.3) and (1.2.4). (In fact, each term in the series satisfies these conditions). The condition (1.2.2) now becomes

$$g(x) = \sum_{n=1}^{\infty} b_n \sin(n\pi x/L) \; ; \tag{1.2.6}$$

but, since g is more or less arbitrary, eqn (1.26) implies that an arbitrary function can be expressed as an infinite series of sines. Assuming the validity of the expansion, the coefficients $b_n$ can be readily determined by using the "orthogonality relations", namely, that for integral m,n

$$\int_o^L \sin(m\pi x/L) \sin(n\pi x/L)\, dx = 0, \quad m \neq n \tag{1.2.7}$$

$$= L/2, \quad m=n \tag{1.2.8}$$

(This is an example of the general orthogonality of normal modes of vibration)

Hence,

$$b_n = (2/L) \int_o^L g(x) \sin(n\pi x/L)\, dx \tag{1.2.9}$$

and the problem is now solved.

One other result might be noted. On multiplying each side of eqn (1.2.6) by itself and integrating, it can be established that

$$\int_o^L \{g(x)\}^2\, dx = (L/2) \sum_{n=1}^{\infty} b_n^2 \tag{1.2.10}$$

This result is generally referred to as Parseval's theorem for a sine series.

Now consider another set of boundary conditions, in particular the case of "free ends" where, instead of eqns (1.2.4), we have

$$u_x(o,t) = u_x(L,t) = 0 \tag{1.2.11}$$

(This slightly artificial case can be motivated by considering the ends of the string as attached to springs (Fig. 1.2) when the boundary conditions are of the form

$$T u_x - Ku = 0 \tag{1.2.12}$$

where K is the stiffness of the springs; for vanishingly small K, eqns (1.2.11) result.) Separation of variables now leads to an expression of the form

$$u(x,t) = a_o/2 + \sum_{n=1}^{\infty} a_n \cos(n\Pi x/L) \cos(n\Pi ct/L) \tag{1.2.13}$$

This satisfies (1.2.1), (1.2.3) and (1.2.11). The condition (1.2.2) becomes

$$g(x) = a_o/2 + \sum_{n=1}^{\infty} a_n \cos(n\Pi x/L) \tag{1.2.14}$$

(The point of associating the factor of 1/2 with the constant term - which physically corresponds to a rigid body motion - will appear shortly.) Thus, it appears that an arbitrary function can also be expressed as an infinite series of cosines. The "orthogonality relations" are now that, for integral m,n (including zero)

$$\int_o^L \cos(m\Pi x/L) \cos(n\Pi x/L)\, dx = 0 \ , \ m \neq n \tag{1.2.15}$$

$$= L/2 \ , \ m = n \neq 0 \tag{1.2.16}$$

$$= L \ , \ m = n = 0 \tag{1.2.17}$$

Hence,

$$a_n = (2/L) \int_o^L g(x) \cos(n\Pi x/L)\, dx \tag{1.2.18}$$

(Use of the factor of 1/2 in (1.2.14) means that eqn (1.2.18) can be used for all integral values of n including zero.)

Parseval's theorem for a cosine series is as follows :

$$\int_o^L \{g(x)\}^2\, dx = (L/2) \left(a_o^2/2 + \sum_{n=1}^{\infty} a_n^2\right) \tag{1.2.19}$$

As already remarked the above arguments, for the sine series at any rate, are essentially due to Bernoulli. Fourier's contribution (10) made in 1822 consisted in the elucidation of many points left obscure by Bernoulli, and included the actual derivation of numerous series; also, he was the sole discoverer of the Fourier integral to be discussed later.

## 1.3 The Different Fourier Series

### 1.3.1 Fourier Sine Series

Recalling the argument for a string with fixed ends, the assertion is that a fairly general function g(x) defined over the interval (0,L) can be represented in the form

$$g(x) = \sum_{n=1}^{\infty} b_n \sin (n\Pi x/L) \qquad (1.3.1)$$

where $b_n = (2/L) \int_o^L g(x) \sin (n\Pi x/L)\, dx$ (1.3.2)

As an example, consider the function

$$g(x) = \exp (x/L) - 1 \qquad (1.3.3)$$

which is shown in Fig.1.3(a). Here the Fourier coefficients are

$$b_n = 2 \{ (-1)^{n+1} \{ (e-1)\, n^2\Pi^2 - 1 \} - 1 \} / \{ n\Pi\, (1+n^2\Pi^2) \} \qquad (1.3.4)$$

The representation of the function that is recovered by summing (1.3.1) up to n=4 is shown in Fig 1.3(b). It might be noted that eqn (1.3.3) violates one of the conditions of the string problem inasmuch as g(L) is non - zero. Whilst the series representation with only four terms reproduces the function at least fairly over most of the range it is badly in error near x = L; there it actually returns the value zero instead of (e-1).

Although in the string problem it is of no concern how the Fourier series behaves outside the interval (0,L), nevertheless it is informative to look at this. Firstly, since the sine is an odd function

the series (1.3.1) always returns the result

$$g(-x) = -g(x) \qquad (1.3.5)$$

Secondly, since for any integer n,

$$\sin \{n\Pi (x + 2L)/l\} = \sin (n\Pi x/L) \qquad (1.3.6)$$

the series returns the result

$$g(x + 2L) = g(x) \qquad (1.3.7)$$

i.e., the sine series represents a periodic function of period 2L. Hence, for the particular function (1.3.3) the series will really be representing the extended function of Fig. 1.3(b). This latter has jump discontinuities at x = L, -L , 3L, -3L etc. and, in returning the value zero there, the series is actually taking the mean of the values on either side of the discontinuity. Also, in the neighbourhood of the discontinuity the series with a finite number of terms oscillates quite widely about the true function; this effect, known as the Gibbs phenomenon, is discernible in Fig. 1.3(b).

### 1.3.2 Fourier Cosine Series

Similarly, the discussion of a string with free ends suggests that a fairly general function g(x) defined over (O,L) can be represented in the alternative form

$$g(x) = a_o/2 + \sum_{n=1}^{\infty} a_n \cos(n\Pi x/L) \qquad (1.3.8)$$

where

$$a_n = (2/L) \int_o^L g(x) \cos (n\Pi x/L)\, dx \qquad (1.3.9)$$

This cosine series can be just as well used as the previous sine series. On applying it to the function (1.3.3) it is found that

$$a_o = 2(e-2), \quad a_n = 2 \{ (-1)^n e-1\} / (1 + n^2\Pi^2) \qquad (1.3.10)$$

The representation that is recovered by summing the cosine series up to n = 4 is shown in Fig. 1.3(c).

The representation given outside the basic interval (O,L) by the cosine series is determined, firstly, by the fact that the cosine is an even function so the series always returns the result

$$g(-x) = g(x) \tag{1.3.11}$$

Secondly, the series has a period of 2L so that (1.3.7) again applies. Thus, for the function (1.3.3) the series is really representing the extended function of Fig. 1.3(c). In this case it happens that the extended function is continuous so that summing to only n = 4 gives quite a good representation, the coefficients $a_k$ decreasing more rapidly than the $b_k$. However, it must be observed that the zero slope end condition imposed in the string problem does not apply to (1.3.3) at either x = o or x = L. The condition is, in a sense, approximately satisfied at x = o because of the even character of the extended function.

### 1.3.3 Fourier Trigonometric Series

If one is only concerned with the representation of a function over the single interval (0, L) - and this is the situation for many boundary value problems - then either the sine or cosine series may be used as convenient. However, if one is concerned with some sort of periodic phenomenon over the whole range of x neither representation may suffice. For example, consider again the function given by eqn (1.3.3) and suppose that it is required to reproduce this function over each interval of length L for all x i.e., the extended function of Fig. 1.3(d) is to be represented. As already seen, neither the sine nor cosine series can do this; however it is possible to develop a combined sine and cosine series which will. The argument which, incidentally, is due to Fourier is as follows.

Any function g(x) can be written in the form

$$g(x) = E(x) + O(x) \tag{1.3.12}$$

where

$$E(x) = (1/2)\ \{g(x) + g(-x)\} \tag{1.3.13}$$

$$O(x) = (1/2)\ \{g(x) - g(-x)\} \tag{1.3.14}$$

Clearly, E(x) is an even function and O(x) an odd function. In the present case g(x) is required to be periodic, with period L i.e.,

$$g(x + L) = g(x) \tag{1.3.15}$$

It follows that E(x) and O(x) are each also periodic with period L.

For the moment consider just E(x). It is an even function of period L and, hence, from the considerations of Section 1.3.2 above can be written in the form

$$E(x) = a_o/2 + \sum_{n=1}^{\infty} a_n \cos(2\Pi nx/L) \tag{1.3.16}$$

where

$$a_n = (4/L) \int_o^{L/2} E(x) \cos(2n\Pi x/L)\, dx \tag{1.3.17}$$

(Note that it is necessary to replace the "L" of eqns (1.3.8) and (1.3.9) by "L/2" here since those equations related to a function of period 2L, not L as is required.) Substituting from eqn (1.3.13) into eqn (1.3.17), and using the periodicity relation, leads to the result

$$a_n = (2/L) \int_o^L g(x) \cos(2n\Pi x/L)\, dx \tag{1.3.18}$$

In a similar fashion it can be shown that

$$O(x) = \sum_{n=1}^{\infty} b_n \sin(2n\Pi x/L) \tag{1.3.19}$$

with

$$b_n = (2/L) \int_o^L g(x) \sin(2n\Pi x/L)\, dx \tag{1.3.20}$$

Summing up then, a more or less arbitrary function of period L can be represented in the form

$$g(x) = a_o/2 + \sum_{n=1}^{\infty} \{ a_n \cos(2n\Pi x/L) + b_n \sin(2n\Pi x/L) \} \tag{1.3.21}$$

where $a_n$ and $b_n$ are given by (1.3.16) and (1.3.20) respectively. Assuming the validity of the expansion (1.3.21), the coefficients $a_n$ and $b_n$ can also be determined directly using the orthogonality relations for the combined cosine and sine function set, namely,

$$\int_o^L u_m u_n\, dx = \int_o^L v_m v_n\, dx = 0,\ m \neq n;\ \int_o^L u_m v_n\, dx = 0,\ \text{all } m, n \tag{1.3.22}$$

where $u_n$ and $v_n$ denote $\cos(2n\pi x/L)$ and $\sin(2n\pi x/L)$ respectively. Parseval's theorem takes the form

$$\int_o^L \{g(x)\}^2\, dx = (L/2)\ \{a_o^2/2 + \sum_{n=1}^{\infty} (a_n^2 + b_n^2)\} \qquad (1.3.23)$$

The representation (1.3.21) is the general form of a Fourier series; the cosine and sine series can be regarded as particular cases appropriate to even or odd functions respectively.

The series (1.3.21) could have been derived from physical considerations by solving eqn (1.2.1) with initial conditions (1.2.2) and (1.2.3) b ut with "periodic boundary conditions" defined by

$$u(o,t) = u(L,t)\ ;\ u_x(o,t) = u_x(L,t) \qquad (1.3.24)$$

(This formulation is appropriate to the longitudinal vibrations of air in a tube closed on itself (Fig. 1.4), assuming that curvature effects are ignorable.)

For the exponential function (1.3.3) it is readily established that

$$a_o = 2(e-2)\ ,\quad a_n = 2(e-1)\ /\ (1 + 4n^2\pi^2)$$
$$b_n = -(e-1)\ 4n\pi\ /\ (1+4n^2\pi^2) \qquad (1.3.25)$$

The representation obtained by summing up to n = 4 is shown in Fig. 1.3(d); since the extended function now has discontinuities at both O and L, the Gibbs phenomenon occurs at both these points.

Sometimes (1.3.21) is written in "polar form", namely,

$$g(x) = a_o/2 + \sum_{n=1}^{\infty} r_n \cos(2n\pi x/L - \phi_n) \qquad (1.3.26)$$

where

$$r_n = (a_n^2 + b_n^2)^{\frac{1}{2}} \text{ and } \tan \phi_n = b_n/a_n \qquad (1.3.27)$$

### 1.3.4 Fourier Complex Exponential Series

Sometimes it is convenient to replace the trigonometric functions appearing in the series (1.3.21) by the equivalent complex exponentials. The result is

$$g(x) = a_o/2 + \sum_{n=1}^{\infty} \{ c_n \exp(2\pi i n x/L) + c_n^* \exp(-2\pi i n x/L) \} \quad (1.3.28)$$

where

$$c_n = (a_n - i b_n)/2 \quad (1.3.29)$$

and

$$c_n^* = (a_n + i b_n)/2 \quad (1.3.30)$$

The result can be written more compactly by letting n range through negative integer values and defining, for $n < o$,

$$a_n = a_{-n} \ , \ b_n = -b_{-n} \ ; \quad (1.3.31)$$

also define

$$b_c = 0 \quad (1.3.32)$$

Then eqn (1.3.28) becomes

$$g(x) = \sum_{n=-\infty}^{\infty} c_n \exp(2\pi i \, nx/L) \quad (1.3.33)$$

with $c_n$ given by eqn (1.3.29) for all n. However, on substituting from eqns (1.3.18) and (1.3.20) into eqn (1.3.29) it follows that

$$c_n = (1/L) \int_o^L g(x) \exp(-2\pi i n \, x/L) \, dx \quad (1.3.34)$$

so that the coefficients can be calculated directly; in general they will be complex. This result (1.3.34) also follows from eqn (1.3.33) by using the orthogonality relation

$$\int_o^L \exp(-2\pi i m x/L) \exp(2\pi i n x/L) \, dx = \begin{cases} 0, & m \neq n \\ L, & m = n \end{cases} \quad (1.3.35)$$

Note that here orthogonality involves an integral of the form

$$\int u_m^* \, u_n \, dx = 0 \qquad (1.3.36)$$

where $u_m$ and $u_n$ are the mth and nth functions of the set and the asterisk denotes a complex conjugate value. Note that the derivation of the coefficients using eqn (1.3.35) is valid when g(x) is a complex function. The case of real g(x) is characterised by the relation

$$c_{-n} = c_n^* \qquad (1.3.37)$$

This follows immediately from (1.3.34). Parseval's theorem is here established by multiplying each side of eqn (1.3.33) by its complex conjugate and integrating over (0,L). The result is

$$\int_o^L g \, g^* \, dx = (1/L) \sum_{n=-\infty}^{\infty} c_n c_n^* \qquad (1.3.38)$$

When applied to the exponential function (1.3.3), the coefficients $c_n$ turn out to be given by

$$c_o = e-2, \; c_n = (e-1) \; / \; (1-2\pi \, in) \qquad (1.3.39)$$

Summing the complex series (1.3.33) from n = -N to n=N gives exactly the same result as summing the trigonometric series from n=o to n=N. It must be borne in mind that a pair of complex terms is needed to give one of the terms in the series (1.3.26); this is sometimes described by saying that "a positive and a negative frequency are needed in the complex representation to give a single frequency in the real representation."

## 1.4 The Fourier Integrals

### 1.4.1 Fourier Complex Exponential Integral

All of the Fourier series have a periodic character and, as already seen, throw up repetitions of the original function defined over the basic interval (O,L). However, in many problems where the independent variable x ranges from $-\infty$ to $\infty$ there is a requirement to represent a function which is non-periodic. (e.g. Referring again to Fig. 1.3(a) it might be required to represent the function precisely as it is shown there; in

particular, it might be required that the representation returns a zero value of the function for all $x < o$ and all $x > L$.) None of the series can do this; however, it can be achieved by a Fourier integral as indicated below.

Consider a function $g(x)$ which is non-periodic and is essentially negligible outside some range but is otherwise more or less arbitrary. Suppose this function is represented by a complex Fourier series of period L where L more than spans the range in which the function is non-zero (Fig. 1.5a). Here it is convenient to take the range as $(-L/2, L/2)$, rather than $(0,L)$ as previously, and it is easily established that the representation now is given by

$$g(x) = \sum_{n=-\infty}^{\infty} c_n \exp(2\pi\, inx/L) \qquad (1.4.1)$$

with

$$c_n = (1/L) \int_{-L/2}^{L/2} g(x) \exp(-2\pi inx/L)\, dx \qquad (1.4.2)$$

This representation, of course, implies the periodic repetitions of Fig.1.5(a). Now, if a larger value of L is chosen, whilst the function remains unaltered, these repetitions will be spaced further apart as in Fig.1.5(b). It might be hoped that in the limit of L approaching infinity the repetitions will be lost altogether; this, in fact, occurs and, concomitantly, the sum (1.4.1) becomes an integral. This can be seen as follows. Think of L as very large but (temporarily) fixed. If a new variable, f, defined by

$$f = n/L \qquad (1.4.3)$$

is introduced then, as n ranges over all integral values from $-\infty$ to $\infty$, f will pass through a sequence of closely spaced values from $-\infty$ to $\infty$ . If L is large enough f will approximate a continuous variable, and the difference between successive values of f can be written as the differential, df

where

$$df = 1/L \qquad (1.4.4)$$

On substituting from (1.4.3) and (1.4.4) into (1.4.2), and letting L approach $\infty$, it follows that

$$c_n = G(f)\, df \qquad (1.4.5)$$

where

$$G(f) = \int_{-\infty}^{\infty} g(x) \exp(-2\pi i f x)\, dx \qquad (1.4.6)$$

Further, on substituting from (1.4.3) and (1.4.5) into (1.4.1), and on replacing the sum of infinitesimals by an integral, it is found that

$$g(x) = \int_{-\infty}^{\infty} G(f) \exp(2\pi i f x)\, df \qquad (1.4.7)$$

The two results (1.4.7) and (1.4.6) represent the complex exponential form of Fourier's integral theorem; they are the respective analogues of eqns (1.3.33) and (1.3.34) for a non-periodic function. Commonly, G(f) as defined by (1.4.6) is said to be the "Fourier transform" of g(x) and the relation (1.4.7) is referred to as the "inversion formula". (Instead of considering the Fourier integral as applying to a non-periodic function, sometimes it is helpful to think of it as applying to a function with an infinite period.)

### 1.4.2 Other Fourier Integrals

The Fourier integral just discussed was derived from, and is closely analogous to, the complex form of the Fourier series. In a parallel way it is possible to derive sine, cosine and trigonometric integrals which are analogous to the other series forms. For details, see the references already cited. In all that follows, however, attention will be restricted to the complex form.

## 1.5 Properties and Simple Examples of Fourier Transforms

### 1.5.1 Basic Properties

Here some of the basic properties of Fourier transforms, which are useful in manipulating with them are listed; these can all be readily proven from the definitions (1.4.6) and (1.4.7). Throughout, the notation of "g" for the function and "G" for its transform will be adopted.

(a) Linearity : If

$$g = c_1 g_1 + c_2 g_2 \qquad (1.5.1)$$

where $c_1$ and $c_2$ are constants, then

$$G = c_1 G_1 + c_2 G_2 \qquad (1.5.2)$$

(b) **Shift Theorem** : If $g_1$ and $g_2$ are such that

$$g_2(x) = g_1(x-a) \tag{1.5.3}$$

where a is a constant, then

$$G_2(f) = \exp(-2\pi i f a)\, G_1(f) \tag{1.5.4}$$

(c) **Transform of Derivative** : If

$$h(x) = dg/dx \tag{1.5.5}$$

then

$$H = 2\pi i f G \tag{1.5.6}$$

(Here it is assumed that g(x) vanishes "sufficiently rapidly" at infinity.)

(d) **Transform of Real Function** : The Fourier transform formulae apply whether g is a real or complex function. If g is real, then

$$G(-f) = G^*(f) \tag{1.5.7}$$

### 1.5.2 Fourier Transform of Rectangular Pulse; The Sinc Function

Consider the function defined by

$$\begin{aligned} g(x) &= 1 && |x| < L/2 \\ &= 0 && |x| > L/2 \end{aligned} \tag{1.5.8}$$

This function, which is shown in Fig. 1.6, is widely used in Fourier analysis. Direct integration readily yields

$$\begin{aligned} G(f) &= \{\sin(\pi f L)\}/(\pi f) \\ &= L\, \mathrm{sinc}(\pi f L) \end{aligned} \tag{1.5.9}$$

Here the functional notation

$$\mathrm{sinc}\, y = \sin y / y \tag{1.5.10}$$

has been introduced. (Sometimes used alternatives to "sinc" are "sync" and "dif"; the last name was presumably chosen because the function has a fundamental role in diffraction problems.)

A sketch of the function sinc y is shown in Fig. 1.7. The function has a maximum value of unity at $y = 0$ and is zero at $y = \pm n\pi$ for $n = 1,2 \cdots$. Its turning points, apart from the origin, are approximately at $y = \pm (2n + 1)\pi/2$. More accurately, the turning point in the vicinity of $y = 3\pi/2 (= 4.71)$ is at $y = 4.49$; the other turning points are nearer the approximate values quoted above. The amplitude of the minimum at $y = 4.49$ is 0.22, and the amplitudes at the other turning points essentially are decreasing as $1/y$. That part of the function between $-\pi$ and $\pi$ is referred to as the "main lobe".

Reverting to the transform (1.5.9), it, of course, also is of the form shown in Fig.1.7; here, the main lobe extends from $f = -1/L$ to $f = 1/L$. Note that decreasing L gives a sharper (or more concentrated) original function but gives a more diffuse (or less concentrated) transform, and conversely. This is a general feature of Fourier transforms; in fact, there exists an "uncertainty principle" (exactly as in Quantum Mechanics) relating the "width" of the function and that of its transform.

Finally, if the pulse under consideration extends from 0 to L, rather than from $-L/2$ to $L/2$, the "shift theorem" as given by eqn (1.5.4) can be used to write down the transform. The result is now

$$G(f) = L \exp(-\pi i f L) \operatorname{sinc}(\pi f L) \qquad (1.5.11)$$

### 1.5.3 Fourier Transform of Triangular Pulse

Now consider the "triangular" function defined by

$$\begin{aligned} g(x) &= (1 + 2x/L) && -L/2 < x \leq 0 \\ &= (1 - 2x/L) && 0 < x < L/2 \\ &= 0 && |x| > L/2 \end{aligned} \qquad (1.5.12)$$

This function is shown in Fig. 1.8; it is also of common occurence in Fourier analysis. Only elementary integration is needed to establish that the transform is

$$G(f) = (2/L) \{\sin^2(\pi f L/2)\} / (\pi^2 f^2). \qquad (1.5.13)$$

It can be seen that the behaviour of the transform is essentially that of the function

$$\sin^2 y / y^2 \qquad (1.5.14)$$

This last is shown in Fig. 1.9. It is of a generally similar character to the sinc function, the most important differences being, firstly, that the present function is always positive and, secondly, there is a much greater concentration of the function in the "main lobe".

## 1.6 The Dirichlet Kernel

The arguments given to date for the development of both Fourier series and integrals are more or less in accord with what took place historically. However, these arguments have been plausible, rather than rigorous. The rigorous proof of the Fourier expansions was given by Dirichlet in 1829 and an outline of this proof is given below for the Fourier integral. (The proof for the series is very similar).

The Fourier integral theorem is embodied in the dual relations

$$g(x) = \int_{-\infty}^{\infty} G(f) \exp(2\pi i f x)\, df \qquad (1.6.1)$$

$$G(f) = \int_{-\infty}^{\infty} g(x) \exp(-2\pi i f x)\, dx \qquad (1.6.2)$$

If these relations are valid then on substituting from (1.6.2) into (1.6.1) an identity should result. It is convenient to commence by taking finite integration terminals in (1.6.1), say -N and N where N is large; the associated function on the left hand side of (1.6.1) will now be written as $g_N(x)$ i.e.,

$$g_N(x) = \int_{-N}^{N} G(f) \exp(2\pi i f x)\, dx \qquad (1.6.3)$$

Thus, it is required to show that as N approaches infinity, $g_N$ approaches g. Substituting for G from (1.6.2) - where u is now written for the integration variable - into (1.6.3) and reversing the order of integration gives

$$g_N(x) = \int_{-\infty}^{\infty} g(u) \{ \int_{-N}^{N} \exp 2\pi i f(x-u)\, df \}\, du \qquad (1.6.4)$$

i.e.,

$$g_N(x) = \int_{-\infty}^{\infty} g(u)\, D_N(x-u)\, du \qquad (1.6.5)$$

where

$$D_N(x-u) = \sin\{2\Pi N(x-u)\}/\pi(x-u) \qquad (1.6.6)$$

$$= 2N \operatorname{sinc}\{2\Pi N(x-u)\} \qquad (1.6.7)$$

If $g_N(x)$ is to approach $g(x)$, then the limiting value $D(x-u)$ of the kernel function $D_N(x-u)$ must have the infinitely strong "focussing power" implied by the equation

$$g(x) = \int_{-\infty}^{\infty} g(u)D(x-u)\,du \qquad (1.6.8)$$

The limit function $D(x-u)$ is termed the "Dirichlet kernel". (From (1.6.7) it is clear that the "main lobe" of the sinc function in this kernel is centred around $x=u$; also that the amplitude of the kernel becomes infinite in the limit.)

Introducing a new variable y defined by

$$y = 2\Pi N(x-u) \qquad (1.6.9)$$

it is easily seen that (1.6.5) becomes

$$g_N(x) = (1/\Pi) \int_{-\infty}^{\infty} g(x - y / (2\Pi N)) \operatorname{sinc} y\,dy \qquad (1.6.10)$$

If N now is let approach infinity, and if use be made of the standard integral,

$$\int_{-\infty}^{\infty} \operatorname{sinc} y\,dy = \Pi \qquad (1.6.11)$$

it follows that $g_N(x)$ approaches $g(x)$ as required.

The above result is valid as long as $g(x)$ is a continuous function (and becomes suitably small at infinity.) If $g(x)$ has a point of discontinuity, then a more rigorous analysis shows that, at such a point, $g_N(x)$ approaches the mean of the values on either side of the discontinuity.

Before passing on it might be observed that the Dirichlet kernel obviously has an intimate connection with the sinc function which, in turn, appeared as the transform of a rectangular pulse. Another kernel function sometimes encountered is the "Fejer kernel"; this has even stronger focussing powers than the Dirichlet kernel and is closely connected with the transform of a triangular pulse.

## 1.7 Delta Functions; Parseval's Theorem for Fourier Integral

### 1.7.1 General

Consider again the Dirichlet kernel D(x-u) just discussed. This was defined as the limit for N approaching infinity of

$$D_N(x-u) = 2N \text{ sinc } \{2 \Pi N(x-u)\} \tag{1.7.1}$$

The kernel has the following properties :

$$\int_{-\infty}^{\infty} D(x-u)\, du = 1 \tag{1.7.2}$$

$$\int_{-\infty}^{\infty} g(u)\, D(x-u)\, du = g(x) \tag{1.7.3}$$

The first of these properties follows from the fact that (1.7.2) holds when $D_N$ replaces D, for all N. (This can be proved by direct integration.) Hence it is also true for the limit function. The second property has already been demonstrated in the previous section.

The relation (1.7.3) shows that D can be regarded as a "weighting function" which gives a zero weight to a function g(u) at all points of an infinite interval save at the single point u=x, where it assigns a unit weight. Ordinary weighting functions will not possess this property. Functions which do are variously termed "delta functions", "distributions", "impulse functions" or "generalised functions". Detailed studies of their properties can be found, for instance, in refs. 11 and 12.

Actually the Dirichlet kernel, although the commonest type of delta function occurring in Fourier analysis, is somewhat more complicated than other delta functions. The simplest such function is that defined by

$$\begin{aligned} \delta(x-u) &= \lim_{\varepsilon \to 0} 1/\varepsilon \quad \text{for } x < u < x + \varepsilon \\ &= 0 \qquad\qquad\quad \text{all other } u \end{aligned} \tag{1.7.4}$$

This function is shown in Fig. 1.10 for (a) non-zero $\varepsilon$ and (b) zero $\varepsilon$. One physical interpretation of it is as a band of uniform (line) pressure which in the limit becomes a concentrated force. It is immediately established that a relation analogous to (1.7.2) holds. To prove the result analogous to

(1.7.3) suppose that g(u) is expanded in a Taylor series about the point x. Then, writing v = u-x, it follows that

$$\int_{-\infty}^{\infty} g(u)\ \delta(x-u)\ du = \lim\ \varepsilon \to 0\ \int_{o}^{\varepsilon}\ (1/\varepsilon)\{\ g(x) + v g^{1}(x) + \cdots\} dv$$

$$= \lim\ \varepsilon \to 0\ \{g(x) + \varepsilon\, g^{1}(x)/2 + \cdots\}$$

i.e.,

$$\int_{-\infty}^{\infty} g(u)\ \delta(x-u) du = g(x) \qquad (1.7.5)$$

However, as already indicated, in most of the following the delta function used will be that associated with the Dirichlet kernel. This can be expressed in the form (using the "δ" notation)

$$\int_{-\infty}^{\infty} \exp\ \{2\pi i\ (f_1 - f)\ x\}\ dx \quad = \quad \delta(f_1 - f) \qquad (1.7.6)$$

Also, it might be noted that since the sinc function is an even one, it follows that here at any rate

$$\delta(f_1 - f) \quad = \quad \delta(f - f_1) \qquad (1.7.7)$$

### 1.7.2 Fourier Transforms involving Delta Functions

Conventional Fourier transforms can only be applied to functions g(x) for which some boundedness condition such as

$$\int_{-\infty}^{\infty} |g(x)|\ \ dx < \ M \qquad (1.7.8)$$

where M is finite, applies. However, using delta functions, they can be fruitfully applied to common functions for which (1.7.8) does not hold.

(a) Transform of constant : Consider the case where

$$g(x) \ = 1 \qquad \text{all } x \qquad (1.7.9)$$

(This can be regarded as the limit of the rectangular pulse discussed in Section 1.5.2 when the length L of the pulse approaches infinity.)

The transform of (1.7.9) is

$$G(f) = \int_{-\infty}^{\infty} \exp(-2\pi i f x)\, dx = \delta(f) \qquad (1.7.10)$$

i.e., the transform is a delta function located at the origin of f. The function and its transform are shown in Fig. 1.11 and it can be seen that this represents an extreme case of the "uncertainty principle" already referred to in Section 1.5.2.

(b) Transform of periodic function : As a second example, consider

$$g(x) = \exp(2\pi i n x/L) \qquad (1.7.11)$$

where n is an integer; this, of course, is the typical term in the complex Fourier series expansion of a function of period L. The transform is easily found to be

$$G(f) = \delta(f - n/L) \qquad (1.7.12)$$

Since an arbitrary periodic function can be represented as an infinite series of terms such as (1.7.11), with n ranging through all positive and negative integral values, its transform will consist of an infinite number of delta functions located at the points f = n/L.

If

$$g(x) = \cos(2\pi n x/L) \qquad (1.7.13)$$

then, immediately,

$$G(f) = (1/2)\{\delta(f-n/L) + \delta(f+n/L)\} \qquad (1.7.14)$$

This function and its transform are shown in Fig. 1.12 for the case n = 2.

### 1.7.3 Parseval's Theorem for Fourier Integral

As a final example of the use of delta functions, Parseval's theorem for the Fourier integral will be proved.

As always,

$$g(x) = \int_{-\infty}^{\infty} G(f)\ \exp(2\pi i f x)\ df \qquad (1.7.15)$$

Taking the conjugate complex of each side, and writing $f_1$ for the integration variable, gives

$$g^*(x) = \int_{-\infty}^{\infty} G^*(f_1)\ \exp(-2\pi i f_1 x)\ df_1 \qquad (1.7.16)$$

Hence,

$$\int_{-\infty}^{\infty} g\ g^*\ dx = \int_{-\infty}^{\infty} G(f)\ \{\int_{-\infty}^{\infty} G^*(f_1)\{\int_{-\infty}^{\infty} \exp 2\pi i\ (f-f_1)\ x\ dx\ \}df_1\}\ df \qquad (1.7.17)$$

The innermost integral is simply $\delta(f-f_1)$ and so the middle integral returns only $G^*(f)$; the final result is

$$\int_{-\infty}^{\infty} g\ g^*\ dx = \int_{-\infty}^{\infty} G\ G^*\ df \qquad (1.7.18)$$

This is Parseval's theorem.

## 1.8 Convolutions

An important tool in all Fourier analysis is the convolution integral. Its introduction can be motivated in a variety of ways. One way is via the following question : Suppose that the Fourier transform of some function $g(x)$ is sought and the direct calculation of the integral is difficult (which is more often the case than might be thought from its rather simple form), but suppose that the function is recognized as the product of two other functions whose transforms are known i.e.,

$$g(x) = g_1(x)\ g_2(x) \qquad (1.8.1)$$

where $G_1(f)$ and $G_2(f)$ are known. Can the transform, G, of g be expressed in terms of $G_1$ and $G_2$ ?

From the definition,

$$G(f) = \int_{-\infty}^{\infty} g_1(x)\, g_2(x) \exp(-2\pi i f x)\, dx \qquad (1.8.2)$$

Also,

$$g_1(x) = \int_{-\infty}^{\infty} G_1(f_1) \exp(2\pi i f_1 x)\, df_1 \qquad (1.8.3)$$

$$g_2(x) = \int_{-\infty}^{\infty} G_2(f_2) \exp(2\pi i f_2 x)\, df_2 \qquad (1.8.4)$$

On substituting from (1.8.3) and (1.8.4) into (1.8.2), and reversing the order of integration so that the x integration is done first, it is found that

$$G(f) = \int_{-\infty}^{\infty} G_1(f_1) \{ \int_{-\infty}^{\infty} G_2(f_2) \{ \int_{-\infty}^{\infty} \exp(2\pi i (f_1 + f_2 - f) x)\, dx \}\, df_2 \}\, df_1 \qquad (1.8.5)$$

The innermost integral can be written as

$$\delta ( f_2 - (f - f_1) )$$

and this, when applied to the middle integral, gives simply

$$G_2(f - f_1)$$

Hence the final result is

$$G(f) = \int_{-\infty}^{\infty} G_1(f_1)\, G_2(f - f_1)\, df_1 \qquad (1.8.6)$$

An integral of this form is termed a "convolution" of the functions $G_1$ and $G_2$ . Sometimes it is denoted by a special symbol e.g.,

$$G = G_1 * G_2 \qquad (1.8.7)$$

(It is easily established that it does not matter which of $G_1$ and $G_2$ has the argument "$f_1$" and which "$f - f_1$".)

A quite analogous proof can be developed to show that, if

$$G(f) = G_1(f)\, G_2(f) \tag{1.8.8}$$

then

$$g(x) = \int_{-\infty}^{\infty} g_1(x_1)\, g_2\,(x-x_1)\, dx_1 \tag{1.8.9}$$

As a simple example of these last relations the "shift theorem" of eqn (1.5.4) will be proved in reverse. Suppose

$$G(f) = \exp\,(-2\pi i f a)\, H\,(f) \tag{1.8.10}$$

where h(x) is known and g(x) is sought. This is a product of the form of (1.8.8). The inverse of the exponential term is

$$\int_{-\infty}^{\infty} \exp(-2\pi i f a)\, \exp(2\pi i f x)\, d\, f = \delta(x-a) \tag{1.8.11}$$

Hence, by the convolution theorem (1.8.9),

$$g(x) = \int_{-\infty}^{\infty} \delta(x_1-a)\, h\,(\, x-x_1)\, dx_1 \tag{1.8.12}$$

i.e.,

$$g(x) = h(x-a) \tag{1.8.13}$$

as required.

## 1.9 Fourier Expansions in Two or More Variables

All the discussion to date has related to Fourier expansions of a function of one variable. However the concepts can be readily extended to functions of two or more variables. This will be demonstrated for the Fourier integral but a similar approach can be used for the series.

Consider a function $g(x_1, x_2)$ and, temporarily thinking of $x_2$ as fixed, take its transform with respect to $x_1$ to get

$$G_1(f_1, x_2) = \int_{-\infty}^{\infty} g(x_1, x_2)\, \exp\,(-2\pi i f_1 x_1)\, dx_1 \tag{1.9.1}$$

with the inverse relation

$$g(x_1,x_2) = \int_{-\infty}^{\infty} G_1(f_1, x_2) \exp(2\pi i f_1 x_1)\, df_1 \qquad (1.9.2)$$

Now take the transform of $G_1$ with respect to $x_2$

to get

$$G(f_1, f_2) = \int_{-\infty}^{\infty} G_1(f_1, x_2) \exp(-2\pi i f_2 x_2)\, dx_2 \qquad (1.9.3)$$

with the inverse relation

$$G_1(f_1,x_2) = \int_{-\infty}^{\infty} G(f_1, f_2) \exp(2\pi i f_2 x_2)\, df_2 \qquad (1.9.4)$$

Substituting from (1.9.1) into (1.9.3) gives

$$G(f_1,f_2) = \int_{-\infty}^{\infty}\int_{-\infty}^{\infty} g(x_1, x_2) \exp\{-2\pi i(f_1 x_1 + f_2 x_2)\}\, dx_1 dx_2 \qquad (1.9.5)$$

and from (1.9.4) into (1.9.2) gives

$$g(x_1, x_2) = \int_{-\infty}^{\infty}\int_{-\infty}^{\infty} G(f_1, f_2) \exp\{2\pi i(f_1 x_1 + f_2 x_2)\}\, df_1 df_2 \qquad (1.9.6)$$

The two relations (1.9.5) and (1.9.6) represent the Fourier integral theorem for a function of two variables. The extensions to functions of more than two variables are obvious.

## References


1. HSU, HWEI P. Fourier Analysis. Simon and Schuster, New York, 1970.

2. CHAMPENEY, D.C. Fourier Transforms and Their Physical Applications. Academic Press, New York, 1973.

3. BRACEWELL, R. The Fourier Transform and Its Applications. McGraw-Hill, New York, 1965.

4. PAPOULIS, A. The Fourier Integral and Its Applications. McGraw-Hill, New York, 1962.

5. CHURCHILL, R.V. Fourier Series and Boundary Value Problems. McGraw-Hill, New York, 1941.

6. SNEDDON, I.N. Fourier Transforms. McGraw-Hill, New York 1951.

7. TITCHMARSH, E.C. Theory of Fourier Integrals. Oxford University Press, 1937.

8. CARSLAW, H.S. Introduction to the Theory of Fourier Series and Integrals. Macmillan, London, 1921.

9. TRUESDELL, C. The Rational Mechanics of Flexible or Elastic Bodies 1638-1788. Orell Fussli, Turici, 1960, pp. 237-300.

10. FOURIER, J. The Analytical Theory of Heat. (Translated by A. Freeman) Dover, New York, 1955.

11. LIGHTHILL, M.J. Introduction to Fourier Analysis and Generalised Functions. Cambridge University Press, 1958.

12. SCHWARTZ, L. Mathematics for the Physical Sciences. Addison-Wesley, Reading, 1966.

## APPENDIX

## End Discontinuity Effects and Hanning

In the earlier "physical" derivation of the different Fourier series it transpired that each form had its own particular boundary conditions associated with the end-points 0 and L of the fundamental interval. Again writing g(x) for the function to be represented, these boundary conditions were as follows :

sine series (period 2L) , $g(o) = g(L) = 0$ (A1)

cosine series (period 2L) , $g^1(o) = g^1(L) = 0$ (A2)

trigonometric series (period L) , $g(o) = g(L)$ and $g^1(o) = g^1(L)$ (A3)

These conditions are not necessary for the validity of the series expansions; however, from the practical viewpoint, the series will generally converge much more rapidly when the conditions are fulfilled.

In some situations the following device is useful. Suppose g(x) is the function which it is wished to represent, but suppose that it does not satisfy the "physical boundary conditions". Let h(x) be another function, which has the same periodicity as the expansion to be used, and which is chosen such that the "modified function"

$$m(x) = g(x)\ h(x) \tag{A4}$$

does have the physical boundary conditions. Then m(x) can be expanded in the same type of series as was planned for g(x) and this series should have good convergence properties.

For example, suppose a sine series is to be used and that $g(o) = 0$ as required (as would be the case for an odd function) but that $g(L) \neq 0$. Here taking

$$h(x) = (1 + \cos \pi x/L)/2 \tag{A5}$$

satisfies the requirement that $h(L) = 0$ and, also, h(x) is of period 2L. This function, which is known as a Hann function (after J. von Hann) is shown in Fig. A1. If the Fourier coefficients, $b_n$, for the sine series for g(x) are known, the coefficients $b_n^1$ for the modified function m(x) can be written down. From the definitions,

$$b_n = (2/L) \int_o^L g(x) \sin(n\pi x/L)\, dx \qquad \text{(A6)}$$

$$b_n^1 = (2/L) \int_o^L g(x)h(x)\sin(n\pi x/L)\, dx \qquad \text{(A7)}$$

With h(x) as given by eqn (A5), it follows that

$$h(x)\sin(n\pi x/L) = (1/4)\sin\{(n-1)\pi x/L\} + (1/2)\sin(n\pi x/L) + (1/4)\sin\{(n+1)\pi x/L\} \qquad \text{(A8)}$$

Hence,

$$b_1^1 = b_1/2 + b_2/4 \qquad \text{(A9)}$$

$$b_n^1 = b_{n-1}/4 + b_n/2 + b_{n+1}/4 \quad , \quad n=2,3 \cdots$$

As an example, consider the Fourier sine series expansion for the function

$$g(x) = \exp(x/L) - 1 \qquad \text{(A10)}$$

This has already been determined in Section 1.3.1. The values of the first few coefficients, $b_n$, and the corresponding "hanned" ones, $b_n^1$, are given in Table 1 below.

| n | $b_n$ | $b_n^1$ |
|---|---|---|
| 1 | 0.876 | 0.305 |
| 2 | -0.533 | 0.041 |
| 3 | 0.356 | -0.023 |
| 4 | -0.272 | 0.007 |

Table 1 : Fourier Coefficients for Exponential Function before and after Hanning.

Clearly the hanned coefficients are decreasing much more rapidly so that taking only 4 terms, say, in the series for the hanned function should give a much better representation of it, than does the same number of terms in the series for the original function. Thus, if one is faced with the problem of recovering a function given its Fourier sine coefficients the following procedure may be useful :

(i) From the original coefficients, determine the hanned coefficients using eqn (A9).

(ii) Recover the modified (or hanned) function by summing the series in the hanned coefficients.

(iii) Recover the original function from the hanned one using g = m/h.

The results of doing this for the exponential function (A10) are shown in Table 2 below (using 4 terms in the series). For comparison the exact results and the results from a direct summation of the series (again with 4 terms) are included.

| x/L | g(x) = exp (x/L) - 1 | | |
|---|---|---|---|
| | Exact | Direct Sum (n=4) | Hanning (n=4) |
| 0 | 0 | 0 | 0 |
| 0.1 | 0.105 | -0.013 | 0.109 |
| 0.2 | 0.221 | 0.186 | 0.222 |
| 0.3 | 0.350 | 0.471 | 0.345 |
| 0.4 | 0.492 | 0.569 | 0.490 |
| 0.5 | 0.649 | 0.520 | 0.656 |
| 0.6 | 0.822 | 0.679 | 0.829 |
| 0.7 | 1.014 | 1.166 | 0.991 |
| 0.8 | 1.226 | 1.521 | 1.186 |
| 0.9 | 1.460 | 1.131 | 1.800 |
| 1.0 | 1.718 | 0 | - |

Table 2 : Hanning with Fourier Sine Series for Exponential

When dealing with a Fourier cosine series for a function which has zero slope at x = 0 but not at x = L exactly the same device can be used. It can be readily established that the modified function (A4) with h(x) again given by (A5) will have a zero slope at both end points. The hanned coefficients, $a_n^1$, are given in terms of the original ones, $a_n$, by

$$a_o^1 = a_o/2 + a_1/2$$

$$a_n^1 = a_{n-1}/4 + a_n/2 + a_{n+1}/4 \qquad \text{(A11)}$$

Finally, when dealing with the general trigonometric series for a function of period L, but which does not satisfy the periodic boundary conditions, use of the Hann function

$$h(x) = (1-\cos 2\pi x/L)/2 \qquad \text{(A12)}$$

leads to a modified function, m(x), which will have periodic boundary conditions. (In fact, m(x) will be zero at x=0 and x=L, as will be its derivative). This Hann function is shown in Fig.A2. By a procedure analogous to that used in establishing eqn (A8) it can be shown that the hanned coefficients $a_n^1$, $b_n^1$ are related to the original ones $a_n$, $b_n$ as follows :

$$a_o^1 = a_o/2 - a_1/2$$

$$a_n^1 = -a_{n-1}/4 + a_n/2 - a_{n+1}/4$$

$$b_1^1 = b_1/2 - b_2/4 \qquad \text{(A13)}$$

$$b_n^1 = -b_{n-1}/4 + b_n/2 - b_{n+1}/4$$

The procedure for using hanning here is completely analogous to that already described for the sine series.

The above is not the only method for dealing with the problem end effects; another way is to subtract off a "linear trend".

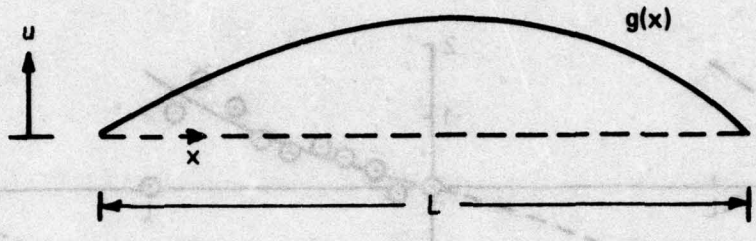


FIG. 1.1 INITIAL CONFIGURATION OF VIBRATING STRING WITH FIXED ENDS

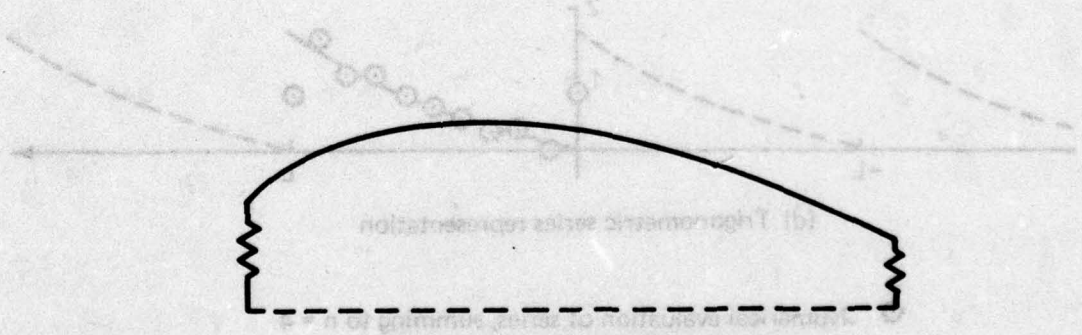

FIG. 1.2 STRING WITH ELASTIC END SUPPORTS

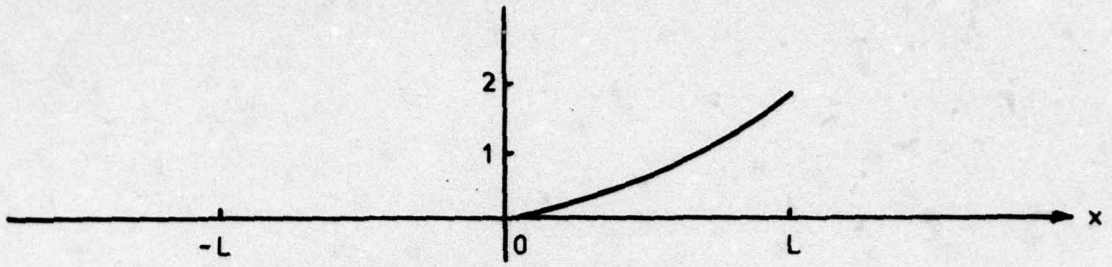


(a) Function EXP(x/L) – 1

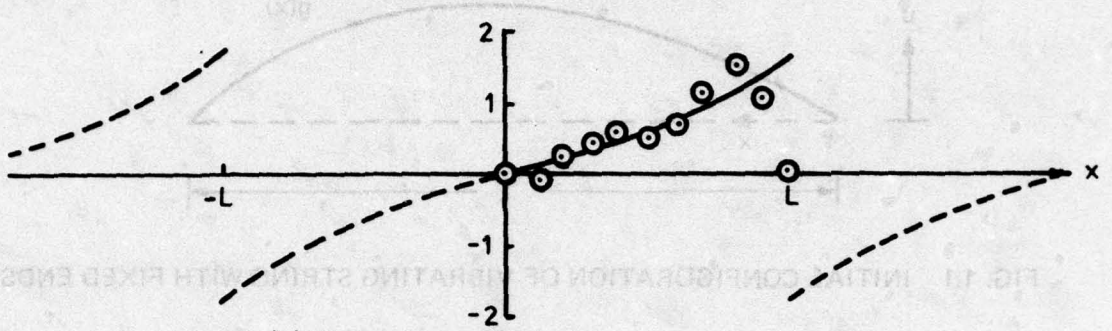


(b) Sine series representation

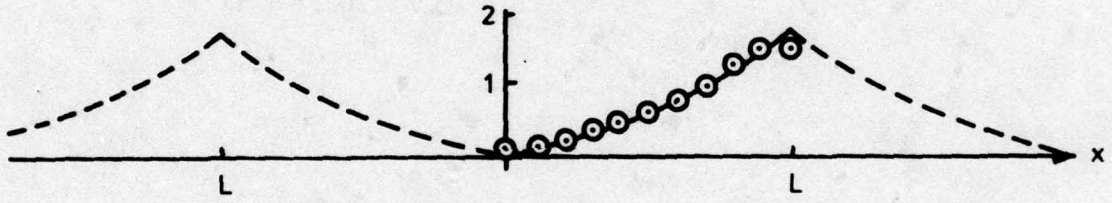


(c) Cosine series representation

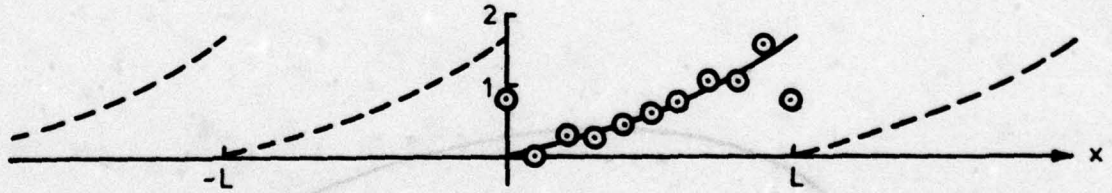


(d) Trigonometric series representation

⊙ Numerical evaluation of series, summing to n = 4
--- Function represented by (infinite) Fourier series outside basic interval

FIG. 1.3 VARIOUS FOURIER SERIES REPRESENTATIONS OF THE ONE FUNCTION: g(x) = EXP(x/L) – 1

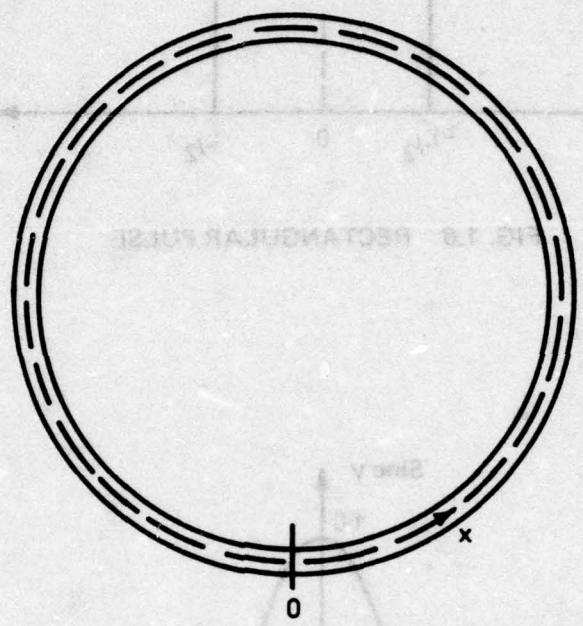


FIG. 1.4 TUBE OF AIR ILLUSTRATING PERIODIC BOUNDARY CONDITIONS (CURVATURE EFFECTS IGNORED SO ONE-DIMENSIONAL WAVE EQUATION APPLIES)

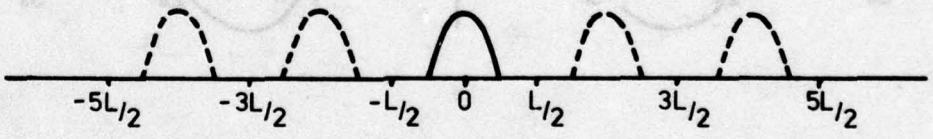


(a) Periodic function, basic interval L

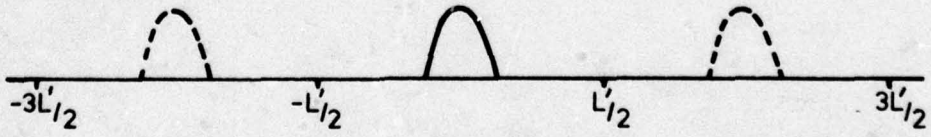


(b) Same periodic function, basic interval $L^1 = 2L$

FIG. 1.5 EFFECT OF INCREASING BASIC INTERVAL ON REPETITIONS OF PERIODIC FUNCTION

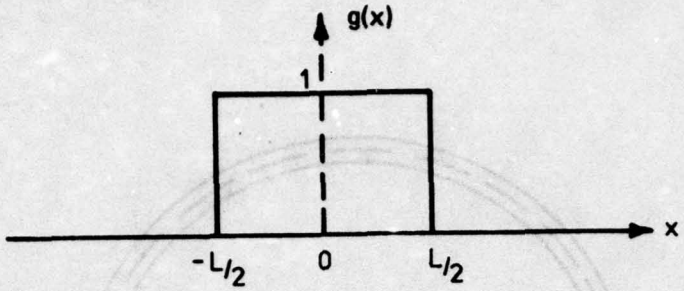


FIG. 1.6 RECTANGULAR PULSE

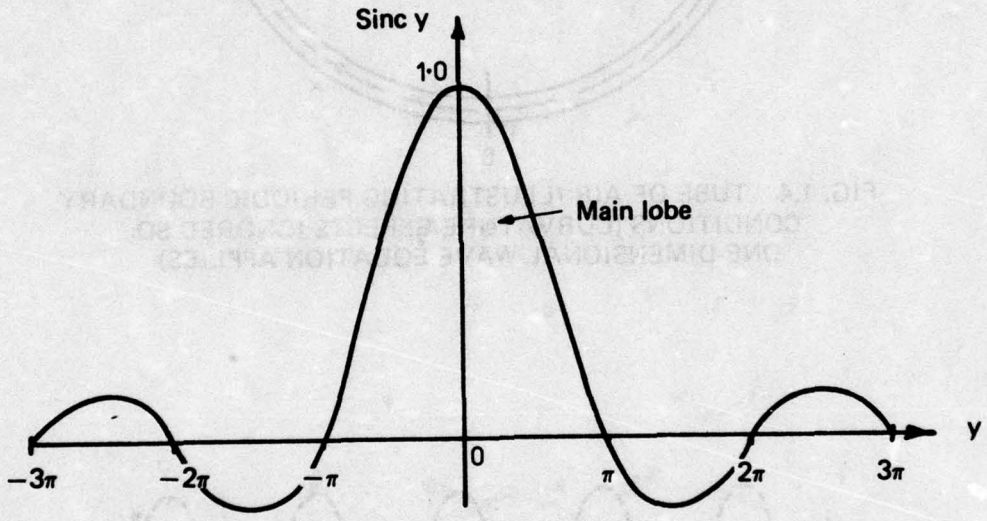


FIG. 1.7 FUNCTION SINC y

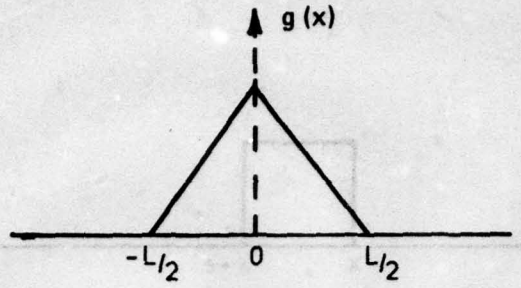


FIG. 1.8 TRIANGULAR PULSE

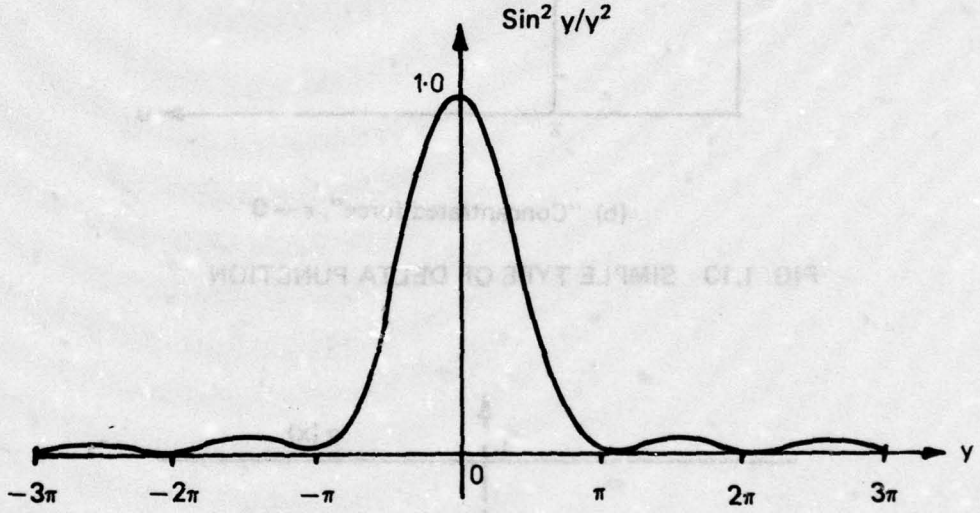


FIG. 1.9 FUNCTION $\sin^2 y/y^2$

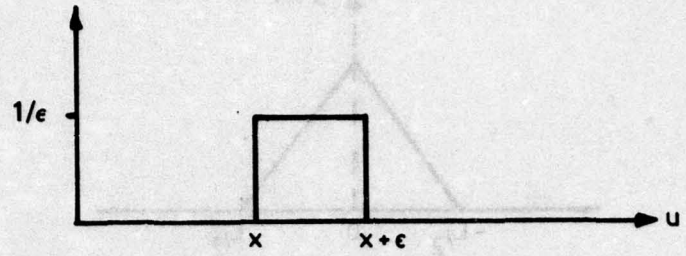


(a) "Band of pressure"

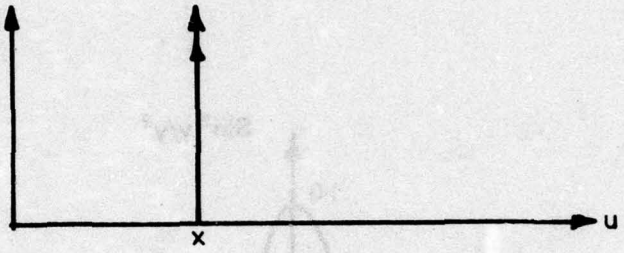


(b) "Concentrated force", $\epsilon \to 0$

FIG. 1.10 SIMPLE TYPE OF DELTA FUNCTION

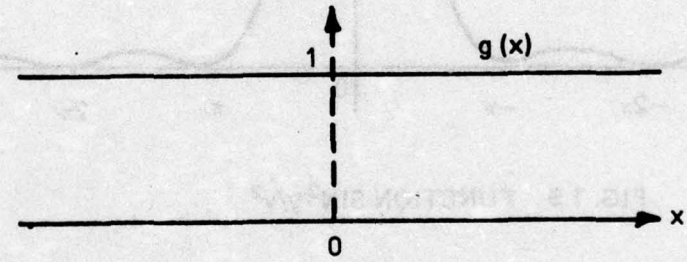


(a) Constant function

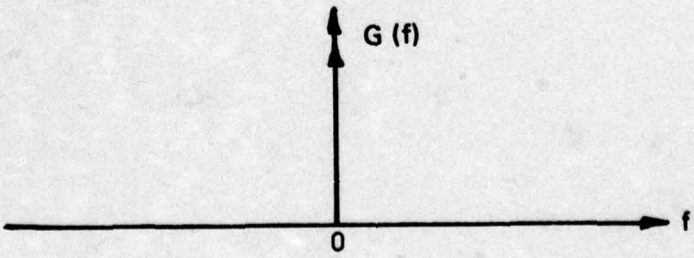


(b) Transform

FIG. 1.11 TRANSFORM OF CONSTANT

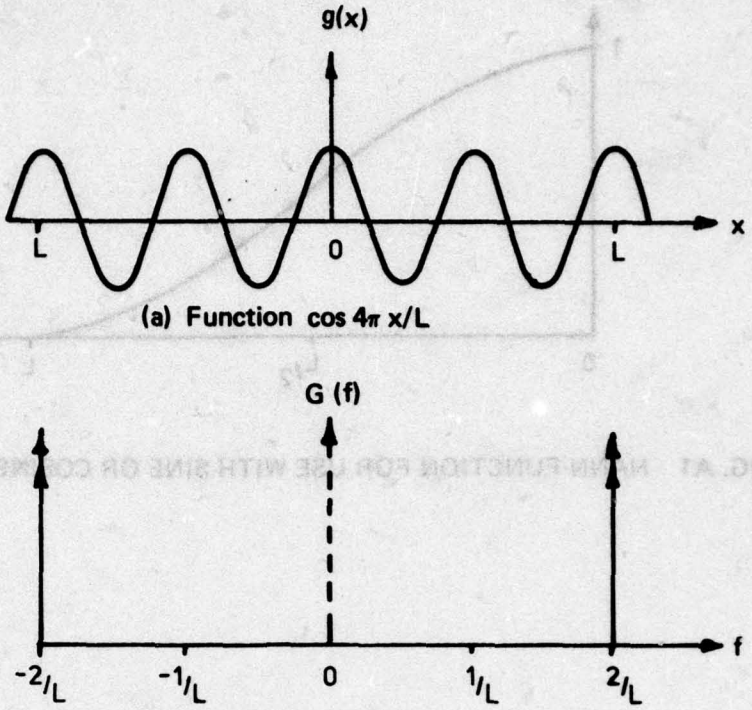


FIG. 1.12 TRANSFORM OF PERIODIC FUNCTION

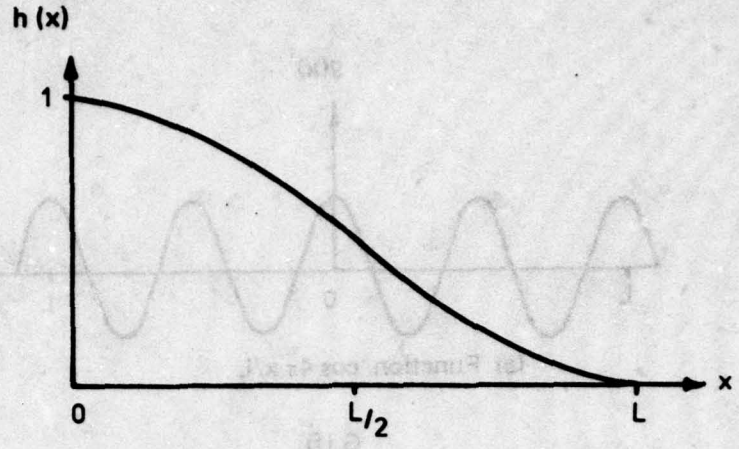


FIG. A1 HANN FUNCTION FOR USE WITH SINE OR COSINE SERIES

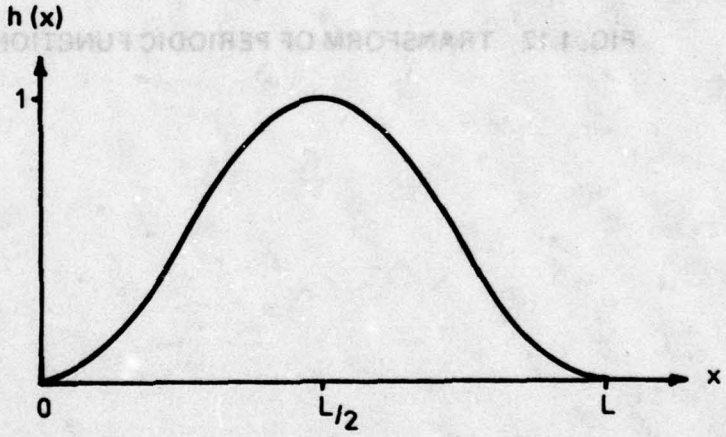


FIG. A2 HANN FUNCTION FOR USE WITH TRIGONOMETRIC SERIES

# CHAPTER 2 : THE DISCRETE FOURIER TRANSFORM

## 2.1 General

The analytical processes associated with the classical Fourier series and integrals can only be conveniently performed when the functions considered are of a relatively simple form. In other cases, and, in particular, for functions that are only specified numerically (as is the general situation when the functions are experimental data) it is necessary to adopt numerical Fourier methods. These have a history as long as the analytical methods, going back to Lagrange who, around 1760, and as a result of studies of the vibration of a string with particles attached, constructed a theory of interpolation using trigonometric functions which is quite analogous to the more familiar theory based on polynomials. Lagrange's results form the basis of what today are called "discrete Fourier transforms" (DFTs).

Sporadic developments in this area occurred over the next two centuries or so. For example, one problem to which Lagrange's results were applied was in the search for hidden periodicities in experimental data; an important tool here was the "periodogram" developed by Schuster around 1900. Also, Runge around the same time developed computational procedures for use in trigonometric interpolation which embodied the key features of the "fast Fourier transform" (FFT) used today. Some account of this early work is given in ref.1. Danielson and Lanczos in 1942 treated several important aspects of numerical Fourier analysis; this work is elaborated on by Lanczos in reference 2 and contains the seeds of many present day developments. In the post World War 2 era the whole subject has been greatly advanced, especially by workers in the field of communication engineering. (See, for example, ref.3) This culminated in 1965, with Cooley and Tukey developing the definitive form of the fast Fourier transform which provided a dramatic reduction in the computing effort previously required.

Nevertheless, amongst the spate of books on general numerical analysis which appeared following the advent of the digital computer, very few made more than a fragmentary reference to numerical Fourier methods; an exception was that by Hamming (4). (See, also, ref.5). It is only over the past two or three years that these methods have been treated in detail in the text book literature (e.g. ref.6).

## 2.2 Physical Motivation for Discrete Fourier Transform

Just as the vibrations of a continuous (heavy) string provided the physical basis for the development of Fourier series, so do the vibrations of a (light) string with discrete masses attached provide a physical basis for the development of the DFT. As already remarked this problem was solved by Lagrange, and details can be found in many texts e.g. that by Hildebrand (7). Only the outlines of the solution will be given here.

Consider the case of N + 1 equal particles uniformly spaced on a string of length L (Fig. 2.1). The particles are numbered "0" to "N" as shown and clearly the base co-ordinate $x_k$ of particle k is given by

$$x_k = k\ L/N \tag{2.2.1}$$

Analogously to the continuous string, first consider the situation when the string has fixed ends (so that the two end particles do not participate in the motion) and commences vibrating with zero initial velocity from some deformed configuration (Fig. 2.2). The initial position of the m th particle is denoted by $g_m$. It is convenient to use vector notation in the following and to write, for example,

$$\vec{g} = \begin{bmatrix} g_1 \\ g_2 \\ . \\ g_{N-1} \end{bmatrix} \tag{2.2.2}$$

Similarly using $\vec{u}$ to denote the set of particle displacements at time t it can be shown that the solution of the (N-1) ordinary differential equations which govern this problem is given by

$$\vec{u}(t) = \sum_{n=1}^{N-1} B_n \vec{e}_n \cos p_n t \tag{2.2.3}$$

where the $B_n$ are integration constants, the $p_n$ are the natural frequency parameters (whose precise values are obtained but are not of concern here), and the $\vec{e}_n$ are the normal modes given by

$$\vec{e}_n = \begin{bmatrix} \sin(n\pi/N) \\ \sin(2n\pi/N) \\ \\ \sin((N-1)n\pi/N) \end{bmatrix} \qquad (2.2.4)$$

(Bearing in mind eqn (2.2.1) it can be seen that (2.2.4) represents an approximation to the n th mode for the continuous string which was $\sin(n\pi x/L)$ .) The expression (2.2.3) satisfies the condition of zero initial velocity whilst the requirement that $\vec{u}(o) = \vec{g}$ implies

$$\vec{g} = \sum_{n=1}^{N-1} B_n \vec{e}_n \qquad (2.2.5)$$

Since equality of a vector relation implies equality of corresponding components eqn (2.2.5) can just as well be written

$$g_m = \sum_{n=1}^{N-1} B_n \sin(mn\pi/N) \qquad (2.2.6)$$

Since the g's are arbitrary, eqn (2.2.6) shows that an arbitrary function defined on a discrete set of uniformly spaced points can be represented by a finite series of sines.

As in the continuous case, the normal modes are orthogonal but here orthogonality is expressed by the vanishing of the scalar product of $\vec{e}_n$ and $\vec{e}_k$ , say; i.e., using the bracket notation for the scalar product,

$$(\vec{e}_n, \vec{e}_k) = \sum_{m=1}^{N-1} \sin(mn\pi/N) \sin(mk\pi/N) = 0, \quad n \neq k \qquad (2.2.7)$$

For an analytical proof of this result, see ref. 7, where it is also shown that

$$(\vec{e}_n, \vec{e}_n) = N/2 \qquad (2.2.8)$$

By virtue of these relations, it follows that

$$B_n = (\vec{g}, \vec{e}_n) \; / \; (\vec{e}_n, \vec{e}_n) \qquad (2.2.9)$$

i.e., $$B_n = (2/N) \sum_{m=1}^{N-1} g_m \sin(mn\pi/N) \qquad (2.2.10)$$

The dual relations (2.2.6) and (2.2.10) constitute a discrete Fourier sine transform (DFST) pair. (Just as a note of historical interest it might be remarked that, whilst Lagrange derived the above results correctly, he then made an error when he proceeded to the limit of a continuous string; this led him to pronounce against Bernoulli's work.)

Finally, on taking the scalar product of each side of eqn (2.2.5) with itself the analogue of Parseval's theorem is obtained in the form

$$\sum_{m=1}^{N-1} g_m^2 = (N/2) \sum_{n=1}^{N-1} B_n^2 \qquad (2.2.11)$$

Continuing on a parallel argument to that adopted for the uniform string, consider the case where the present string has "free ends". Now, the two end particles will participate in the motion. It turns out that the result analogous to eqn (2.2.6) is

$$g_m = \sum_{n=o}^{N}{}'' A_n \cos(mn\pi/N) \qquad (2.2.12)$$

where m is in the range (0,N) and the two accents on the summation indicate that the first and last terms are each taken with a weight factor of 1/2 e.g. the first term in (2.2.12) is Ao/2. Again, there exist orthogonality relations for the discrete cosine functions analogous to eqns (2.2.7) and (2.2.8), and these can be used to show that

$$A_n = (2/N) \sum_{m=o}^{N}{}'' g_m \cos(mn\pi/N) \qquad (2.2.13)$$

Since the g's are arbitrary, eqn (2.2.12) shows that an arbitrary function defined on a discrete set of uniformly spaced points can be represented by a finite series of cosines. (The reason for the weight factors of 1/2 on the first and last terms is, broadly, that in considering the discrete case as an approximation to the continuous case, the first and last particles are associated with a sub-interval that is only half the length of that associated with an interior particle.)

Parseval's theorem here takes the form

$$\sum_{m=o}^{N}{}'' g_m^2 = (N/2) \sum_{n=o}^{N}{}'' A_n^2 \qquad (2.2.14)$$

## 2.3 The Different DFTs

### 2.3.1 The DFST

The previous discussion has shown that a function, g, defined at a discrete set of uniformly spaced points over an interval (0,L) can be represented as a finite sine series :

$$g_m = \sum_{n=1}^{N-1} B_n \sin(mn\pi/N) \qquad (2.3.1)$$

where

$$B_n = (2/N) \sum_{m=1}^{N-1} g_m \sin(mn\pi/N) \qquad (2.3.2)$$

Also, it will be recalled,

$$x_m = m\, L/N \qquad (2.3.3)$$

$$g_m = g(x_m) \qquad (2.3.4)$$

As with the infinite series, it is useful to look at the function which is represented by the finite series at points outside the basic interval (0,L). From (2.3.3), negative values of x correspond to negative values of m and, since the sine is an odd function, the series (2.3.1) returns the result

$$g_{-m} = -g_m \qquad (2.3.5)$$

Also, since

$$\sin(mn\pi/N) = \sin\{(m+2N)n\pi/N\} \qquad (2.3.6)$$

the series (2.3.1) represents a periodic function of period 2N. These results are completely analogous to the continuous case. (Note that 2N points span a length of 2L.)

### 2.3.2. The DFCT

Likewise, the point function g can be represented as a finite cosine series :

$$g_m = \sum_{n=o}^{N}{}'' A_n \cos(mn\pi/N) \qquad (2.3.7)$$

where

$$A_n = (2/N) \sum_{m=o}^{N}{}'' g_m \cos(mn\pi/N) \qquad (2.3.8)$$

The series (2.3.7) is again of period 2N but now returns a result of the form

$$g_{-m} = g_m \qquad (2.3.9)$$

i.e. the series represents an even function.

### 2.3.3. The DFTT

If it is required to represent a function g on the same set of points as in the above but now with the requirement that, outside the basic interval (0,L), the extended function is defined by the requirement that it has a period of N (or L) it is necessary to use a finite series of combined sines and cosines. This may be designated the discrete Fourier trigonometric transform (DFTT). The argument is basically parallel to the infinite series case.

The periodicity requirement can be expressed as

$$g_m = g_{m+N} \quad ; \qquad (2.3.10)$$

in particular note that

$$g_o = g_N \qquad (2.3.11)$$

so that here one can only specify N arbitrary values of g. (In the DFCT one could also specify $g_N$ arbitrarily; in the DFST, $g_o$ and $g_N$ were implicitly assumed to be zero.)

As in the continuous function case, write $g$ as the sum of an even and an odd point function :

$$g_m = E_m + O_m \tag{2.3.12}$$

where

$$E_m = (1/2)\ (g_m + g_{-m}) \tag{2.3.13}$$

$$O_m = (1/2)\ (g_m - g_{-m}) \tag{2.3.14}$$

Both $E$ and $O$ will be of period $N$; hence, these last two relations can be just as well written as

$$E_m = (1/2)\ (g_m + g_{N-m}) \tag{2.3.15}$$

$$O_m = (1/2)\ (g_m - g_{N-m}) \tag{2.3.16}$$

For the convenience it will be assumed that $N$ is an even number. (As will be seen later, in practice $N$ is generally a power of 2.) In Fig.2.3, $E_m$ and $O_m$ are shown for the point function $g_m$ derived from the continuous function

$$g(x) = \exp(x/L) - 1 \tag{2.3.17}$$

taking $N=10$. It will be noted that $E_m$ is symmetric about the midpoint $m = N/2$ and that $O_m$ is skew-symmetric about that point. These results are, of course, implied by eqns (2.3.15) and (2.3.16).

Consider first $E_m$ and initially limit attention to the range $m = o$ to $N/2$ i.e., $x = o$ to $L/2$. Since $E_m$ is an even function it can be expanded in a cosine series of the form

$$E_m = \sum_{n=o}^{N/2}{}'' A_n \cos(2mn\pi/N) \tag{2.3.18}$$

where

$$A_n = (4/N) \sum_{m=o}^{N/2}{}'' E_m \cos(2mn\pi/N) \tag{2.3.19}$$

These results follow from eqns (2.3.7) and (2.3.8) on replacing N by N/2. On substituting for $E_m$ from (2.3.15) in (2.3.19) there results

$$A_n = (2/N) \sum_{m=o}^{N/2}{}'' g_m \cos(2mn\pi/N) +$$

$$+(2/N) \sum_{m=o}^{N/2}{}'' g_{N-m} \cos(2mn\pi/N) \qquad n = 0,\cdots,N/2 \qquad (2.3.20)$$

In the second series, write

$$k = N - m \qquad (2.3.21)$$

The summation terminals for k are N and N/2, and since

$$\cos\{ 2(N-k)\, n\pi/N \} = \cos(2kn\pi/N) \qquad (2.3.22)$$

it can be seen that (2.3.20) simplifies to

$$A_n = (2/N) \sum_{m=o}^{N}{}'' g_m \cos(2mn\pi/N) \qquad n = 0,\cdots,N/2 \qquad (2.3.23)$$

Recalling (2.3.11) this finally becomes

$$A_n = (2/N) \sum_{m=o}^{N-1} g_m \cos(2mn\pi/N) \qquad (2.3.24)$$

A similar sort of calculation shows that, again for the half range m = o to N/2,

$$O_m = \sum_{n=1}^{N/2-1} B_n \sin(2mn\pi/N) \qquad (2.3.25)$$

with

$$B_n = (2/N) \sum_{m=1}^{N-1} g_m \sin(2mn\pi/N) \qquad n = 1,\cdots,N/2-1 \qquad (2.3.26)$$

Thus, using (2.3.12), it follows that for m = 0 to N/2,

$$g_m = A_o/2 + \sum_{n=1}^{N/2-1} \{ A_n \cos(2mn\pi/N) + B_n \sin(2mn\pi/N) \} + (A_{N/2}/2) \cos m\pi \qquad (2.3.27)$$

where $A_n$ and $B_n$ are given by (2.3.24) and (2.3.26).

Now consider the case of m greater than N/2 (i.e. x in the range L/2 to L). As already remarked

$$E_m = E_{N-m} \qquad (2.3.28)$$

where now (N-m) will be in the range (O,N/2). Thus, one can use eqn (2.3.18) and simply replace "m" by "N-m" ; but by virtue of a relation such as (2.3.22) it follows that (2.3.18) is also valid for the present range of m. Again,

$$O_m = -O_{N-m} \qquad (2.3.29)$$

and $O_{N-m}$ is obtained by replacing "m" by "N-m" in eqn (2.3.25). Since

$$\sin \{ 2(N-m)\, n\pi/N \} = - \sin (2mn\pi/N) \qquad (2.3.30)$$

it follows that (2.3.25) is also valid for $m > N/2$. Hence, the result (2.3.27) is valid for all m in (O,N-1).

It is most import to note, though, that whilst the suffix m , which is associated with the original variable ranges from O to N-1, the suffix n associated with the transform only ranges from O to N/2.

The validity of the expansion (2.3.27), with the associated relations (2.3.24) and (2.3.26) can be established directly using orthogonality relations for the combined set of sines and cosines.

### 2.3.4 The Complex Form of the DFT

The commonest form of DFT encountered, and that which will be used almost universally in all the following, is that obtained from the DFTT by replacing the sines and cosines by complex exponentials; in fact, this will be simply denoted by "DFT".

The DFTT was defined by

$$g_m = A_o/2 + \sum_{n=1}^{N/2-1} \{ A_n \cos(2mn\pi/N) + B_n \sin(2mn\pi/N) \} + \\ + (A_{N/2}/2) \cos m\pi \qquad (2.3.31)$$

with

$$A_n = (2/N) \sum_{m=0}^{N-1} g_m \cos(2mn\pi/N) \qquad (2.3.32)$$

$$B_n = (2/N) \sum_{m=1}^{N-1} g_m \sin(2mn\pi/N) \qquad (2.3.33)$$

On introducing the complex exponentials, (2.3.31) becomes

$$g_m = A_o/2 + \sum_{n=1}^{N/2-1} C_n \exp(2\pi imn/N) + (A_{N/2}/2) \exp im\pi + \\ + \sum_{n=1}^{N/2-1} C_n^* \exp(-2\pi imn/N) \qquad (2.3.34)$$

where

$$C_n = (A_n - iB_n)/2 \qquad (2.3.35)$$

$$C_n^* = (A_n + iB_n)/2 \qquad (2.3.36)$$

Consider the second series. Clearly

$$\exp\{ 2\pi im (N-n)/N \} = \exp(-2\pi i\, mn/N) \qquad (2.3.37)$$

and introducing a new summation index $k$ with

$$k = N-n \qquad (2.3.38)$$

the summation terminals for $k$ will be $(N/2 + 1, N-1)$

It follows from (2.3.32) and (2.3.33) that

$$A_{N-k} = A_k \tag{2.3.39}$$

$$B_{N-k} = -B_k \tag{2.3.40}$$

so that, defining for $k > N/2$, $C_k$ by

$$C_k = C_n^* = C_{N-k}^* = (A_k - i\, B_k)/2 \tag{2.3.41}$$

the second series can be written

$$\sum_{k=N/2+1}^{N-1} C_k \exp(2\pi i\, mk/N) \tag{2.3.42}$$

Since $k$ is only a dummy suffix, and since one can take

$$B_o = B_{N/2} = 0 \tag{2.3.43}$$

it follows that eqn (2.3.34) can be re-written as

$$g_m = \sum_{n=0}^{N-1} C_n \exp(2\pi i\, mn/N) \tag{2.3.44}$$

Also, since eqn (2.3.35) now can be taken to hold for all $n$, on substituting from eqns (2.3.32) and (2.3.33) into it, one obtains

$$C_n = (1/N) \sum_{m=0}^{N-1} g_m \exp(-2\pi i\, mn/N) \tag{2.3.45}$$

The two relations (2.3.44) and (2.3.45) constitute a DFT pair. The second is sometimes called "the transform" and the first "the inversion formula" in analogy with the integral case.

The validity of the above relations can be established directly and, because of their importance, this will be done. Assuming the expansion (2.3.44) exists, multiply both sides by $\exp(-2\pi i\, mk/N)$, where $k$ is in $(0,N-1)$, and sum over $m$. The result is

$$\sum_{m=0}^{N-1} g_m \exp(-2\pi i\, mk/N) = \sum_{n=0}^{N-1} C_n \{ \sum_{m=0}^{N-1} \exp(2\pi i\, m(n-k)/N) \} \tag{2.3.46}$$

The inner sum on the right hand side of (2.3.46) is just a geometric series, first term unity and common ratio $\exp(2\pi i(n-k)/N)$. Hence

$$\sum_{m=0}^{N-1} \exp(2\pi i m(n-k)/N) = \{1-\exp 2\pi i(n-k)\} \,/\, \{1-\exp(2\pi i(n-k)/N\} \tag{2.3.47}$$

i.e.,

$$\sum_{m=0}^{N-1} \exp(2\pi i m(n-k)/N) = N\,\delta_{nk} \tag{2.3.48}$$

where $\delta_{nk}$ is the Kronecker delta defined by

$$\begin{aligned} \delta_{nk} &= 0 \qquad n \neq k \\ &= 1 \qquad n = k \end{aligned} \tag{2.3.49}$$

The relation (2.3.48) may be deemed the analogue of the Dirichlet kernel for a finite series. Using (2.3.48) in (2.3.46) establishes the required result (2.3.45).

It should be noted that this last proof of the DFT is valid for complex, as well as real, $g_m$. Parseval's theorem obtained by multiplying each side of (2.3.44) by its conjugate and summing over $m$ takes the form

$$\sum_{m=0}^{N-1} g_m\, g_m^* = N \sum_{n=0}^{N-1} C_n\, C_n^* \tag{2.3.50}$$

Before passing on attention is drawn to the fact that when $g_m$ is real (as was assumed in the first derivation of the DFT given above) then,

$$C_n = C^*_{N-n} \tag{2.3.51}$$

This relation is simply (2.3.41) rewritten.

## 2.4 A Real DFT as an Interpolation Formula

One interpretation of a real DFT that is often useful is as a trigonometric interpolation formula. That this is a valid interpretation can be readily seen as follows for the case of the DFST. (The argument is quite analogous for the other real DFT's).

Consider a function $g(x)$ which is defined over the interval $(0,L)$ by the relation

$$g(x) = \sum_{n=1}^{N-1} B_n \sin(n\pi x/L) \tag{2.4.1}$$

where

$$B_n = (2/N) \sum_{m=1}^{N-1} g_m \sin(m\, n\pi/N) \tag{2.4.2}$$

The notation $g_m$ is here used to denote

$g(x_m)$ where

$$x_m = m\, L/N \qquad m=1,\cdots, N-1 \tag{2.4.3}$$

Now, the function defined by (2.4.1) exists at ALL values of x in $(0,L)$. Also, it follows from the formulae for a DFST that, at a point $x_m$ given by eqn (2.4.3), the series (2.4.1) will return the value $g_m$. Hence the two relations (2.4.1) and (2.4.2) do indeed provide a formula which interpolates the points $(x_m, g_m)$. The analogy with polynomial interpolation can be displayed by substituting from (2.4.2) into (2.4.1), and reversing the order of summation when, after some trigonometric manipulations, the result becomes

$$g(x) = \sum_{m=1}^{N-1} g_m S_m(x) \tag{2.4.4}$$

with

$$S_m(x) = \frac{(1/2N)(-1)^m \sin(m\pi/N)\sin(N\pi x/L)}{\sin\{\pi(x/L - m/N)/2\}\sin\{\pi(x/L + m/N)/2\}} \tag{2.4.5}$$

It can be readily established that

$$\begin{aligned} S_m(x_k) &= 0 \qquad k \neq m \\ S_m(x_m) &= 1 \end{aligned} \tag{2.4.6}$$

as is required for an interpolation function.

Analogous results can be established for the DFCT and the DFTT; for example, in the case of the latter it can be proved that the appropriate interpolation formula is

$$g(x) = \sum_{m=0}^{N-1} g_m T_m(x) \tag{2.4.7}$$

where

$$T_m(x) = \frac{(1/N)(-1)^m \sin(N\pi x/L)\cos\{\pi(x/L - m/N)\}}{\sin\{\pi(x/L - m/N)\}} \tag{2.4.8}$$

The $T_m$, of course, have the properties (2.4.6). For the simple case of $N = 4$, they are shown in Fig. 2.4.

It might be worth noting that the above interpolation formulae can be used, in turn, for developing schemes for numerical integration and the like.

## 2.5 A DFT as a Sampling Formula; Aliasing

### 2.5.1 General

In practice any DFT is generally used as an approximation to some function defined for continuous values of $x$ ; if this function is periodic then the DFT may be regarded as approximating an infinite Fourier series whilst if it is aperiodic the DFT may be regarded as approximating a Fourier integral. Now, a DFT exactly reproduces the values of the function it is approximating at a finite number of equally spaced points; hence, it can be regarded as a "sampling" of the function over these points. In this Section some account is given of the errors that can arise in the approximation of a continuously defined function by a DFT due to the necessarily finite distance between samples.

### 2.5.2 Sampling from a Periodic Function

Suppose $g(x)$ is a real, periodic function defined over the basic interval $(0,L)$. Then it can be represented exactly by a Fourier series as follows :

$$g(x) = \sum_{k=-\infty}^{\infty} c_k \exp(2\pi ikx/L) \qquad (2.5.1)$$

with

$$c_k = (1/L) \int_0^L g(x) \exp(-2\pi ikx/L)\, dx \qquad (2.5.2)$$

and

$$c_{-k} = c_k^* \qquad (2.5.3)$$

the asterisk denoting a complex conjugate.

On the basis of a subdivision at the $N$ points

$$x_m = mL/N \qquad m=0,\cdots N-1 \qquad (2.5.4)$$

the DFT representation of the same function is

$$g_m = \sum_{n=0}^{N-1} C_n \exp(2\pi imn/N) \qquad (2.5.5)$$

with

$$C_n = (1/N) \sum_{m=0}^{N-1} g_m \exp(-2\pi imn/N) \qquad (2.5.6)$$

and

$$C_{N-n} = C_n^* \qquad (2.5.7)$$

A relation between the C's and the c's can be obtained as follows. From (2.5.1) it can be seen that

$$g_m = \sum_{k=-\infty}^{\infty} c_k \exp(2\pi ikm/N) \qquad (2.5.8)$$

Substituting from this last into (2.5.6) and reversing the order of summation gives

$$C_n = \sum_{k=-\infty}^{\infty} c_k \{(1/N) \sum_{m=0}^{N-1} \exp(2\pi im(k-n)/N)\} \qquad (2.5.9)$$

It is convenient to consider the value of the inner bracketed sum over different ranges of $k$ separately.

(i) $k$ in $(0,N-1)$

From the basic orthogonality relation (2.3.48), the sum is just $\delta_{kn}$

(ii) $k$ in $(-N,-1)$

Write

$$k = j-N \qquad (2.5.10)$$

so $j$ is in $(0,N-1)$. Since

$$\exp(2\pi im(j-N)/N) = \exp(2\pi imj/N) \tag{2.5.11}$$

the sum is $\delta_{jn}$ or, equivalently, $\delta_{k,n-N}$ (2.5.12)

Proceeding in the same way for all such ranges and inserting the results in (2.5.9) gives

$$C_n = c_n + c_{-(N-n)} + c_{N+n} + c_{-(2N-n)} + \cdots \tag{2.5.13}$$

or

$$C_n = c_n + c^*_{N-n} + c_{N+n} + c^*_{2N-n} + \cdots \tag{2.5.14}$$

In order to interpret this relation it is a little simpler to revert to real variables. Consider first the case when $n \leq N/2$. Then

$$C_n = (A_n - iB_n)/2 \quad ; \quad c_n = (a_n - ib_n)/2 \tag{2.5.15}$$

where A's and a's are the coefficients of the cosine terms in the DFTT and the Fourier trigonometric series respectively; and likewise the B's and b's are coefficients of the sine terms. On substituting from (2.5.15) into (2.5.14) and equating real and imaginary parts the result is

$$A_n = a_n + a_{N-n} + a_{N+n} + a_{2N-n} + \cdots \tag{2.5.16}$$

$$B_n = b_n - b_{N-n} + b_{N+n} - b_{2N-n} + \cdots \tag{2.5.17}$$

Adopting, for the moment, the interpolation viewpoint for the DFTT, it can be regarded as representing an approximating function $g_s(x)$ given by

$$g_s(x) = \sum_{n=0}^{N/2_{11}} \{A_n \cos(2\pi nx/L) + B_n \sin(2\pi nx/L)\} \tag{2.5.18}$$

On the other hand, the exact function is given by

$$g(x) = \sum_{n=0}^{\infty_1} \{a_n \cos(2\pi nx/L) + b_n \sin(2\pi nx/L)\} \tag{2.5.19}$$

(In the above, the single accent on the summation sign indicates that a weight factor of 1/2 is to be assigned to the first term; the double accent has the same meaning as earlier.)

Now substitute from (2.5.16) and (2.5.17) into (2.5.18) and compare the result with (2.5.19). It can be seen that, in the sample function, the coefficients of these trigonometric terms having a given value of $n$ ($\leq N/2$) consist not only of the "true" coefficients $a_n$ and $b_n$ but also an infinite set of other coefficients having suffices out beyond N/2. This phenomenon is known as "aliasing" or "spectrum folding". The reason for the second name can be seen from Fig.2.5. If, on a strip of paper, the number $n$ and all its "aliases" are marked as in Fig.2.5(a), and if then the strip is folded at the points N/2, N, 3N/2 etc. the original number and all its aliases sit one upon the other as in Fig.2.5(b).

Consider now the circumstances under which aliasing does not occur. This will only be the case if the $a_k$ and $b_k$ are all zero (or ignorably small) for $k > N/2$. This, then, imposes a constraint on the choice of N; equivalently, since the distance, $h$, between adjacent sample points is simply

$$h = L/N \tag{2.5.20}$$

it is a constraint on $h$. It is necessary to choose $N$ sufficiently large, or $h$ sufficiently small, so that the aliasing error is small.

The above condition is usually stated in the context of frequency analysis. The last trigonometric term in (2.5.18) is $\cos(2\pi Nx/2L)$ and this represents an oscillation of frequency

$$f_{NY} = N/2L \tag{2.5.21}$$

This frequency is known as the Nyquist frequency. The requirement that there should be no terms in the series (2.5.19) with $n > N/2$ can be stated as follows. "The maximum frequency, $F$ say, in the true function must not exceed the Nyquist frequency of the sample function." This is the Nyquist criterion for the prevention of aliasing and can be written as

$$h \leq 1/(2F) \tag{2.5.22}$$

In this form, the criterion stipulates how closely together samples must be taken.

A simple example of how aliasing arises is shown in Fig.2.6. There $N = 4$ (and $L = 1$ for simplicity). The function $\cos 2\pi x$ corresponds to $n = 1$ in the above; since $N-n$ is 3, the first alias function is $\cos 6\pi x$. As seen from the Figure, these two functions coincide at the sample points and so are indistinguishable.

A physical example of aliasing is the stroboscopic effect.

Finally, it will be recalled that in all the discussion following eqn (2.5.14) it was assumed that $n \leqslant N/2$. However when $n > N/2$ (but $\leqslant N-1$) it is easy to show, by writing $n=N-k$ that instead of eqn (2.5.14) one obtains its conjugate complex. The subsequent relations for the real variables (where $n$ is always less than $N/2$) are unaltered.

### 2.5.3 Sampling from an Aperiodic Function

It has just been shown that a "band-limited" periodic function (i.e. one whose maximum frequency is bounded) can be reconstructed exactly from a number of equally spaced samples provided these samples are sufficiently closely spaced. A similar result applies to a band limited aperiodic function (Fig.2.7), where it generally goes under the title of Nyquist's theorem. An outline of the proof is given below.

If $g(x)$ is the function, then the statement that it is band-limited means that

$$G(f) = 0 \qquad |f| > F \tag{2.5.23}$$

where $F$ is considered known. Hence one can write

$$g(x) = \int_{-F}^{F} G(f) \exp(2\Pi i f x)\, df \tag{2.5.24}$$

Suppose now that $G$ is expanded as a complex Fourier series over the basic interval $(-F,F)$. The result may be written

$$G(f) = \sum_{n=-\infty}^{\infty} c_n \exp(-2\pi i n f/2F) \tag{2.5.25}$$

with

$$c_n = (1/2F) \int_{-F}^{F} G(f) \exp(2\pi inf/2F)\ df \qquad (2.5.26)$$

(Here a slightly different form of the series has been used to that given in Chapter 1.) Comparing eqns (2.5.26) and 2.5.24) it can be seen that

$$c_n = (1/2F) g(n/2F) \qquad (2.5.28)$$

Consider now a sampling of $g(x)$ done at the points (Fig.2.8)

$$x = n\,h \qquad n = 0, 1, -1, \cdots \qquad (2.5.29)$$

where

$$h = 1/2F \qquad (2.5.30)$$

and, as usual, write

$$g_n = g(nh) \qquad (2.5.31)$$

It is readily established that the sample function

$$g_s(x) = \sum_{n=-\infty}^{\infty} g_n \operatorname{sinc} 2\pi F(x-nh) \qquad (2.5.32)$$

returns the values $g_n$ at $x_n$ provided $h$ is related to $F$ by eqn (2.5.30). (This is a valid interpolation formula whatever be the significance of $F$.) The transform $G_s$ of $g_s$ can be obtained by first recalling that a rectangular pulse of height 1/2F, and extending from $-F$ to $F$, has the transform sinc $2\pi Fx$; and, so, vice-versa. In order to obtain the transform of the translated sinc functions occurring in eqn (2.5.32) the shift theorem is then used. In this way it is established that

$$G_s(f) = (1/2F) \sum_{n=-\infty}^{\infty} g_n \exp(-2\pi ifnh), \quad |f| < F$$
$$= 0 \qquad\qquad |f| > F \qquad (2.5.33)$$

As long as $h$ is chosen in accord with eqn (2.5.30), it can be seen that $G_s$ coincides with $G$. Since a function is uniquely determined by its

transform (through the inversion integral) it follows that the sample function coincides with the original one.

If $h$ is chosen smaller than is required by (2.5.30) the argument remains valid. A smaller value of $h$ may be considered to correspond to a larger value $F^1$ of the bandwidth; however, a function which has a bandwidth $F$ can certainly be deemed to have a bandwidth $F^1 > F$.

On the other hand if $h$ is chosen larger than required by (2.5.30) the argument breaks down. The transforms $G$ and $G_s$ will no longer coincide, and it can be shown that the errors involved in using $G_s$ can be interpreted in terms of aliasing.

## 2.6 Truncation and End Effects; Windows

### 2.6.1 General

Consider an aperiodic function $g(x)$ which, by definition, is given over an infinite range of $x$. When approximating this function by a DFT, one necessarily is working only with some finite range $(0,L)$ of $x$. The question is, what error is involved in this "truncation" of the true function. This will now be taken up.

It turns out that the same sort of error arises when the DFT is used to approximate a periodic function but when the length $L$ does not coincide with the period (or some integral multiple of the period.) This, of course, might have been expected on the basis of the remark made earlier that an aperiodic function can be thought of as a periodic one but with infinite period.

### 2.6.2 Truncation of Interval

If the true function under consideration is $g(x)$ then the truncated function $g_t(x)$ is given by (Fig. 2.9)

$$\begin{aligned} g_t(x) &= g(x) && 0 < x < L \\ &= 0 && \text{elsewhere} \end{aligned} \qquad (2.6.1)$$

It is clear that one can write

$$g_t(x) = g(x)\, w(x) \tag{2.6.2}$$

where w(x) is the "rectangular window" function defined by

$$\begin{aligned} w(x) &= 1 && 0 < x < L \\ &= 0 && \text{elsewhere} \end{aligned} \tag{2.6.3}$$

(The terminology, of course, arises from the fact that the truncated function can be considered as a restricted "view" of the true one through the "window".)

Since (2.6.2) is a product, the transform $G_t$ can be written as a convolution. The transform of w was shown in Section 1.5.2 to be

$$W(f) = L \exp(-\pi i f L)\, \mathrm{sinc}(\pi f L) \tag{2.6.4}$$

Hence, by the convolution theorem,

$$G_t(f) = \int_{-\infty}^{\infty} G(u)\, L \exp\{-\pi i (f-u)L\}\, \mathrm{sinc}\{\pi(f-u)L\}\, du \tag{2.6.5}$$

In order to interpret this result, consider the case where g(x) is a pure (complex) oscillation corresponding to a frequency $f_1$, say i.e.,

$$g(x) = \exp(2\pi i f_1 x) \tag{2.6.6}$$

Then,

$$G(f) = \delta(f-f_1) \tag{2.6.7}$$

and

$$G_t(f) = L \exp\{-\pi i (f-f_1)\}\ \mathrm{sinc}\{\pi(f-f_1)L\} \tag{2.6.8}$$

In particular, the magnitude of $G_t$ is given by

$$|G_t(f)| = L\, |\, \mathrm{sinc}\ \{\pi(f-f_1)\, L\}\, | \tag{2.6.9}$$

Comparing (2.6.7) and (2.6.9) it can be seen that, whereas the transform of the true function is a "spike" at the point $f_1$, the transform of the truncated function gives a "diffraction pattern" centred about $f_1$ (Fig.2.10). If one were dealing with a function that comprised the sum of two oscillations whose frequencies were close together then the two diffraction patterns would overlap; in such a case it may not be clear from a study of the transform what the true situation is. This phenomenon, where truncation effects lead to the replacement of a "spike" by a diffraction pattern, is known as "leakage".

### 2.6.3 DFT of a Function "Not Periodic in the Window"

A DFT defined over the interval (0,L) represents, outside that interval, the periodic repetitions of the original function. Here one is concerned with the case where the original function is periodic but its period (or an integral multiple of it) may not be equal to L. Simple examples of this situation are shown in Fig.2.11; there, the first example $\sin(2\pi x/L)$ does have a period L but the second $\sin(1.5\pi x/L)$ does not. In the first case the extended function is continuous whilst in the second the extended function has discontinuities at the end points. It is these discontinuities which cause trouble.

Consider the complex oscillation of frequency $f_1$ (and hence period $L_1 = 1/f_1$) given by

$$g(x) = \exp(2\pi i f_1 x) \tag{2.6.10}$$

Recalling the general formulae for a DFT, namely,

$$g_m = \sum_{n=0}^{N-1} C_n \exp(2\pi i m n/N) \tag{2.6.11}$$

and

$$C_n = (1/N) \sum_{m=0}^{N-1} g_m \exp(-2\pi i m n/N) \tag{2.6.12}$$

it is easily seen that if

$$f_1 = k/L \qquad (k \text{ integer}) \tag{2.6.13}$$

then

$$C_k = 1 \quad , \quad C_n = 0 \qquad n \neq k \tag{2.6.14}$$

However, suppose

$$f_1 = (k + p)/L \quad , \quad o < p < 1 \tag{2.6.15}$$

Now

$$g_m = \exp \{2\pi i(k+p)m/N \} \tag{2.6.16}$$

On substituting from (2.6.16) into (2.6.12), and noting that the result is a geometric series similar to eqn (2.3.46), it is found that

$$C_n = (1/N)\exp\{\pi i(k+p-n)(1-1/N) \}\sin\{\pi(k+p-n) \}/\sin\{\pi(k+p-n)/N\} \tag{2.6.17}$$

Confining attention to the magnitude of the coefficients, it can be seen that

$$|C_n| = (1/N)\left| \sin\{\pi(k+p-n)\} /\sin\{\pi(k+p-n)/N\}\right| \tag{2.6.18}$$

The ratio of the two sines occurring in (2.6.18) has a behaviour generally similar to the sinc function. In general all the $C_n$ are non-zero, although the largest coefficients are $C_k$ and $C_{k+1}$ as might be expected.

Again, this represents "leakage" compared with the "true" situation as represented by something like (2.6.14). Leakage may be considered here as the error arising from an incorrect choice of the length of the basic interval or because "the function is not periodic in the window". The evaluation of eqn (2.16.18) for the case N=16, k+p=3.5 is shown in Fig.2.12.

### 2.6.4 Reduction of Leakage by Hanning

As already seen, the problem of "leakage" is associated with end-effects which arise when the function is not periodic in the window. One way of ameliorating this problem is to use the concept of hanning already introduced in the Appendix to Chapter 1. It will be recalled that there, instead of dealing with the original function g(x), one considered a modified function p(x) say, given by

$$p(x) = g(x)\ (1-\cos 2\pi x/L)/2 \qquad (2.6.19)$$

The modified function will be periodic in the window. The discrete form of eqn (2.6.19) is, of course,

$$p_m = g_m\ (1-\cos\ 2\pi m/N)/2 \qquad (2.6.20)$$

By writing the cosine in terms of exponentials and applying the general formula for a DFT to $p_m$ it is readily found that, if $C_n$ denotes the transform of g, and $C^1_n$ denotes the transform of p, then

$$C^1_n = -C_{n-1}/4 + C_n/2 - C_{n+1}/4 \qquad (2.6.21)$$

where n is in the range (0,N-1). (Values of C for subscripts lying outside this range are obtained from periodicity considerations). The results of applying eqn (2.6.21) to eqn (2.6.17) are shown in Fig.2.12 and it can be seen that the leakage has been decreased. As with the continuous case, if the modified function is reconstructed using the hanned coefficients, the original function can be obtained from eqn (2.6.20)

Some light is thrown on hanning by considering the continuous transform of the "Hann window",

$$w(x) = (1-\cos 2\pi x/L)/2 \qquad 0 \leq x \leq L$$
$$= 0 \qquad |x| > L \qquad (2.6.22)$$

After some routine calculations it is found that

$$W(f) = \{(-1)(L/2)\exp(-\pi ifL)\sin(\pi fL)\} / \{\pi L^3 f(f-1/L)(f+1/L)\} \qquad (2.6.23)$$

The modulus of this function has been shown in Fig.2.13 along with the corresponding result for a rectangular window (where the transform, of course, was basically $\mathrm{sinc}\pi fL$). The main points are

(i) the height of the main lobe is here half that for the rectangular window,

(ii) the width of the main lobe is here twice that for the rectangular window (which is a detrimental effect as regards the resolution of close frequencies),

(iii) the maximum amplitudes in the minor lobes drop off much more rapidly than for a rectangular window and this reduces leakage. (Basically, these amplitudes are now dropping of as $1/f^3$ rather than $1/f$ for the rectangular window.)

## 2.7. The Discrete Convolution

### 2.7.1 The Convolution Theorem

It is possible to derive a convolution theorem for a DFT which is quite analogous to that for a continuous transform. Suppose that it is required to evaluate the transform $Z_n$ of a point function $z_m$ which can be considered as the product of two other point functions, $h_m$ and $y_m$, say, whose transforms $H_n$, $Y_n$ are known; the question is, to express $Z_n$ in terms of $H_n$ and $Y_n$.

It is given that

$$z_m = y_m h_m \qquad m = 0, \cdots, N-1 \tag{2.7.1}$$

where

$$y_m = \sum_j Y_j \exp(2\pi imj/N)$$
$$h_m = \sum_k H_k \exp(2\pi imk/N) \tag{2.7.2}$$

(For brevity, the summation terminals of 0 and N-1 have been omitted.) From the definition, and using (2.7.1),

$$g_n = (1/N) \sum_m y_m h_m \exp(-2\pi imn/N) \tag{2.7.3}$$

On substituting from (2.7.2) into (2.7.3), and altering the order of summation, one gets

$$g_n = (1/N) \sum_j \sum_k Y_j H_k \{\sum_m \exp(2\pi im(j+k-n)/N)\} \tag{2.7.4}$$

From the orthogonality relation, the inner sum has the value

$$N \delta_{k,n-j}$$

Hence,

$$g_n = \sum_{j=0}^{N-1} Y_j H_{n-j} \tag{2.7.5}$$

This last summation is termed a discrete convolution of the functions H and Y.

If, instead of (2.7.1), one is given that

$$g_n = Y_n H_n \tag{2.7.6}$$

then a parallel argument shows that

$$z_m = (1/N) \sum_{k=0}^{N-1} y_k h_{m-k} \tag{2.7.7}$$

### 2.7.2 Wrap-Around Errors

Consider again the discrete convolution given by

$$z_m = \sum_{k=0}^{N-1} y_k \; h_{m-k} \qquad m=0,\cdots,N-1 \qquad (2.7.8)$$

where, for brevity, the constant factor (1/N) has been omitted. First note that the suffix (m-k) takes values in the range -(N-1) to (N-1). Secondly, in all calculations using the DFT it is implicit that any function appearing is of period N. In the present case, then

$$h_{-j} = h_{N-j} \qquad (2.7.9)$$

These two points create difficulties when a discrete convolution is used as an approximation to the continuous convolution integral.

The continuous convolution to which (2.7.8) may be regarded as some sort of approximation will be of the form

$$z(x) = \int_{-\infty}^{\infty} y(\xi)\; h(x-\xi)\; d\xi \qquad (2.7.10)$$

If this is approximated by a sum using the same sub-division as employed in the discrete case, but extended at each end, this will be of the form

$$z_m = \sum_{k=-\infty}^{\infty} y_k \; h_{m-k} \qquad m=-\infty,\cdots,\infty \qquad (2.7.11)$$

where, again in the interests of brevity, a constant factor giving the length of sub-interval has been omitted.

If the infinite sum represented by (2.7.11) is to coincide with the finite one (2.7.8) for values of m in (0,N-1) i.e., "in the window", then clearly at least one of the functions appearing in the convolution must be zero over "most of the range". From here on, it is simplest to consider a concrete case. Hence, take N=8 and suppose that, whilst y is in general non-zero everywhere, h is only non-zero at the points 0,-1,-2 and -3 (i.e., only N/2 values of h are non-zero). Considering the infinite sum first, the only non-zero terms occurring are those denoted by an asterisk in Fig.2.14(a). For example

$$z_2 = y_2 h_0 + y_3 h_{-1} + y_4 h_{-2} + y_5 h_{-3} \qquad (2.7.8)$$

and

$$z_6 = y_6 h_0 + y_7 h_{-1} + y_8 h_{-2} + y_9 h_{-3} \qquad (2.7.9)$$

Turning now to the discrete case, an analogous table is shown in Fig.2.14(b). Comparison of the two tables shows that for $z_o$ to $z_4$ inclusive, the infinite and finite sums provide the same result. On the other hand, for $z_5$ to $z_7$ the two sums give different results. For example in $z_6$, as seen from eqn (2.7.9), the infinite sum has terms involving $y_8$ and $y_9$ whilst the finite sum has no such terms. However, the finite sum as well as returning the first two terms in (2.7.9), returns terms in $y_o$ and $y_1$ since it assumes that

$$h_6 = h_{-2} \quad , \quad h_5 = h_{-3} \qquad (2.7.10)$$

and these are non-zero. This type of error is known variously as "wrap-around" or "overlap" or, sometimes, as an "end-effect". Because of it, valid convolution results are only obtained for "half of the window". If one wished to obtain the missing (or, rather, presently invalid) results it would be necessary to repeat the calculation with the window differently located.

It might be noted that if a different number of non-zero values of $h$ had been used, a different number of valid convolution results would have been obtained. (Increasing the number of non-zero values of $h$ decreases the number of valid results; in practice it is usual to take N/2 values as above). A detailed account of convolution calculations has been given by Brigham (6).

## References


1 WHITTAKER,E.T. and ROBINSON,G. The Calculus of Observations. Blackie, London, 1924.

2 LANCZOS,C. Applied Analysis. Pitman, London, 1957.

3 BLACKMAN,R.B. AND TUKEY,J.W. The Measurement of Power Spectra. Dover, New York, 1958.

4 HAMMING,R.W. Numerical Methods for Scientists and Engineers. McGraw-Hill, New York, 1962.

5 HAMMING,R.W. The Frequency Approach to Numerical Analysis. pp.151-175 of "Studies in Numerical Analysis" (ed. by B.K.P. Scaife). Academic Press, New York, 1974.

6 BRIGHAM,E. ORAN The Fast Fourier Transform. Prentice-Hall, Englewood Cliffs, 1974.

7 HILDEBRAND,F.B. Methods of Applied Mathematics. Prentice-Hall, Englewood Cliffs, 1952 p.272.

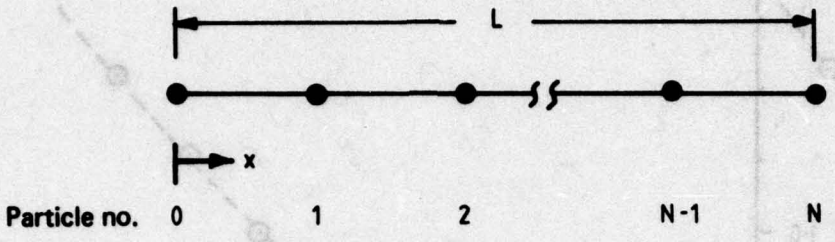


FIG. 2.1 STRING WITH (N + 1) UNIFORMLY SPACED PARTICLES

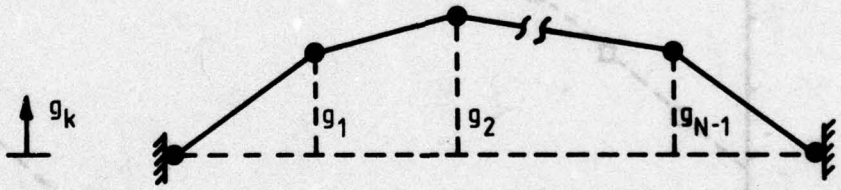


FIG. 2.2 INITIAL CONFIGURATION OF STRING WITH FIXED ENDS

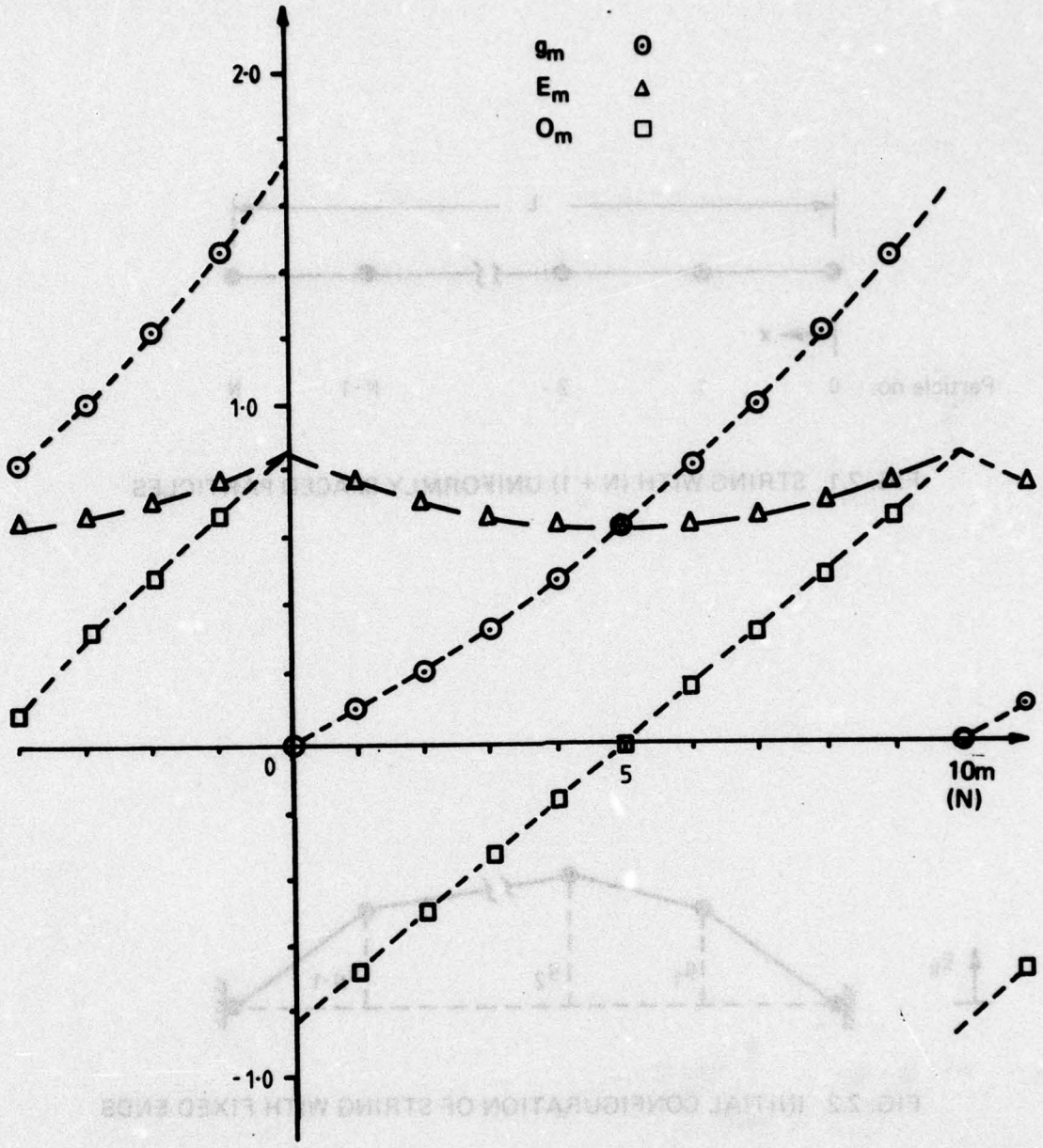


FIG. 2.3 EVEN AND ODD POINT FUNCTIONS FOR
$\begin{cases} g(x) = \exp(x/L) - 1, & 0<x<L \text{ WITH } N = 10 \\ g(x + L) = g(x) \end{cases}$

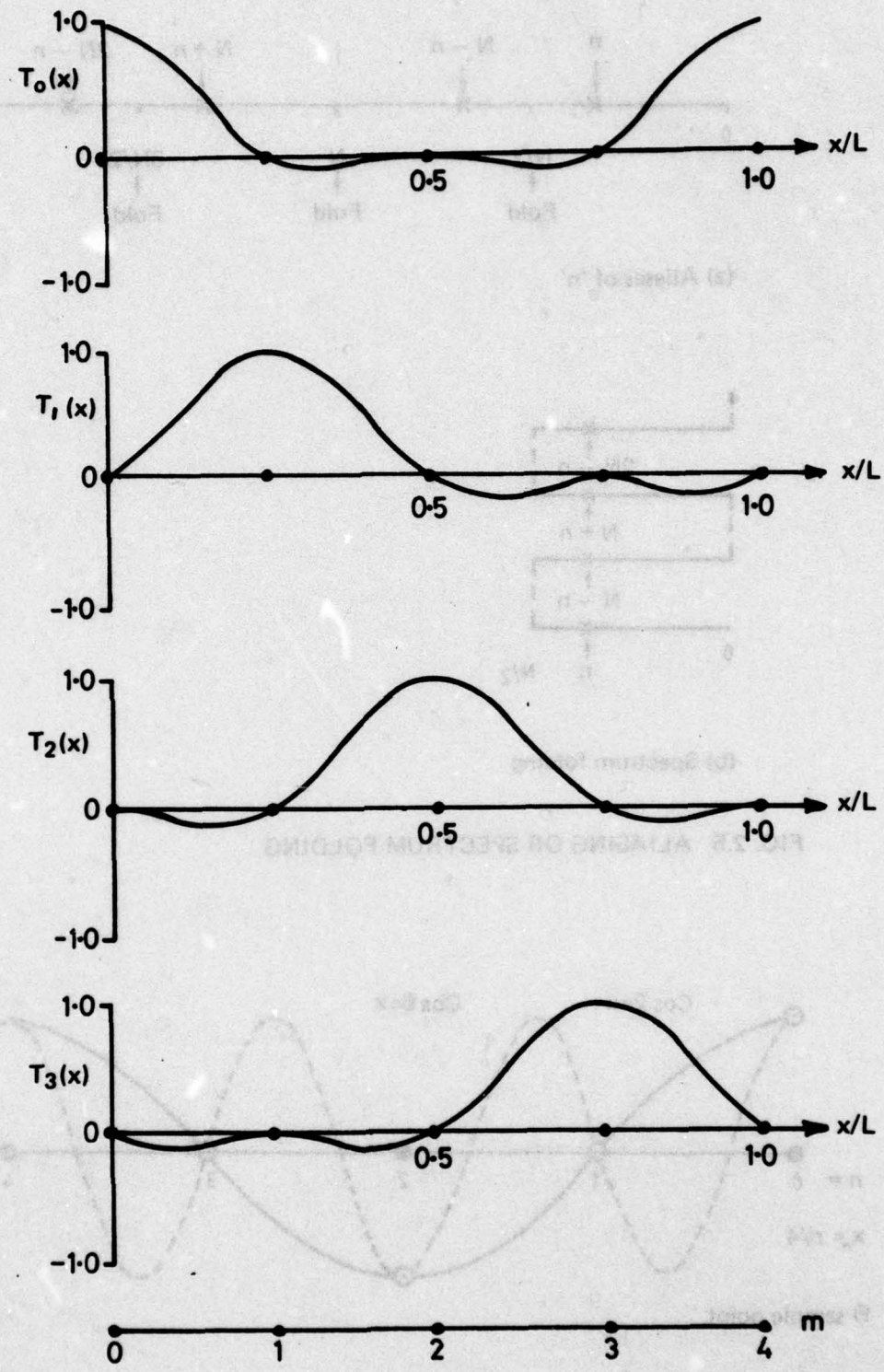


FIG. 2.4 TRIGONOMETRIC INTERPOLATION FUNCTIONS (N = 4)

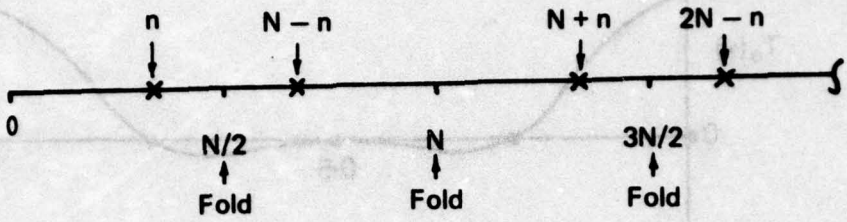


(a) Aliases of 'n'

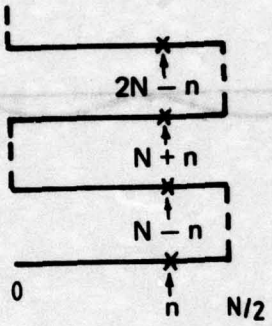


(b) Spectrum folding

FIG. 2.5 ALIASING OR SPECTRUM FOLDING

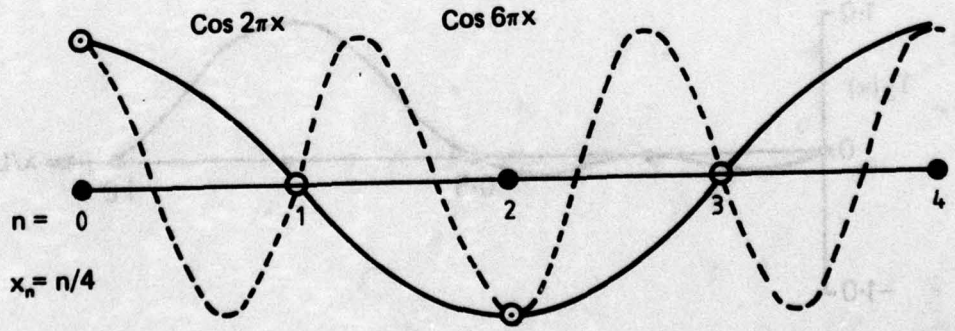


⊙ sample point

FIG. 2.6 ALIASING OF TWO COSINE FUNCTIONS

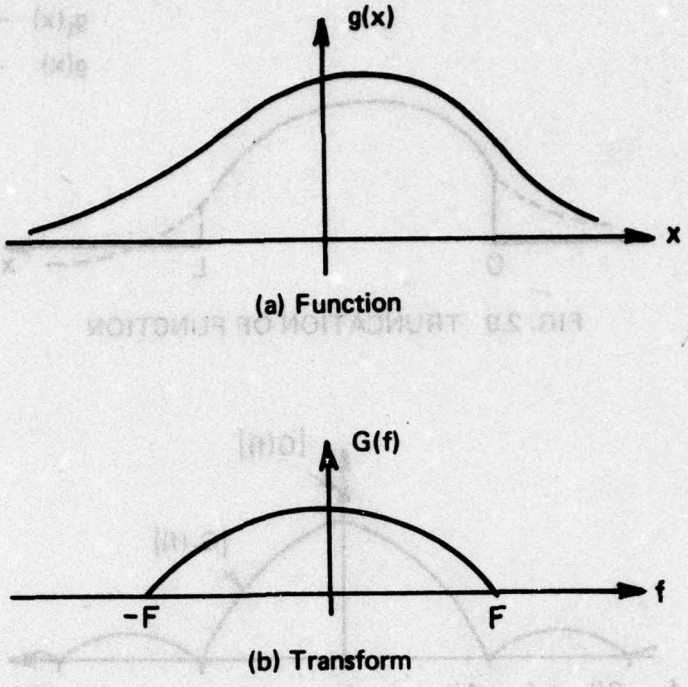


FIG. 2.7 BAND LIMITED FUNCTION

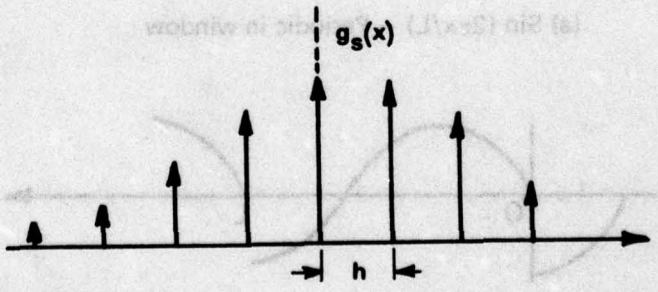


FIG. 2.8 SAMPLED FUNCTION

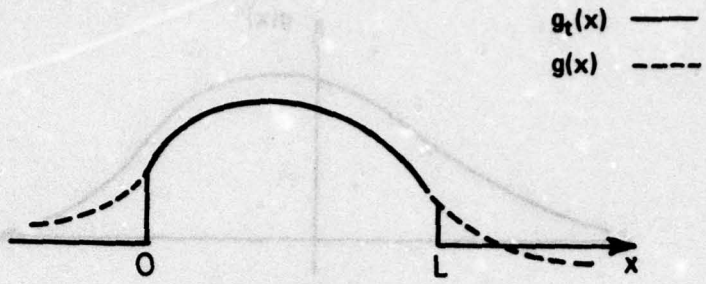


FIG. 2.9 TRUNCATION OF FUNCTION

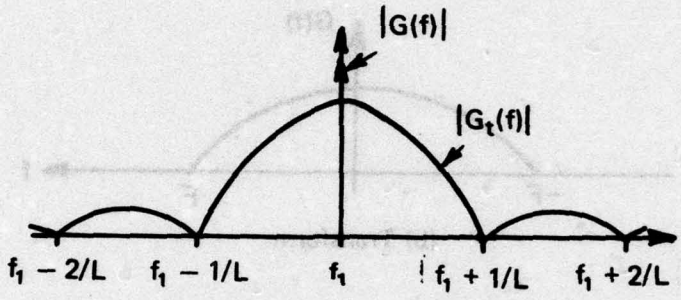


FIG. 2.10 EFFECT OF TRUNCATION ON TRANSFORM OF (COMPLEX) OSCILLATION

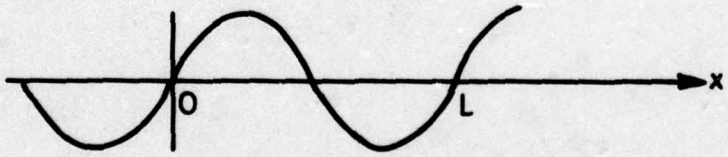


(a) Sin ($2\pi x/L$) – Periodic in window


(b) Sin ($1.5\pi x/L$) – Not periodic in window

FIG. 2.11 TRUNCATION EFFECTS FOR PERIODIC FUNCTIONS

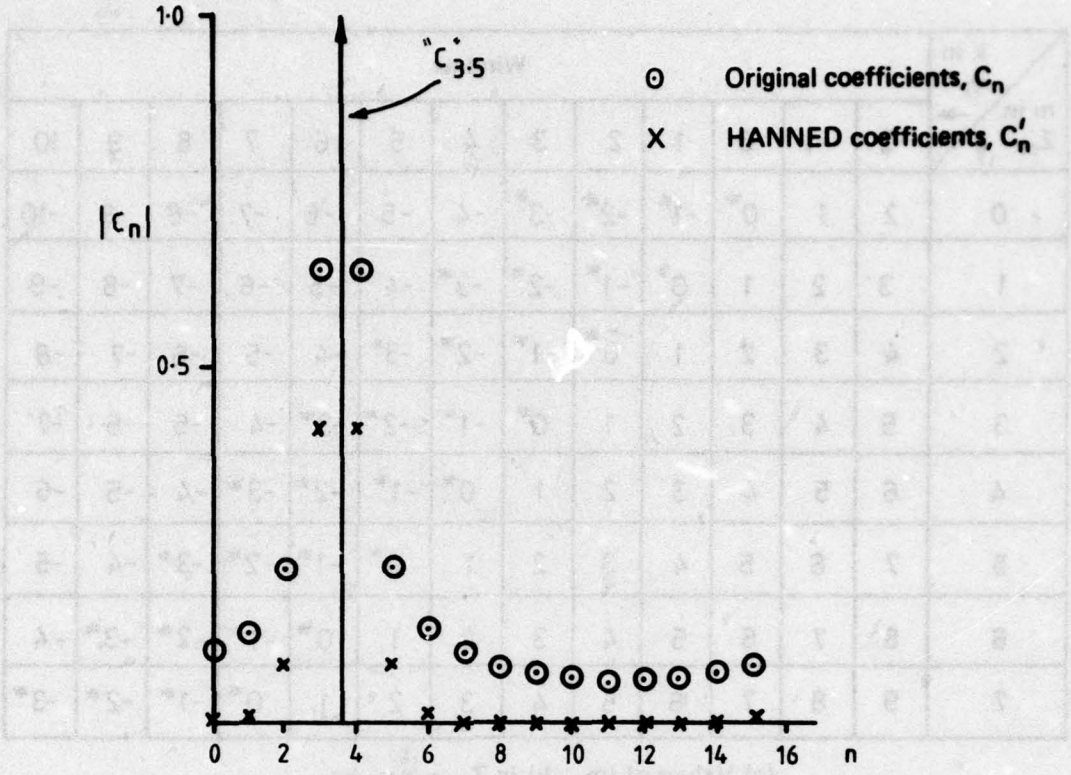


FIG. 2.12 16 POINT TRANSFORM OF EXP. $(2\pi i(3.5)x/L)$

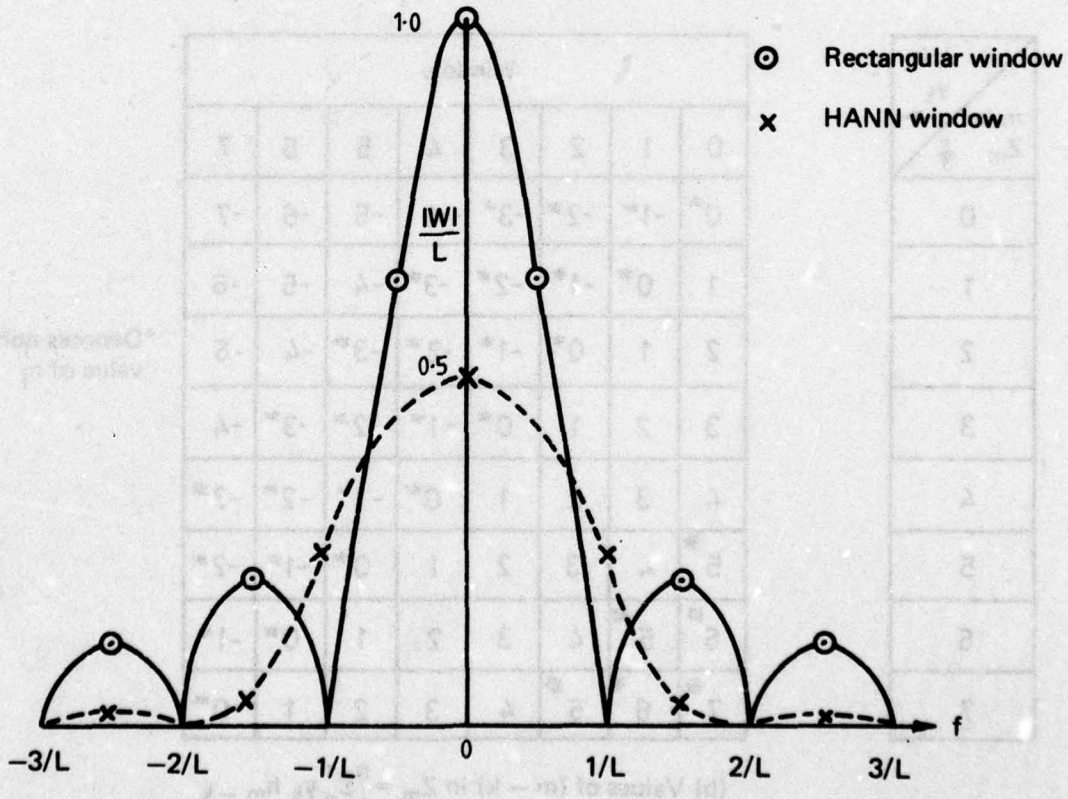


FIG. 2.13 TRANSFORMS OF RECTANGULAR AND HANN WINDOWS

| m in $Z_m$ \ k in $y_k$ | Window | | | | | | | | | | | | |
|---|---|---|---|---|---|---|---|---|---|---|---|---|---|
| | -2 | -1 | 0 | 1 | 2 | 3 | 4 | 5 | 6 | 7 | 8 | 9 | 10 |
| 0 | 2 | 1 | 0* | -1* | -2* | -3* | -4 | -5 | -6 | -7 | -8 | -9 | -10 |
| 1 | 3 | 2 | 1 | 0* | -1* | -2* | -3* | -4 | -5 | -6 | -7 | -8 | -9 |
| 2 | 4 | 3 | 2 | 1 | 0* | -1* | -2* | -3* | -4 | -5 | -6 | -7 | -8 |
| 3 | 5 | 4 | 3 | 2 | 1 | 0* | -1* | -2* | -3* | -4 | -5 | -6 | -7 |
| 4 | 6 | 5 | 4 | 3 | 2 | 1 | 0* | -1* | -2* | -3* | -4 | -5 | -6 |
| 5 | 7 | 6 | 5 | 4 | 3 | 2 | 1 | 0* | -1* | -2* | -3* | -4 | -5 |
| 6 | 8 | 7 | 6 | 5 | 4 | 3 | 2 | 1 | 0* | -1* | -2* | -3* | -4 |
| 7 | 9 | 8 | 7 | 6 | 5 | 4 | 3 | 2 | 1 | 0* | -1* | -2* | -3* |

(a) Values of $(m - k)$ in $Z_m = \sum_{k=-\infty}^{\infty} y_k \, h_{m-k}$

| m in $Z_m$ \ k in $y_k$ | Window | | | | | | | |
|---|---|---|---|---|---|---|---|---|
| | 0 | 1 | 2 | 3 | 4 | 5 | 6 | 7 |
| 0 | 0* | -1* | -2* | -3* | -4 | -5 | -6 | -7 |
| 1 | 1 | 0* | -1* | -2* | -3* | -4 | -5 | -6 |
| 2 | 2 | 1 | 0* | -1* | -2* | -3* | -4 | -5 |
| 3 | 3 | 2 | 1 | 0* | -1* | -2* | -3* | -4 |
| 4 | 4 | 3 | 2 | 1 | 0* | -1* | -2* | -3* |
| 5 | 5* | 4 | 3 | 2 | 1 | 0* | -1* | -2* |
| 6 | 6* | 5* | 4 | 3 | 2 | 1 | 0* | -1* |
| 7 | 7* | 6* | 5* | 4 | 3 | 2 | 1 | 0* |

*Denotes non-zero value of $h_j$

(b) Values of $(m - k)$ in $Z_m = \sum_{k=0}^{N-1} y_k \, h_{m-k}$

FIG. 2.14 WRAP-AROUND ERROR IN CONVOLUTION

# CHAPTER 3 : THE FAST FOURIER TRANSFORM ALGORITHM

## 3.1 Introduction

The DFT has been defined previously as:

$$G_n = G(f_n) = (1/N) \sum_{m=o}^{N-1} g_m \exp(-2\pi imn/N) \qquad (3.1.1)$$

where $n = 0, 1, \cdots N-1$

with an inverse given by:

$$g_m = g(x_m) = \sum_{n=o}^{N-1} G_n \exp(+2\pi imn/N) \qquad (3.1.2)$$

where $m = 0, 1, \cdots N-1$.

Using the common notation

$$W_N = \exp(-2\pi i/N) = \cos(2\pi/N) - i \sin(2\pi/N) \qquad (3.1.3)$$

for the N th root of unity eqns (3.1.1) and (3.1.2) may be written concisely as follows :

$$G_n = (1/N) \sum_{m=o}^{N-1} W_N^{mn} g_m \qquad n=0,1\cdots N-1 \qquad (3.1.4)$$

and

$$g_m = \sum_{n=o}^{N-1} W_N^{-mn} G_n \qquad m=0,1,\cdots N-1 \qquad (3.1.5)$$

Clearly any method for calculating the transform may easily be adapted to calculate the inverse by using the complex conjugate of the exponential terms $W_N^{nm}$ and deleting the factor 1/N. In the following discussion of computational procedures it is therefore sufficient to consider only the forward transform without the factor 1/N i.e.,

$$G_n = \sum_{m=o}^{N-1} W_N^{mn} gm \qquad n=0,1,\cdots N-1 \qquad (3.1.6)$$

In many cases it is convenient to write the N equations (3.1.6) in matrix notation :

$$\vec{G} = M_N \vec{g} \tag{3.1.7}$$

where

$$M_N = \begin{bmatrix} W^0 & W^0 & W^0 & \cdots & W^0 \\ W^0 & W^1 & W^2 & \cdots & W^{N-1} \\ W^0 & W^2 & W^4 & \cdots & W^{2(N-1)} \\ . & . & . & \cdots & . \\ W^0 & W^{N-1} & W^{2(N-1)} & \cdots & W^{(N-1)(N-1)} \end{bmatrix} \tag{3.1.8}$$

The matrix representation shows that the direct calculation of the DFT (or its inverse) requires the multiplication of the N-element complex vector $\vec{g}$ by the N x N complex matrix $M_N$ to form the N complex elements of the transform vector $\vec{G}$. Assuming that the $N^2$ elements of the matrix $M_N$ have been calculated once and for all, the complete matrix multiplication requires $N^2$ operations of complex multiplication and addition. In typical practical problems, N may be of the order of $10^3$ and so $N^2$ is of the order of $10^6$. In the past, the usefulness of the DFT as a numerical tool was limited by the fact that the computation time was proportional to $N^2$.

The publication of the paper by Cooley and Tukey (1) revolutionised the approach to wave-form analysis (i.e. DFT calculations). They showed that if the number of samples, N, is a composite number having factors $r_1, r_2, \cdots r_k$, the number of operations required to calculate the DFT may be reduced from

$$N^2 = N (r_1 . r_2 . r_3 \ldots r_k)$$

to

$$N(r_1 + r_2 + r_3 + \ldots + r_k)$$

Their method, and similar later ones, for calculating the DFT have become known as the Fast Fourier Transform (FFT). It should be emphasized again that the FFT is simply an algorithm for calculating the DFT; the numerical result is the same as if the full matrix multiplication had been performed.

The advantage of the FFT is a dramatic reduction in computational time achieved by use of an algorithm which is an efficient rearrangement of the process used for matrix multiplication. A second, but less important advantage, is a possible saving in computer memory by the use of "in-place" computation. This last aspect will be discussed in a subsequent chapter.

Here, the basic two factor algorithm will be derived using summation notation. Most references use this notation, presumably because of the origin of the DFT as an approximation to the classical Fourier integral. However, as the matrix notation has special advantages, the FFT algorithm will be described in this form as well. Finally, a description of multifactor FFT's will be given.

## 3.2 The Basic Fast Fourier Transform Algorithm

The FFT is an algorithm for computing the $N$ elements $G(n)$ in (3.1.6) using less than $N^2$ operations. The method is only applicable when $N$ is non-prime.

The algorithm for $N$ even, which exploits the factor 2, is often given as an introductory example, e.g. refs.(2) and (3), since it may readily be derived from first principles. As this approach rather obscures the generality of the FFT, the algorithm derived below is for $N$ having two arbitrary factors.

If $N = r_1 . r_2$ then the $N$ elements $g_m$

of the original function and the $N$ elements $G_n$ of the transform may be grouped as either $r_1$ groups of $r_2$ elements or as $r_2$ groups of $r_1$ elements. The basis of the FFT algorithm is to group the elements of the original function by the first method and the elements of the transform

by the second. It will be convenient to consider the successive groups of the elements $g_m$ as being the columns of an $r_2 \times r_1$ array and the successive groups of the elements $G_n$ as the columns of an $r_1 \times r_2$ array.

With this convention the index $m$ ($m = 0, 1, \cdots N-1$) which tags the original elements is written

$$m = m_o + m_1 r_2 \tag{3.2.1}$$

where "row" index $m_o = 0, 1, \ldots r_2 - 1$

and "column" index $m_1 = 0, 1, \cdots r_1 - 1$

Hence one can write

$$g(m) = g(m_1, m_o)$$

Analogously, the index $n$ which tags the elements of the transform is written

$$n = n_o + n_1 r_1 \tag{3.2.2}$$

where "column" index $n_o = 0, 1, \ldots r_1 - 1$

and "row" index $n_1 = 0, 1, \cdots r_2 - 1$

Thus, $G(n) = G(n_1, n_o)$

For example, if

$N = 12 = 4 \times 3$, the two groupings are as shown in Fig. 3.1.

Using the above representations of the indices $m$ and $n$, the exponent $n m$ in eqn (3.1.6) becomes

$$n.m = (n_o + n_1 r_1)(m_o + m_1 r_2)$$

$$= r_1 n_1 m_o + n_o m_o + r_2 n_o m_1 + r_1 r_2 n_1 m_1$$

Thus, the factor $W_N^{nm}$ of eqn (3.1.6) becomes

$$W_N^{nm} = W_N^{r_1 n_1 m_o} \; W_N^{n_o m_o} \; W_N^{r_2 n_o m_1} \qquad (3.2.3)$$

since

$$W_N^{r_1 r_2 n_1 m_1} = (W_N^N)^{n_1 m_1} = 1$$

With the above notation the expression (3.1.6) for the DFT becomes

$$G(n_1, n_o) = \sum_{m_o=0}^{r_2-1} \sum_{m_1=0}^{r_1-1} W_N^{r_1 n_1 m_o} \; W_N^{n_o m_o} \; W_N^{r_2 n_o m_1} \; g(m_1, m_o) \qquad (3.2.4)$$

with $n_1 = 0, 1, \ldots r_2-1$

$n_o = 0, 1, \ldots r_1-1$

This double sum (3.2.4) is the basis of the FFT. However, there are two similar but quite distinct forms that the sum may take.

Firstly, using the fact that

$$W_N^{r_2} = \exp(-2\pi i r_2/r_1 r_2) = \exp(-2\pi i/r_1) = W_{r_1}$$

the double sum may be reorganised as

$$G(n_1, n_o) = \sum_{m_o=0}^{r_2-1} W_N^{(n_o+n_1 r_1)m_o} \left\{ \sum_{m_1=0}^{r_1-1} W_{r_1}^{n_o m_1} \; g(m_1, m_o) \right\} \qquad (3.2.5)$$

with $n_1 = 0, 1, \ldots r_2-1$

$$n_o = 0, 1, \cdots r_1 - 1$$

This relation is the essence of the Cooley-Tukey version of the FFT algorithm, also referred to as "decimation in time". The inner sums which depend only on $m_o$ and $n_o$, and are performed first are :

$$\mathcal{G}(n_o, m_o) = \sum_{m_1=0}^{r_1-1} W_{r_1}^{n_o m_1} g(m_1, m_o) \qquad (3.2.6)$$

with

$$n_o = 0, 1, \cdots r_1 - 1$$

Each of these expressions is precisely an $r_1$-point DFT of each of the $r_2$ rows of $g$ in Fig.3.1. Since each $r_1$-point DFT requires $r_1^2$ operations, the total number of operations required to form all the inner sums is $r_2 . r_1^2 = N r_1$. For each value of $n = n_o + n_1 r_1$ in (3.2.5) the outer sum is :

$$G(n_1, n_o) = \sum_{m_o=0}^{r_2-1} W_N^{nm_o} \mathcal{G}(n_o, m_o) \qquad (3.2.7)$$

with

$$n = 0, 1 \ldots N-1$$

Each sum is a weighted sum of $r_2$ of the $N$ results so far formed. The outer sums thus involve $r_2$ operations carried out $N$ times (one for each value of $n$). The grand total of operations is therefore only $N(r_1 + r_2)$ rather than $N^2 = N r_1 r_2$ for the direct evaluation of the N-point DFT.

The two operations specified by (3.2.6) and (3.2.7) may be described by the use of a signal flow graph. The Cooley-Tukey algorithm for $N = 12 = 4 \times 3$ is shown in Fig.3.2.

The alternative rearrangement of the double sum (3.2.4) is

$$G(n_1, n_o) = \sum_{m_o=0}^{r_2-1} W_{r_2}^{m_o n_1} \left\{ \sum_{m_1=0}^{r_1-1} W_N^{(m_o + m_1 r_1) n_o} g(m_1, m_o) \right\} \qquad (3.2.8)$$

with $n_1 = 0,1, \cdots, r_2 - 1$

$n_o = 0,1, \cdots, r_1 - 1$

This relation is the essence of the Sande-Tukey version of the FFT algorithm, also referred to as "decimation in frequency" (4). In this version the weighted sums of the N elements of g taken $r_1$ at a time are formed first as specified by the inner bracket. This requires $Nr_1$ operations. The outer sums are then $r_2$-point DFT's of which there are $r_1$ in all. The grand total of operations is again $N(r_1+r_2)$. The Sande-Tukey algorithm for N=12=3X4 is shown in the signal flow graph of Fig.3.3.

At first sight the two versions may appear to differ merely in the interchange of the roles of $r_1$ and $r_2$. However, also involved is an interchange of the roles of m and n. In fact, the Sande-Tukey version is the inverse of the Cooley-Tukey version. This inverse relationship is the reasoning behind the terms "decimation in time" and "decimation in frequency". In the Cooley-Tukey version, the $r_1$-point DFT's of the inner sum are performed on elements of the original or "time" function spaced $r_2$ apart, whereas in the Sande-Tukey version the results of the final $r_2$-point transforms generate elements of the transformed or "frequency" function spaced $r_1$ apart. This inverse relationship will be discussed further in a later section. However, at this stage it is important to emphasize that, in the present context, the two versions are equally efficient.

## 3.3 Matrix Description of FFT Algorithm

In the previous section the basic two-factor algorithm was derived using summation notation. However matrix notation, although not used by most authors in this field, has several advantages. For example, any operations involved are more apparent and manipulation of the matrix factors is easy. For this reason a matrix description of the FFT algorithm will be given below.

The summation forms of the FFT developed in Section 3.2 may be concisely expressed as a factorisation of the matrix $M_N$. The elements of

$M_N$ are all powers of a primitive N th root of unity, so each of the elements must be one of the N such roots. Hence, among the $N^2$ elements there are only N distinct values. When N is not a prime number repetitive patterns of elements appear in the matrix $M_N$. These allow the factorisation of $M_N$ into a product of several sparse matrices. If trivial operations are not performed, the series of matrix multiplications specified by the factors is more efficient than the single matrix multiplication.

The key to the Cooley-Tukey FFT factorisation lies in the rearrangement of the sequence of input elements. This rearrangement or permutation is achieved by hypothetically entering the elements of g, column by column, in an $r_2 \times r_1$ array and then extracting them, row by row, to form the input data sequence. In matrix notation this re-ordering or "shuffling" of the input data corresponds to a multiplication by the permutation matrix $P = P_{r_1,r_2}$. The matrix $P_{4,3}$ and its effect on g are both shown in Fig.3.4. Referring back to eqn(3.1.7) the matrix $M_N$ operates on the elements of the vector g in numerical order to form the elements of the vector G, also in numerical order. If the elements of g are permuted by P then the columns of $M_N$ in (3.1.8) must be similarly permuted by post-multiplication by $P^{-1}$ to maintain the correct result, i.e.

$$\vec{G} = (MP^{-1})\ P\ \vec{g} \qquad (3.3.1)$$

When the permutation of the columns of $M_N$ has been performed, and the resulting permuted matrix $M'_N = M_N P^{-1}$ is partitioned into $r_1 \times r_1$ submatrices the factorisation of $M'_m$ becomes more apparent.

The factorisation may be carried out in general terms but it is more informative to use a concrete example. The steps in the factorisation of $M_6$ for N = 6 = 3 X 2 are shown in Fig.3.5. (For simplicity only the exponents of $W_6$ have been shown.) The steps involved are :-

a) write the matrix in terms of $W_6^{mn}$,

b) reduce the exponents modulo 6 ,

c) shuffle the columns according to the permutation $P_{3,2}$ and partition the matrix ,

d) factorise the individual elements according to eqn (3.2.3) ,

(At this stage note that

(i) within each partition, the first factor of each element is the same,

(ii) the last factor in each element is the same at corresponding positions in each partition,

(iii) the middle factor of each element is the same in each row within each partition, and is also the same as those in the corresponding rows of all other partitions in the same column.)

e) factorise the individual partitions and hence the complete matrix. (This operation is possible because of the repetitions specified above).

The right hand factor is a replication of the matrix $M_3$ along the diagonal partitions. Normally $M_3$ would be written in terms of $W_3$ but here it is expressed in terms of $W_6$ where $W_3 = W_6^2$. Consequently each element has been raised to the second power i.e., its exponent has been multiplied by 2.

The middle factor is a diagonal matrix whose $(3m_o + n_o)$ th element is given by $W_6^{n_o m_o}$ where $n_o = 0,1,2$ and $m_o = 0,1$

The left hand factor contains the elements of the matrix $M_2$ repeated along the diagonal in each partition. Again $M_2$ would normally be written in terms of $W_2$ but, analogously to the first case, each element is raised to the third power since it is written in terms of $W_6$.

Pease (5) has suggested the use of the Kronecker, or direct, products of matrices to represent the replications shown in the right and left factors. The Kronecker product of a matrix A and the 3 x 3 matrix B is

$$A \times B = \begin{bmatrix} b_{11}A & b_{12}A & b_{13}A \\ b_{21}A & b_{22}A & b_{23}A \\ b_{31}A & b_{32}A & b_{33}A \end{bmatrix} \qquad (3.3.2)$$

With this notation the two forms of replication expressed by the right and left factors in Fig.3.5 may be simply expressed. The left factor is $I_3 \times M_2$ and the right factor is $M_3 \times I_2$. Thus the Cooley-Tukey version of the 6-point transform may be written as

$$\vec{G} = M_6 \vec{g}$$

$$= (I_3 \times M_2)\, D_{3,2} (M_3 \times I_2)\, P_{3,2} \vec{g} \qquad (3.3.3)$$

The general case where $N = r_1 . r_2$ may be written with the same notation as

$$\vec{G} = M_{r_1 r_2} \vec{g}$$

$$= (I_{r_1} \times M_{r_2})\, D_{r_1,r_2} (M_{r_1} \times I_{r_2})\, P_{r_1,r_2} \vec{g} \qquad (3.3.4)$$

where the $(n_o + m_o r_1)$th element of the diagonal matrix $D_{r_1,r_2}$ is given by $W_N^{m_o n_o}$ where

$$n_o = 0,1,\cdots r_1 - 1$$

$$m_o = 0,1,\cdots r_2 - 1$$

The above matrix description has been developed for the Cooley-Tukey FFT. The Sande-Tukey version may be derived in a similar manner but in that version the rows rather than the columns of $M_N$ are permuted by pre-multiplication by $P^{-1}_{r_1 r_2} = P_{r_2 r_1}$. This has the effect of producing the same matrix factors but written in the reverse order, viz.

$$\vec{G} = P_{r_2 r_1} (M_{r_1} \times I_{r_2}) D_{r_1,r_2} (I_{r_1} \times M_{r_2})\, \vec{g} \qquad (3.3.5)$$

The inverse of (3.3.5) is given by

$$\vec{g} = (I_{r_1} \times M_{r_2})^{-1}\, D^{-1}_{r_1,r_2} (M_{r_1} \times I_{r_2})^{-1}\, P^{-1}_{r_2,r_1} \vec{G}$$

Using the property of the Kronecker products that

$$(A \times B)^{-1} = A^{-1} \times B^{-1}$$

this last becomes

$$\vec{g} = (I_{r_1} \times M_{r_2}^{-1})\, D_{r_1,r_2}^{-1}\, (M_{r_1}^{-1} \times I_{r_2})\, P_{r_1,r_2}\, \vec{G} \qquad (3.3.6)$$

When this equation is compared with the Cooley-Tukey version (3.3.4) the terms "decimation in time" and "decimation in frequency" become clear.

In this description of the FFT algorithm, matrix notation has been used. As has been demonstrated, the advantages of this notation are that it is compact and that it is completely general. Furthermore, it allows reorganisations of the basic algorithm to be developed by making use of the properties of ordinary and Kronecker matrices.

In this section the basic Cooley-Tukey algorithm has been described in matrix notation using the Kronecker matrix product. This is equivalent to the more commonly quoted summation form. The matrix approach has also been used to reveal the inverse relationship between the Cooley-Tukey and Sande-Tukey versions of the FFT algorithm.

*Only the two-factor* algorithm has been described at this stage. This is fundamental to the more useful multi-factor FFT which is treated in the next Section. The matrix approach will prove especially advantageous there, allowing the iterative development for more than two factors to be written explicitly.

## 3.4 Multi-factor FFT Algorithm

The use of the matrix notation facilitates the development of algorithms when N has many factors. In this Section an expression is derived for the multi-factor Cooley-Tukey algorithm. This expression is then used to derive the algorithm when all the factors are equal to a general radix r. The two most important cases of radix-2 and radix-4 are then discussed.

In what follows

$$N = r_1.r_2.r_3 \ldots r_k$$

It is therefore more convenient to consider the initial factorisation in terms of the factors $r_1$ and $N/r_1$. With this change in notation the two-factor algorithm (3.3.4) may be rewritten by direct substitution as:

$$\vec{G} = (I_{N/r_1} \times M_{r_1})\, D_{N/r_1,r_1}\, (M_{N/r_1} \times I_{r_1})\, P_{N/r_1,r_1}\, \vec{g} \qquad (3.4.1)$$

Since $N/r_1$ is also non-prime it may be written as

$$N/r_1 = (r_3.r_4 \ldots r_k).r_2 = \{N/(r_1.r_2)\}.r_2$$

The factor $M_{N/r_1}$ in (3.4.1) may thus be factorised in a similar manner and becomes

$$M_{N/r_1} = (I_{N/r_1r_2} \times M_{r_2})\, D_{N/r_1r_2,r_2}\, (M_{N/r_1r_2} \times I_{r_2})\, P_{N/r_1r_2,r_2} \qquad (3.4.2)$$

The Kronecker product has the following properties :

$$(A\ B\ C) \times I = (A \times I)\ (B \times I)(C \times I)$$

and $$I_a \times I_b = I_{ab}$$

Using these with eqn (3.4.2) it follows that

$$M_{N/r_1} \times I_{r_1} = (I_{N/r_1r_2} \times M_{r_2} \times I_{r_1})(D_{N/r_1r_2,r_2} \times I_{r_1}).$$
$$(M_{N/r_1r_2} \times I_{r_1r_2})(P_{N/r_1r_2,r_2} \times I_{r_1}) \qquad (3.4.3)$$

When the expression (3.4.3) is substituted into (3.4.1) the FFT becomes

$$\vec{G} = (I_{N/r_1} \times M_{r_1})\, D_{N/r_1,r_1}\,.$$
$$(I_{N/r_1r_2} \times M_{r_2} \times I_{r_1})(D_{N/r_1r_2,r_2} \times I_{r_1}).$$

$$(M_{N/r_1r_2} \times I_{r_1r_2}).$$

$$(P_{N/r_1r_2,r_2} \times I_{r_1}) P_{N/r_1,r_1} \vec{g} \qquad (3.4.4)$$

This process of substitution may be continued until all the factors of $N$ (and the authors) are exhausted. As an example, take

$$N = 12 = 3 \times 2 \times 2$$

The expression (3.4.4) then becomes

$$\vec{G} = (I_4 \times M_3) D_{4,3}.$$

$$(I_2 \times M_2 \times I_3)(D_{2,2} \times I_3).$$

$$(M_2 \times I_6).$$

$$(P_{2,2} \times I_3) P_{4,3} \vec{g} \qquad (3.4.5)$$

If all the factors of $N$ are equal the complete factorisation is known as the radix-$r$ FFT. Using the three-factor expression (3.4.4) as a model the radix-$r$ transform (where $N = r^k$) may be written concisely as

$$\vec{G} = \{ \prod_{p=k} (I_{r^{p-1}} \times M_r \times I_{N/r^p})(D_{r^{p-1},r} \times I_{N/r^p})\}.$$

$$. A_{N,r} \vec{g} \qquad (3.4.6)$$

Here,

(i) The permutation matrix $A_{N,r}$ is given by

$$A_{N,r} = (P_{1,r} \times I_{N/r})(P_{r,r} \times I_{N/r^2}) \ldots (P_{N/r^2,r} \times I_r) P_{N/r,r}$$

(3.4.7)

This permutation reorders the input elements into the sequence defined by reversing the digits of their original sequence position expressed as a number to base $r$.

(ii) The second factor in the continued product of eqn (3.4.6) is always diagonal and consists of the $r^p \times r^p$ matrix $D_{r^{p-1},r}$ repeated $N/r^p$ times along the diagonal. As before, the $(n_o + m_o N/r^{p-1})$th element of $D_{N/r^{p-1},r}$ is $(W_{r^p})^{m_o n_o}$ where

$$n_o = 0,1, \cdots N/r^{p-1}-1$$

$$m_o = 0,1, \cdots r-1$$

The only operations involved in each pass or stage of a radix-r FFT are the weighting of the input vector to each pass by a diagonal matrix and the calculation of N/r r-point DFT's. The only differences from pass to pass are the values of the weights and the selection of the r elements upon which to perform the r-point DFT's.

The formal number of operations required for a radix-r FFT ($N=r^k$) is

$$Nrk = Nr \log_r N$$

The improvement factor over direct evaluation of the DFT is

$$N^2/(Nr \log_r N) = (N/\log N)(\log r/r)$$

and is thus proportional to log r/r. The values of this function are shown in the following table :

| r | log r/r |
|---|---|
| 2 | 0.347 |
| 3 | 0.366 |
| 4 | 0.347 |
| 5 | 0.322 |
| 6 | 0.299 |
| 7 | 0.278 |
| 8 | 0.260 |
| 9 | 0.244 |
| 10 | 0.230 |

The function has a maximum for r=3 with the values for r=2 and r=4 (which are equal) being slightly smaller. For increasing values of r the function decreases slowly. This suggests that radix-3 is formally the most efficient. However, the radices 2 and 4 provide significant

simplification to the addressing when the FFT is performed on a binary computer.

More importantly, however, both radix-2 and radix-4 algorithms may be considerably simplified by taking advantage of the 2 and 4 fold symmetries of the sine and cosine functions.

As stated previously a radix-r FFT involves many r-point DFT's at each pass. The advantage of radix-2 and radix-4 algorithms lies in the fact that both a 2-point and a 4-point DFT may be performed using only additions and subtractions - no multiplications are required. This can be seen as follows :-

$$M_2 = \begin{bmatrix} W_2^0 & W_2^0 \\ W_2^0 & W_2^1 \end{bmatrix} = \begin{bmatrix} 1 & 1 \\ 1 & -1 \end{bmatrix} \qquad (3.4.8)$$

since $W_2 = \exp(-2\pi i/2) = -1$

Furthermore,

$$M_4 = \begin{bmatrix} W_4^0 & W_4^0 & W_4^0 & W_4^0 \\ W_4^0 & W_4^1 & W_4^2 & W_4^3 \\ W_4^0 & W_4^2 & W_4^4 & W_4^6 \\ W_4^0 & W_4^3 & W_4^6 & W_4^9 \end{bmatrix} = \begin{bmatrix} 1 & 1 & 1 & 1 \\ 1 & -i & -1 & i \\ 1 & -1 & 1 & -1 \\ 1 & i & -1 & -i \end{bmatrix} \qquad (3.4.9)$$

since $W_4 = \exp(-2\pi i/4) = -i$

As no multiplications are involved in the r-point DFT's, the only multiplications required are the initial weighting of the input vector to each pass by the diagonal matrix. These weightings or phase changes to the input elements to each pass have been called "twiddling" the data. Consequently the radix-2 and radix-4 algorithms are known as the twiddle factor algorithms.

AD-A062 156 AERONAUTICAL RESEARCH LABS MELBOURNE (AUSTRALIA) F/G 12/1
LECTURES ON MODERN FOURIER TRANSFORM METHODS.(U)
FEB 78 B C HOSKIN

UNCLASSIFIED ARL/STRUC-TM-276 NL

2 OF 3
AD A062156

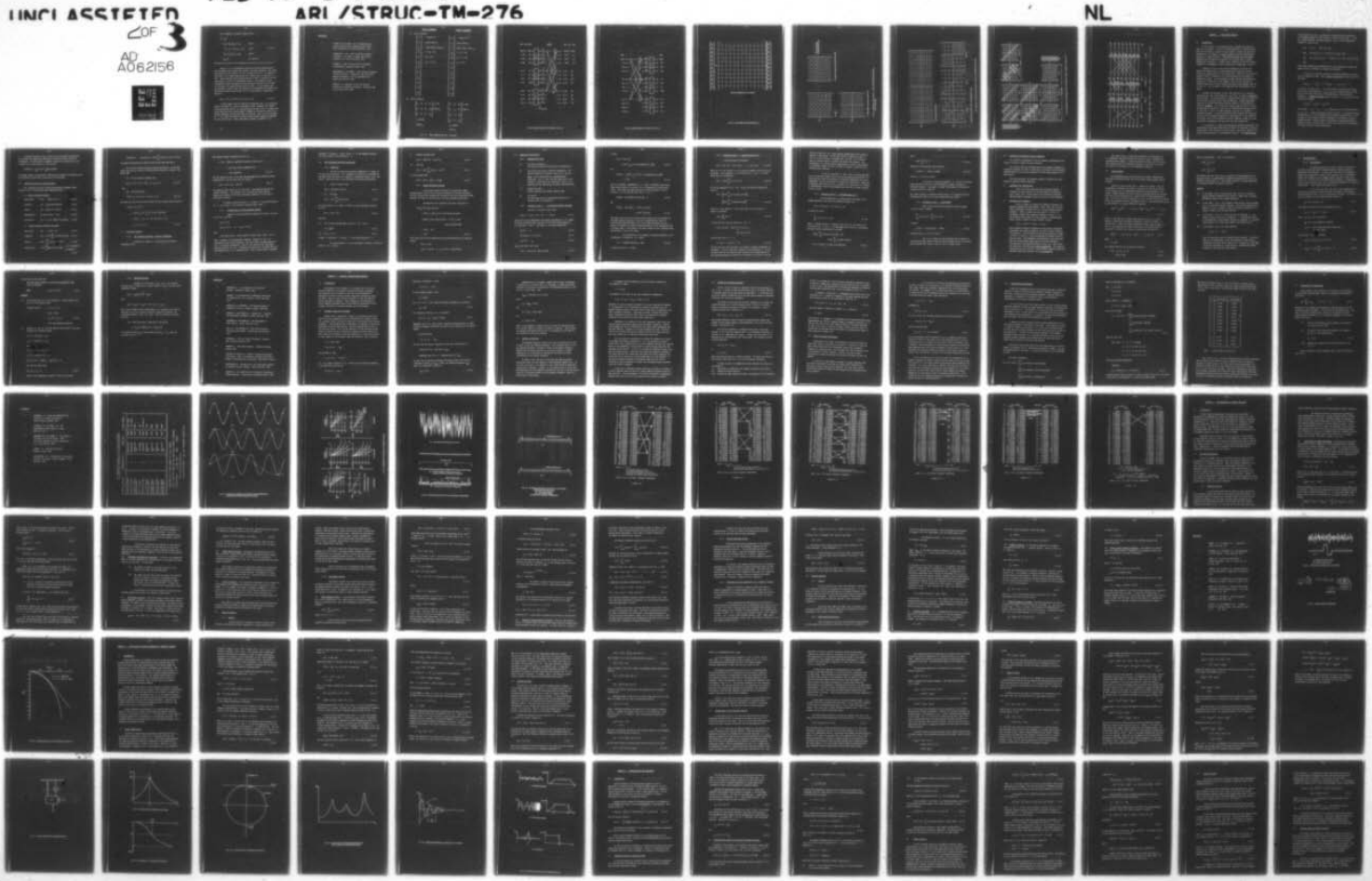

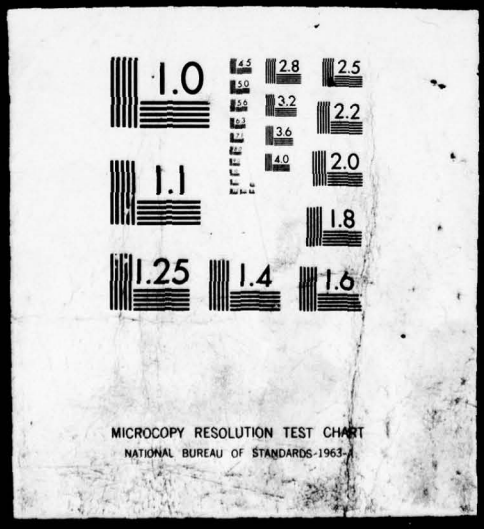

As an example, an 8-point radix-2 FFT is

$$\vec{G} = M_8 \vec{g}$$

$$= (I_4 \times M_2)(D_{4,2} \times I_1). \qquad \text{Pass 3}$$

$$(I_2 \times M_2 \times I_2)(D_{2,2} \times I_2). \qquad \text{Pass 2} \qquad (3.4.10)$$

$$(M_2 \times I_4)(D_{1,2} \times I_4). \qquad \text{Pass 1}$$

$$A_{8,2}\,\vec{g} \qquad \text{Bit Reverse}$$

The matrices involved in this expression are shown in full in Fig.3.6.

There is a 1:1 correspondence between the matrix representation and the commonly used signal flow graph of the same transform. The signal flow graph for the transform (3.4.10) is shown in Fig.3.7. It should be noted that in all matrix expressions the "signal flow" is from right to left. Each successive matrix multiplication of Fig.3.6 starting from the right yields a vector of intermediate results. The elements of this intermediate vector correspond to each successive vertical line of nodes in the signal flow graph starting from the left. If the original data are supplied in normal order the operation of rearranging the elements into bit-reversed order is given from (3.4.7) as the product of permutation matrices :

$$A_{8,2} = (P_{1,2} \times I_4)(P_{2,2} \times I_2)(P_{4,2} \times I_1) \qquad (3.4.11)$$

It might appear from the preceding discussion that it is irrelevant whether the radix-2 or radix-4 algorithm is used. However, the twiddle factor algorithms involve $N$ multiplications in each of the $k$ passes and, since there are half as many passes in radix-4 as in radix-2, there is an obvious advantage in using the radix 4 algorithm. When $N$ is an odd power of 2 it is most efficient to perform as many radix-4 passes as possible and one radix-2 pass. These algorithms are known as "radix-4 + 2".

## References


1 COOLEY,J.W. and TUKEY, J.W. An Algorithm for Machine Calculation of Complex Fourier Series. Math. Computation, vol.19, pp.297-301, 1965.

2 COCHRAN,W.T. et al. What is the Fast Fourier Transform? IEEE Trans. on Audio and Electro-acoustics, vol. AU-15, pp.45-55, 1967.

3 BRIGHAM, E. ORAN The Fast Fourier Transform. Prentice-Hall, Englewood Cliffs, 1974.

4 GENTLEMAN,W.M. and SANDE,G. Fast Fourier Transforms for Fun and Profit. AFIPS Proc. 1966 Fall Joint Computer Conference, vol.29, Washington D.C. : Spartan pp. 563-578, 1966.

5 PEASE,M.C. An Adaption of the Fast Fourier Transform for Parallel Processing. Journal of ACM, vol.15, pp.252-264, 1968.

**INPUT ELEMENTS** **OUTPUT ELEMENTS**

(a) Vector Grouping

| | | | |
|---|---|---|---|
| $g_o$ | 4 groups of 3 | $G_o$ | 3 groups of 4 |
| $g_1$ | group index $m_1$ | $G_1$ | group index $n_1$ |
| $g_2$ | index within group $m_o$ | $G_2$ | index within group $n_o$ |
| $g_3$ | $m = m_o + 3m_1$ | $G_3$ | $n = n_o + 4n_1$ |
| $g_4$ | $m_o = 0,1,2$ | $G_4$ | $n_o = 0,1,2,3$ |
| $g_5$ | $m_1 = 0,1,2,3$ | $G_5$ | $n_1 = 0,1,2$ |
| $g_6$ | | $G_6$ | |
| $g_7$ | | $G_7$ | |
| $g_8$ | | $G_8$ | |
| $g_9$ | | $G_9$ | |
| $g_{10}$ | | $G_{10}$ | |
| $g_{11}$ | | $G_{11}$ | |

(b) Matrix Grouping

$$\begin{bmatrix} g_o & g_3 & g_6 & g_9 \\ g_1 & g_4 & g_7 & g_{10} \\ g_2 & g_5 & g_8 & g_{11} \end{bmatrix}$$

$r_2$ rows

index $m_o$

$r_1$ columns

index $m_1$

$$\begin{bmatrix} G_o & G_4 & G_8 \\ G_1 & G_5 & G_9 \\ G_2 & G_6 & G_{10} \\ G_3 & G_7 & G_{11} \end{bmatrix}$$

$r_1$ rows

index $n_o$

$r_2$ columns

index $n_1$

FIG. 3.1 DATA INDEXING FOR FFT : N=12=4X3

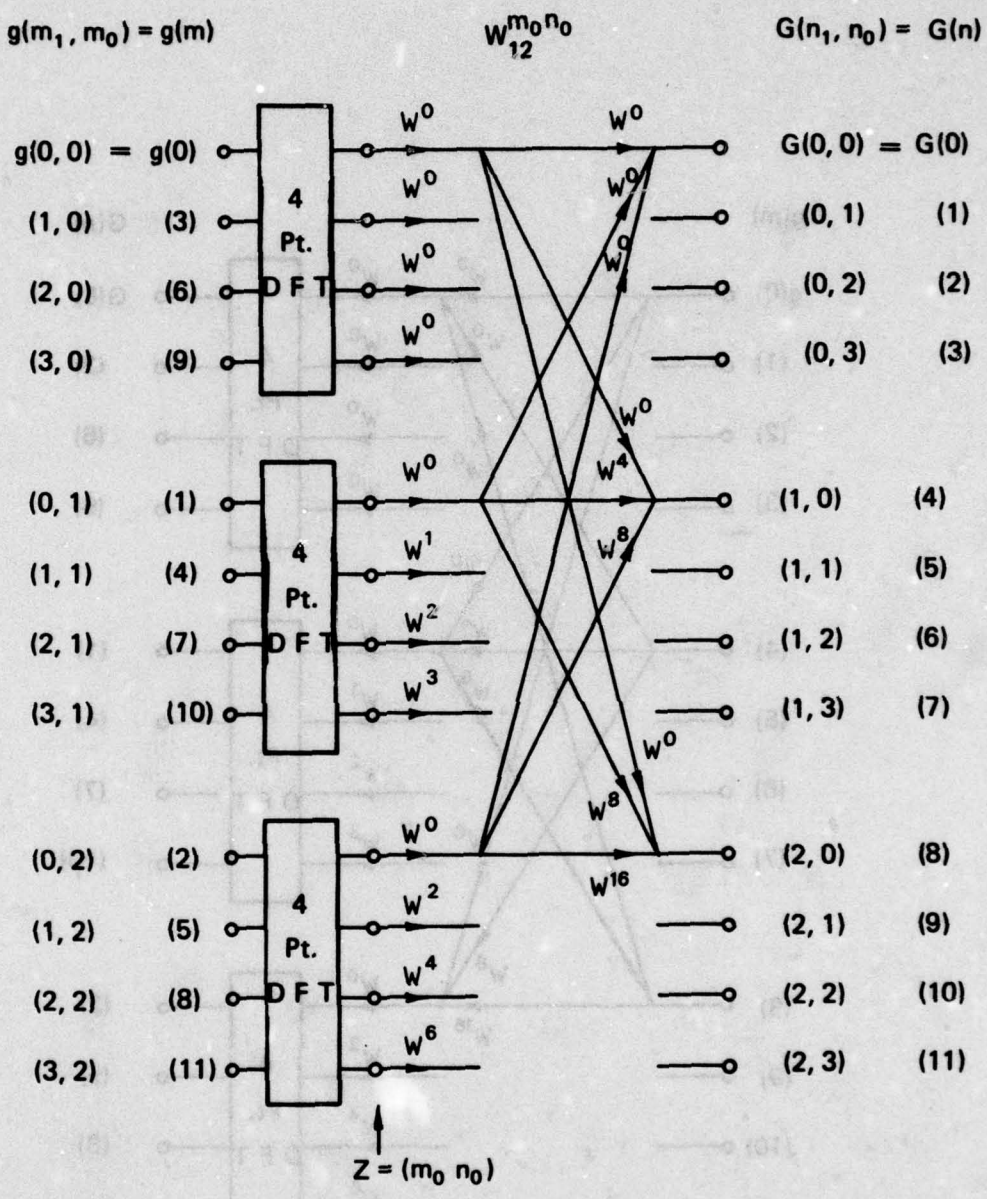


FIG. 3.2 COOLEY-TUKEY FFT FOR N = 12 = 4 x 3

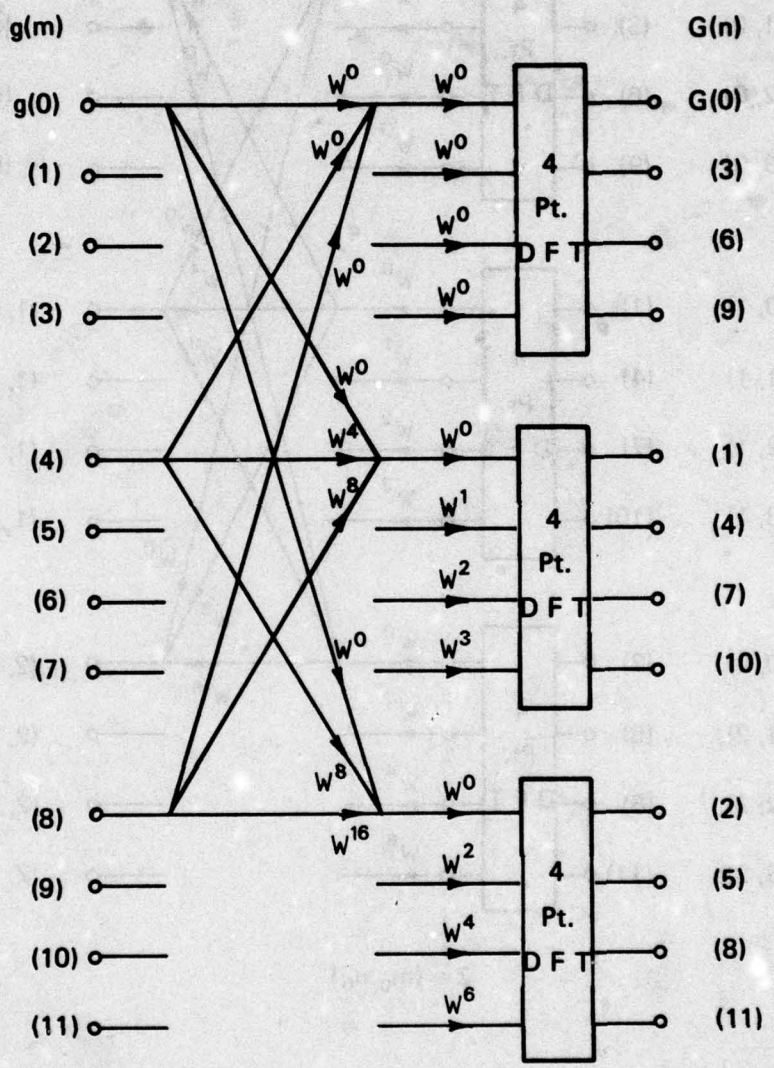


FIG. 3.3 SANDE-TUKEY FFT FOR N = 12 = 3 x 4

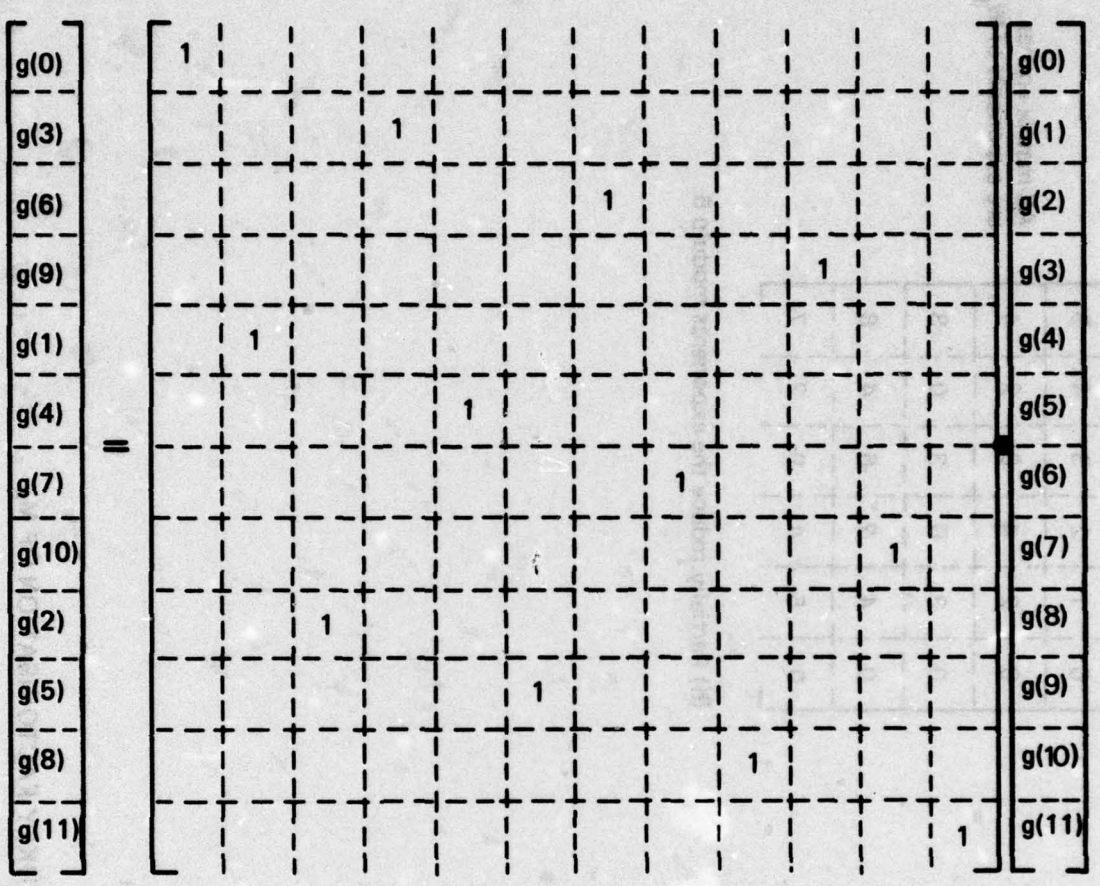


Zeros are indicated by vacant spaces

FIG. 3.4 THE PERMUTATION MATRIX $P_{4,3}$

$$M_6 = \begin{bmatrix} 0 & 0 & 0 & 0 & 0 & 0 \\ 0 & 1 & 2 & 3 & 4 & 5 \\ 0 & 2 & 4 & 6 & 8 & 10 \\ 0 & 3 & 6 & 9 & 12 & 15 \\ 0 & 4 & 8 & 12 & 16 & 20 \\ 0 & 5 & 10 & 15 & 20 & 25 \end{bmatrix}$$

(a) $[W_6^{mn}]$

$$= \begin{bmatrix} 0 & 0 & 0 & 0 & 0 & 0 \\ 0 & 1 & 2 & 3 & 4 & 5 \\ 0 & 2 & 4 & 6 & 2 & 4 \\ 0 & 3 & 0 & 3 & 0 & 3 \\ 0 & 4 & 2 & 6 & 4 & 8 \\ 0 & 5 & 4 & 9 & 2 & 7 \end{bmatrix}$$

All matrix entries are exponents of $W_6$

(b) Partially reduce the exponents modulo 6

$$M_6^1 = \left[\begin{array}{ccc|ccc} 0 & 0 & 0 & 0 & 0 & 0 \\ 0 & 2 & 4 & 1 & 3 & 5 \\ 0 & 4 & 2 & 2 & 6 & 4 \\ \hline 0 & 0 & 0 & 3 & 3 & 3 \\ 0 & 2 & 4 & 4 & 6 & 8 \\ 0 & 4 & 2 & 5 & 9 & 7 \end{array}\right]$$

(c) Rearrange the columns and partition

FIG. 3.5 STAGES IN THE COOLEY-TUKEY FACTORISATION OF $M_6$

(Cont. over page)

$M_6^1 =$

| | | | | | |
|---|---|---|---|---|---|
| 0 + 0 + 0 | 0 + 0 + 0 | 0 + 0 + 0 | 0 + 0 + 0 | 0 + 0 + 0 | 0 + 0 + 0 |
| 0 + 0 + 0 | 0 + 0 + 2 | 0 + 0 + 4 | 0 + 1 + 0 | 0 + 1 + 2 | 0 + 1 + 4 |
| 0 + 0 + 0 | 0 + 0 + 4 | 0 + 0 + 2 | 0 + 2 + 0 | 0 + 2 + 4 | 0 + 2 + 2 |
| 0 + 0 + 0 | 0 + 0 + 0 | 0 + 0 + 0 | 3 + 0 + 0 | 3 + 0 + 0 | 3 + 0 + 0 |
| 0 + 0 + 0 | 0 + 0 + 2 | 0 + 0 + 4 | 3 + 1 + 0 | 3 + 1 + 2 | 3 + 1 + 4 |
| 0 + 0 + 0 | 0 + 0 + 4 | 0 + 0 + 2 | 3 + 2 + 0 | 3 + 2 + 4 | 3 + 2 + 2 |

(d) Factorize the elements

$M_6^1 =$

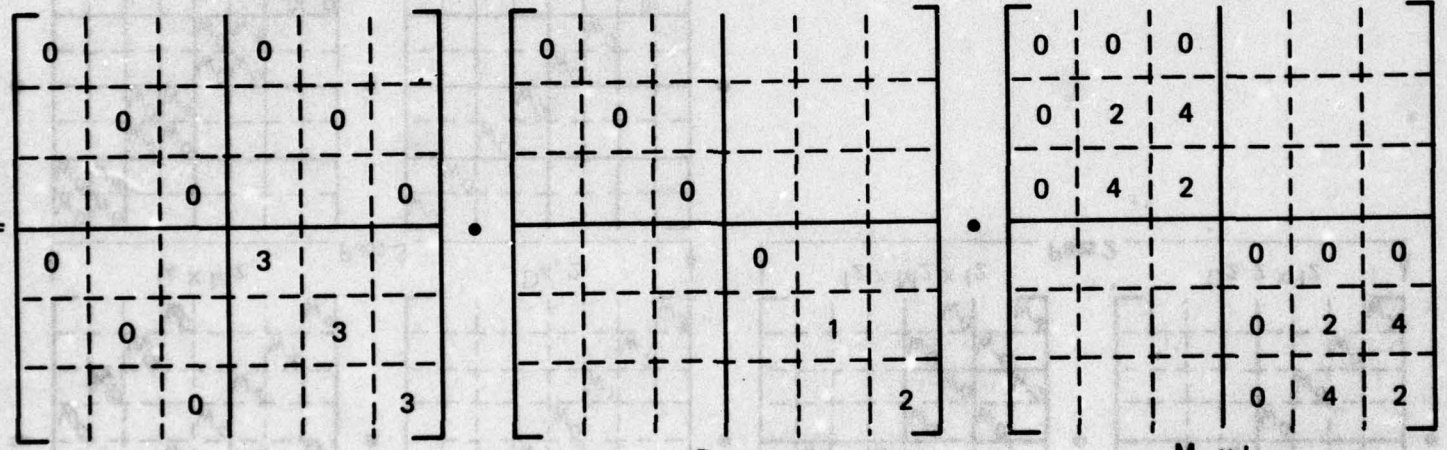


(e) Factorize the matrix (N.B. Vacant spaces are zero)

FIG. 3.5 (cont.) STAGES IN THE COOLEY-TUKEY FACTORISATION OF $M_6$

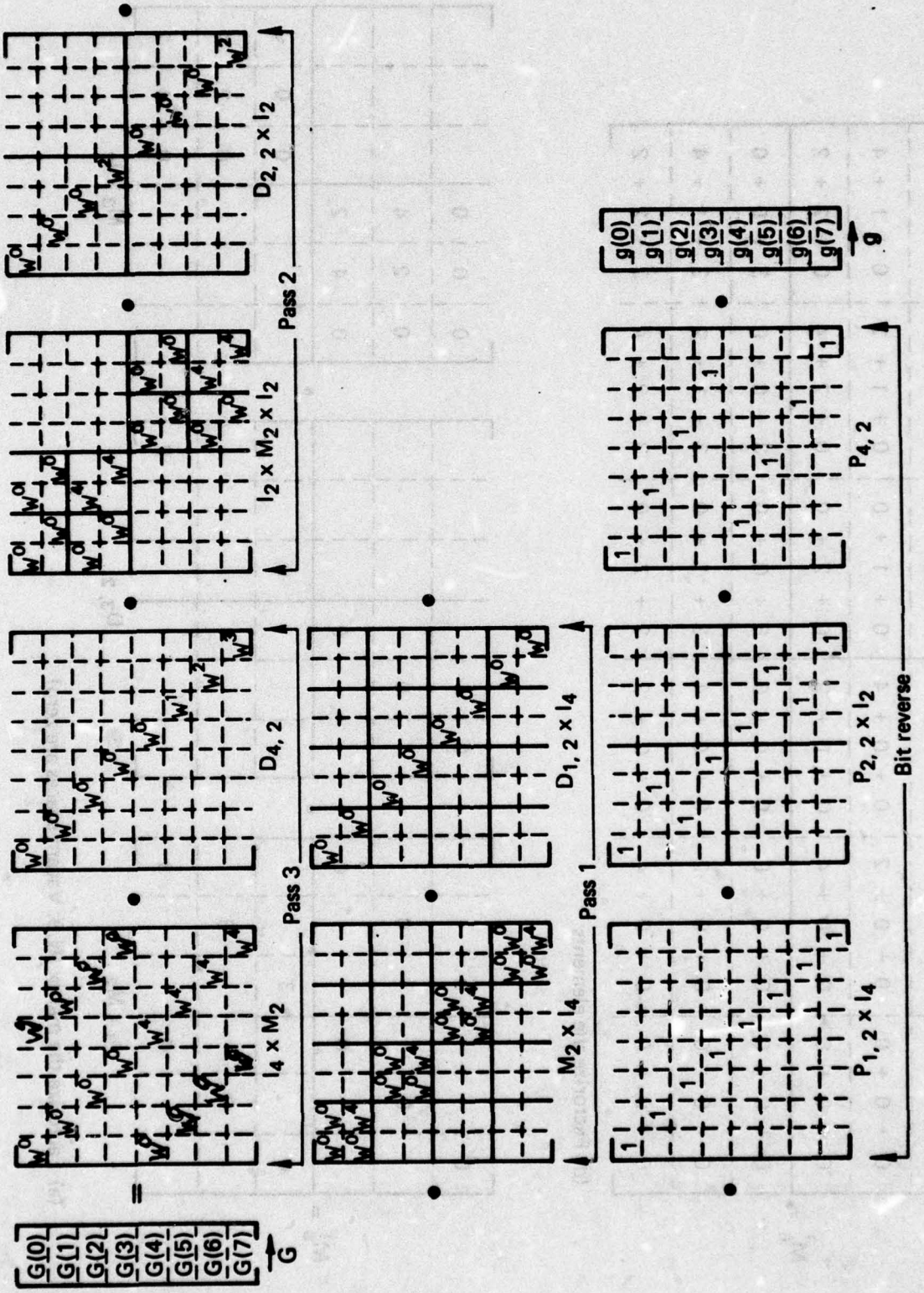


FIG. 3.6 MATRIX FACTORISATION OF AN 8-POINT RADIX 2 COOLEY-TUKEY FFT

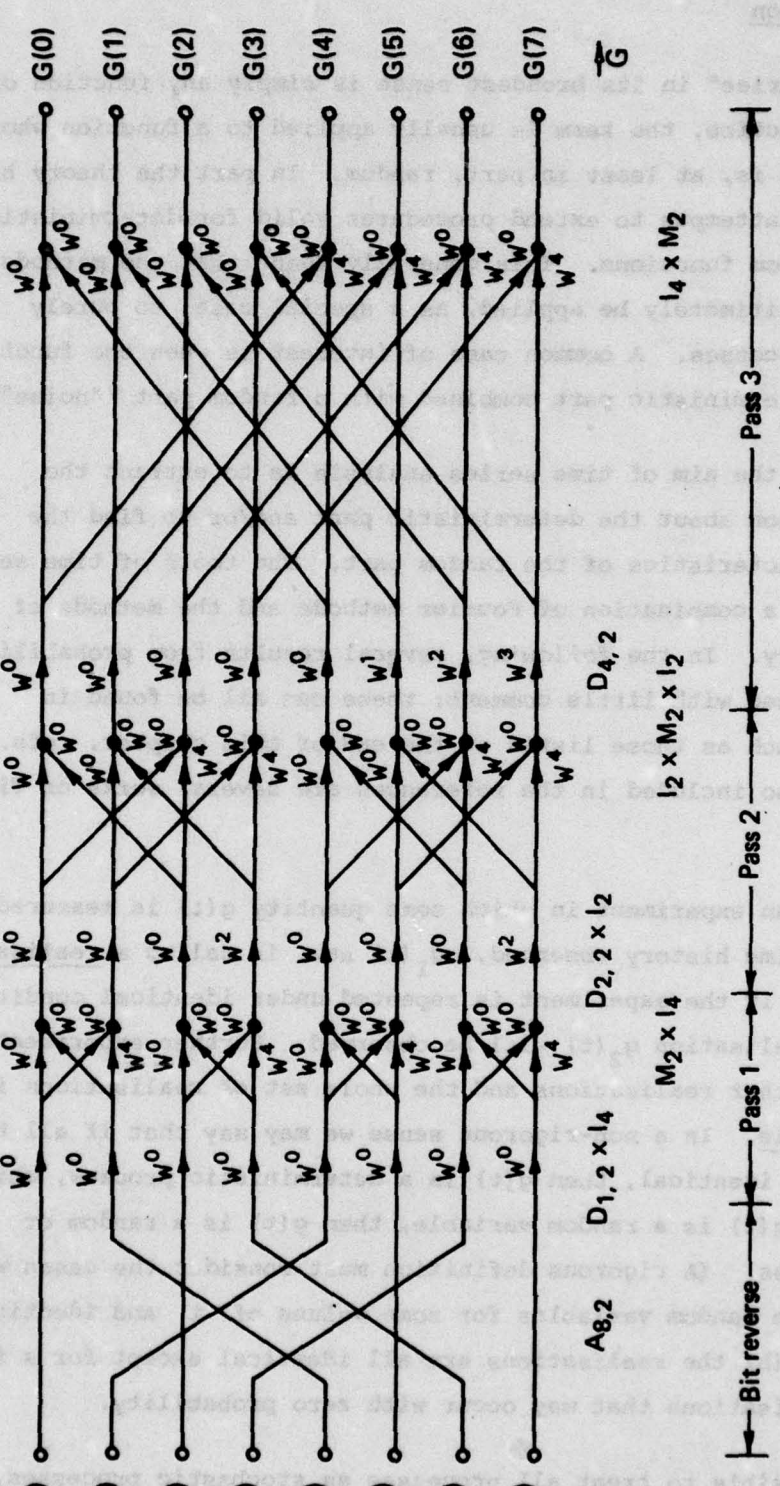


FIG. 3.7 SIGNAL FLOW GRAPH OF AN 8-POINT RADIX 2 COOLEY-TUKEY FFT

# CHAPTER 4 : TIME SERIES ANALYSIS

## 4.1 Introduction

A "time series" in its broadest sense is simply any function of time, but, in practice, the term is usually applied to a function whose value at any time is, at least in part, random. In part the theory has developed out of attempts to extend procedures valid for deterministic functions to random functions. This generally means that the methods developed can legitimately be applied, as a special case, to purely deterministic processes. A common case of interest is when the function consists of a deterministic part combined with a random part ("noise").

Generally the aim of time series analysis is to extract the maximum information about the deterministic part and/or to find the statistical characteristics of the random part. The tools of time series analysis involve a combination of Fourier methods and the methods of probability theory. In the following, several results from probability theory will be used with little comment; these can all be found in standard texts such as those listed at the end of this chapter, refs.(1), (2) and (3). Also included in the references are several works on Time Series.

Consider an experiment in which some quantity $g(t)$ is measured. The particular time history observed, $g_1(t)$ say, is called a realisation of the process. If the experiment is repeated under identical conditions then a second realisation $g_2(t)$ will be observed. Further experiments give rise to further realisations and the whole set of realisations is termed an ensemble. In a non-rigorous sense we may say that if all the realisations are identical, then $g(t)$ is a deterministic process, whilst if, for each $t$, $g(t)$ is a random variable, then $g(t)$ is a random or stochastic process. (A rigorous definition must consider the cases when (a) the $g_i(t)$ are random variables for some values of $t$ and identical for others, and (b) the realisations are all identical except for a few exceptional realisations that may occur with zero probability.

It is possible to treat all processes as stochastic processes, the deterministic ones simply being those in which, for each time $t$, there is zero scatter in the values of the time series. This would, however, be a rather wide definition of a deterministic process.) The expected value

of some function of $g(t)$ is simply the average over all realisations (the ensemble average) of that function. Since for each time, $t$, $g(t)$ is a random variable, the process defines a set of finite dimensional probability distributions

$$\underline{1\text{-D}} \quad F(x_1;t_1) = P[g(t_1) < x_1]$$

$$\underline{2\text{-D}} \quad F(x_1,x_2;t_1,t_2) = P[g(t_1) < x_1,\ g(t_2) < x_2]$$

$$\underline{3\text{-D}} \quad F(x_1,x_2,x_3;t_1,t_2,t_3) = P[g(t_1) < x_1,\ g(t_2) < x_2, g(t_3) < x_3]$$

etc

These finite dimensional distributions are also sufficient to define the random process, according to a theorem of Kolmogorov.

A stationary stochastic process is one whose probability structure does not change with time. Thus a strictly stationary process will be one for which

$$F(x_1,x_2,\cdots;\ t_1,t_2,\cdots) = F(x_1,x_2,\cdots;\ t_1+\tau,\ t_2+\tau\ \cdots)$$

is true for all values of $\tau$. (In other words the distributions depend only one the time differences $t_2-t_1$, $t_3-t_1$ etc.) However there are some parts of the theory which can be developed from a less restrictive assumption. A weakly stationary process of order $\ell$ is one for which the multivariate moments

$$E\{g(t_1)^{\ell_1}\ g(t_2)^{\ell_2}\cdots g(t_n)^{\ell_n}\}$$

up to order $\ell = \ell_1 + \ell_2 + \cdots + \ell_n$ depend only on the time differences $t_2 - t_1$ etc. A weakly stationary process of order 2 is the most commonly considered case. If the probability distribution associated with any set of times is a multivariate normal distribution, the process is called a Gaussian process. Since a normal distribution is fully characterised by moments of first and second order, in this case second order stationarity is enough to produce strict stationarity.

An ergodic process is one in which all the different realisations of a process are adequately represented by different parts of any one realisation. In other words an ensemble average of any function of $g(t)$ is equal to the time average of that function.

$$E\{\phi[g(t)]\} = \lim_{T\to\infty} (1/2T) \int_{-T}^{T} \phi[g(t+t^1)]\,dt^1$$

An ergodic process is necessarily stationary and values of the process which are sufficiently separated in time must be uncorrelated.

## 4.2 Results from Fourier Transform Theory

For convenience the main results from Fourier transform theory required in the following have been summarised below:

### a) Fourier Integral Transform

Time series ; $g(t)$ : $\int_{-\infty}^{\infty} |g(t)|^2\,dt < \infty$ (4.2.1)

Transform ; $G(f) = \int_{-\infty}^{\infty} g(t)\exp(-2\pi i f t)\,dt$ (4.2.2)

Inverse ; $g(t) = \int_{-\infty}^{\infty} G(f)\exp(2\pi i f t)\,df$ (4.2.3)

Orthogonality ; $\int_{-\infty}^{\infty} \exp(2\pi i f t)\,dt = \delta(f)$ (4.2.4)

Convolution ; $g_1(t) * g_2(t) = \int_{-\infty}^{\infty} g_1(s)\, g_2(t-s)\,ds$ (4.2.5)

### b) Discrete Fourier Transform (N points)

Time series ; $g(t)$ : $g(t+N) = g(t)$ (4.2.6)

Transform ; $G(n) = (1/N) \sum_{t=o}^{N-1} g(t)\exp(-2\pi i n t/N)$ (4.2.7)

Inverse ; $g(t) = \sum_{n=o}^{N-1} G(n)\exp(2\pi i n t/N)$ (4.2.8)

Orthogonality ; $(1/N) \sum_{t=o}^{N-1} [\exp 2\pi i t(r-n)/N] = \begin{cases} 1 \text{ if } r=n \text{ modulo } N \\ 0 \text{ otherwise} \end{cases}$ (4.2.9)

$$\text{Convolution} \quad ; \quad g_1(t) * g_2(t) = (1/N) \sum_{s=o}^{N-1} g_1(s)\, g_2\,(t-s) \qquad (4.2.10)$$

(A somewhat abbreviated but obvious notation has been used here.)

All the above results have been derived previously. One further result which can be called the "multiplication theorem" is needed. This states that

(a) for the Fourier Integral case

$$\int_{-\infty}^{\infty} g_1\,(t)\; g_2\,(t)\; dt = \int_{-\infty}^{\infty} G_1\,(-f)\; G_2\,(f)\; df \qquad (4.2.11)$$

and

(b) for the DFT case

$$(1/N) \sum g_1\,(t)\; g_2\,(t) = \sum G_1(-n)\; G_2\,(n) \qquad (4.2.12)$$

The proof for the DFT case follows (that for the integral being parallel):

$$(1/N) \sum_t g_1\,(t)\; g_2\,(t)$$

$$= (1/N) \sum_t g_1\,(t) \{ \sum_n G_2\,(n) \exp\,(2\pi int/N) \}$$

$$= (1/N) \sum_n \{ \sum_t g_1\,(t) \exp\,(2\pi int/N) \}\, G_2\,(n)$$

$$= \sum_n G_1\,(-n)\; G_2\,(n) \qquad (4.2.13)$$

## 4.3 The Power Spectrum

### 4.3.1 An Invariance Property of Fourier Transforms

Consider the effect of a time shift on the Fourier transform of g(t).

The Fourier integral transform of g(t-a) is

$$G'(f) = \int_{-\infty}^{\infty} g(t-a) \exp[-2\pi i f(t-a)] \exp(-2\pi i f a)\, d(t-a)$$

$$= \int g(t) \exp(-2\pi i f t) \exp(+2\pi i f a)\, dt$$

$$= G(f) \exp(+2\pi i f a) \qquad (4.3.1)$$

The two quantities G(f), G'(f) have the same modulus but different phases. Alternatively it may be said that the quantity

$$P(f) = G^*(f)\, G(f) = |G(f)|^2 \qquad (4.3.2)$$

is invariant under shifts in the time scale. (The asterisk denotes the complex conjugate.) The quantity P(f) is called the power spectral density and, because of the above invariance property, is a key tool in time series analysis.

It might be noted that when $g$ is real, $P$ is an even function of $f$. In the past it was generally analysed using a DFCT.

### 4.3.2 Interpretation of Power Spectral Density

Suppose in the multiplication theorem for the DFT, as given by (4.2.12), one sets

$$g_2(t) = g(t)$$

$$g_1(t) = g^*(t) \quad \text{so} \quad G_1(-n) = G^*(n)$$

then

$$(1/N)\, \Sigma g^*(t)\, g(t) = (1/N)\, \Sigma |g(t)|^2 = \Sigma G^*(n)\, G(n) = \Sigma P(n) \qquad (4.3.3)$$

This, of course, is just Parseval's theorem. However if $g(t)$ is interpreted as the current through a unit resistance, the mean square of $g(t)$ is the power dissipation. This is the reason for the term power spectral density, for $P(n)$ represents that portion of the power which is contributed by the $n$'th frequency band. Thus a signal having a periodic

component of frequency $n/(N\Delta t)$, where $\Delta t$ is the sampling interval, will have a spike in the spectrum at $n$.

## 4.4 Auto Covariance and Auto Correlation

### 4.4.1 Definition

One way of looking for periodic components in a signal is via the "auto-covariance". If a component of period $k\,\Delta t$ is present in the signal then there will be a degree of correlation between $g(t)$ and $g(t+k)$. This idea leads to the definition of the auto-covariance by

a) Fourier integral case

$$C(t) = \int_{-\infty}^{\infty} g^*(s)\, g(s+t)\, ds \qquad (4.4.1)$$

b) DFT Case

$$C(t) = (1/N) \sum_{s=o}^{N-1} g^*(s)\, g(s+t) \qquad (4.4.2)$$

For many purposes it is useful to define an auto-correlation function $R(t)$ by

$$R(t) = C(t) / C(o) \qquad (4.4.3)$$

Note that

(i) $C(o)$ is just the mean square value of $g(t)$ and so

$$C(o) = \sum P(n) \qquad (4.4.4)$$

(ii) $$C(-t) = C^*(t) \qquad (4.4.5)$$

so when $g$ and hence $C$ is real, $C$ is an even function of $t$.

For some purposes it is also convenient to define a structure function $D(t)$ given by

a) Fourier Integral Case

$$D(t) = \int_{-\infty}^{\infty} |g(s+t) - g(s)|^2 \, ds \tag{4.4.6}$$

b) DFT Case

$$D(t) = (1/N) \sum_{s=o}^{N-1} |g(s+t) - g(s)|^2 \tag{4.4.7}$$

It can be shown that

$$D(t) = 2\,C(o) - \left[C(t) + C^*(t)\right] \tag{4.4.8}$$

### 4.4.2 Wiener Khintchine Theorem

If the power spectral density of a stationary random process exists, then it is the Fourier transform of the auto-covariance. We will not prove this theorem for the general case of a stationary random process, but only for the particular DFT case considered previously.

By definition the transform of the auto covariance is

$$(1/N) \sum_t C(t) \exp(-2\pi int/N)$$

$$= (1/N) \sum_t \{(1/N) \sum_s g^*(s)\, g(s+t)\} \exp(-2\pi int/N)$$

$$= \{(1/N) \sum_s g^*(s) \exp(2\pi isn/N)\} \{(1/N) \sum_t g(s+t) \exp\left[-2\pi i(s+t)n/N\right]\}$$

$$= G^*(n)\; G(n)$$

$$= P(n) \tag{4.4.9}$$

This result can also be established using the multiplication theorem and taking

$$g_1(t) = g(t)$$

$$g_2(t) = g^*(t-k) \quad \text{so} \quad G_2(-n) = G^*(n) \exp(2\pi ikn/N)$$

## 4.5 Examples of Time Series

### 4.5.1 Deterministic Cases

a) Sine Wave, frequency f.
The spectrum consists of two lines at frequencies ±f.

b) Two or more sine waves, different frequencies. The spectrum consists of discrete lines at $\pm f_1$, $\pm f_2$ etc.
Note: If two frequencies are incommensurable magnitudes, (e.g. f, $\sqrt{2}f$) then the time series is not periodic. Nevertheless the spectrum is still a line spectrum and the time series is called "quasi-periodic".

c) Damped sine wave.
Greater damping gives broader spectral peak.

d) An impulse.
The power spectrum of a Dirac Delta function is a constant over all frequencies.

### 4.5.2 Stochastic Case 1 - Uncorrelated Random Variables

Consider a (discrete) time series

$$\{g(t)\} = \{\varepsilon(o), \varepsilon(1), \varepsilon(2), \cdots, \varepsilon(N-1)\} \qquad (4.5.1)$$

where the $\varepsilon(t)$ are independent identically distributed (i i d) random variables, with zero mean, variance $\sigma^2$ and finite fourth moment $\mu_4$. i.e. for each t and s and using E to denote expectation

$$E\{\varepsilon(t)\} = 0 \qquad (4.5.2)$$

$$E\{\varepsilon(t)\varepsilon(s)\} = \sigma^2 \delta(t-s) \qquad (4.5.3)$$

$$E\{\varepsilon(t)^4\} = \mu_4 \qquad (4.5.4)$$

Taking the DFT of g(t) gives

$$G(n) = (1/N) \sum_t \varepsilon(t) \exp(-2\pi int/N) \qquad (4.5.5)$$

so that

$$P(n) = G^*(n)\, G(n)$$

$$= (1/N^2) \sum_t \sum_s \varepsilon^*(s)\varepsilon(t)\exp\left[-2\pi i n(t-s)/N\right] \qquad (4.5.6)$$

and

$$E\{P(n)\} = (1/N^2) \sum_t \sum_s E\{\varepsilon^*(s)\ \varepsilon(t)\}\exp\left[-2\pi i n(t-s)/N\right]$$

$$= \sigma^2/N \qquad (4.5.7)$$

This is a constant, independent of n. Such a stochastic time series, whose power spectrum is constant for all frequencies is termed white noise. (Note that the power spectrum of a delta function is also a constant.) It can also be shown that if $m \neq n$ :

$$E\{\left[P(m) - E\{P(m)\}\right]\left[P(n)-E\{P(n)\}\right]\} \simeq 0 \qquad (4.5.8)$$

and

$$E\{\left[P(n) - E\{P(n)\}\right]^2\} \simeq (\sigma^4/N^2)\ \left[1+\delta(n)\right]$$

$$= E\{P(n)^2\}\left[1+\delta(n)\right] \qquad (4.5.9)$$

This means that for any two given distinct frequencies the estimates of the power spectral density at those two frequencies are a pair of uncorrelated random variables, and at any single frequency the non-negative estimates of the power spectral density will be distributed with a variance equal to the square of the mean (except at zero frequency where the variance is twice this value).

The reliability of an estimate is usually indicated by the "coefficient of variation", C.V., where

$$\text{C.V.} = \text{standard deviation / mean} \qquad (4.5.10)$$

In this case the C.V. is unity.

### 4.5.3 Stochastic Case 2 - Moving Average (m.a.)

A moving average is defined by

$$g(t) = \alpha(o)\ \varepsilon(t) + \alpha(1)\ \varepsilon(t-1) + \ldots + \alpha(m)\ \varepsilon(t-m) \qquad (4.5.11)$$

where the $\varepsilon(t)$ are defined as in the previous example, and the $\alpha(t)$ are constants. If we suppose $m < N-1$ and that $\alpha(j) = o$ for $j > m$ we may write this as a convolution

$$g(t) = (1/N) \sum_{j=o}^{N-1} N\ \alpha(j)\ \varepsilon(t-j) \qquad (4.5.12)$$

of the two sequences $N\,\alpha(t)$, $\varepsilon(t)$, so that the Fourier transform is given by

$$G(n) = \left[(1/N) \sum_{t=o}^{N-1} N\ \alpha(t) \exp(-2\pi i n t/N)\right] \cdot$$

$$\left[(1/N) \sum_{t=o}^{N-1} \varepsilon(t) \exp(-2\pi i n t/N)\right] \qquad (4.5.13)$$

Writing $z = \exp(-2\pi i n/N)$ it can be seen that the first bracket is simply a polynomial

$$A(z) = \sum_{t=o}^{m} \alpha(t)\ z^t \qquad (4.5.14)$$

so that the power spectral density of $g(t)$ is

$$P(n) = |A(z)|^2\ (1/N^2) \sum_t \sum_s \varepsilon^*(s)\ \varepsilon(t)\ .$$

$$\exp -2\pi i n(t-s)/N$$

and the mean value of $P$ is

$$E\{P(n)\} = |A(z)|^2\ \sigma^2\ /N \qquad (4.5.15)$$

In this case the power spectrum is no longer a constant independent of frequency. It has a shape which depends on the polynomial A. It may be shown that any well behaved power spectrum can be approximated to any prescribed degree of accuracy by a function of the form A, and the

resultant values of $\alpha(t)$ give a moving average which can be used to simulate a time series. If the time series is known up to time $t^1$, then it is also possible to estimate the $\varepsilon(t)$ for $t \leq t^1$ and use these as starting values to predict the future time history. The disadvantage of a moving average representation is that it may require a considerable number of terms (m large) to achieve a good fit to an arbitrary power spectrum.

It may be shown that $E\{P(m)\ P(n)\}$ has the same form as in the previous example, apart from the multiplying polynomials, so that once again spectral estimates at different frequencies are nearly independent, and the coefficient of variation is again unity. Note that a necessary condition for the m.a. process to be invertible (i.e. useful in forecasting) is that the polynomial $A(z)$ have all its roots outside the unit circle.

### 4.5.4 Stochastic Case 3 - Autoregression (a.r.)

An autoregression is a process where the value at one instant depends on the values at previous instants e.g.

$$g(t) = 0.5\ g(t-1) + 0.1\ g(t-2) + \varepsilon(t)$$

In general we write

$$\sum_{j=o}^{m} \beta(j)\ g\ (t-j) = \varepsilon(t) \qquad (4.5.16)$$

(Note: A Markov process is a special case of an a.r. for which m=1) By defining $\beta(j) = 0$ for $j > m$ we may again write this as a convolution, and upon Fourier transformation we obtain

$$\left[(1/N) \sum_{t=o}^{N-1} N\beta(t)\exp(-2\pi int/N)\right]\ G(n)$$

$$= (1/N) \sum_{t=o}^{N-1} \varepsilon(t)\exp(-2\pi int/N)$$

$$G(n) = \left[(1/N) \sum_{t} \varepsilon(t)\exp(-2\pi int/N)\right] / B(z) \qquad (4.5.17)$$

where

$$B(z) = \sum_{t=0}^{m} \beta(t)\, z^t \qquad (4.5.18)$$

Similarly to the previous case we obtain

$$E\{P(n)\} = (\sigma^2/N) \,/\, |B(z)|^2 \qquad (4.5.19)$$

and the c.v. of P(n) is unity.

By fitting a suitable polynomial, B, to any well behaved power spectrum we may use an autoregression to model or predict a stochastic process. Once again, a rather large number of terms may be required to obtain a good fit.

Note that to obtain a stationary power series it is necessary that the polynomial B(z) have all its roots outside the unit circle.

### 4.5.5 Stochastic Case 4 - Mixed Model

This is also called an autoregression moving average (a.r.m.a.) model. Taking

$$\sum_{j=o}^{m_1} \beta(j)\, g(t-j) = \sum_{j=o}^{m_2} \alpha(j)\, \varepsilon(t-j) \qquad (4.5.20)$$

we obtain

$$E\{P(n)\} = \left|A(z)/B(z)\right|^2 \quad (\sigma^2/N) \qquad (4.5.21)$$

and again the c.v. of P(n) is unity.

The a.r.m.a. model has the advantage that in general it requires many fewer terms to obtain a given goodness of fit to a general power spectrum than either of the m.a. or a.r. models alone.

## 4.6 Reliability of Spectral Density Estimates

If a signal is deterministic then one example (realisation) of the signal is enough to define the power spectrum.

On the other hand the preceding three (very general) examples of stochastic processes all have a coefficient of variation (of the spectral density estimate at any given frequency) of unity, which implies a very high scatter.

There are basically two different methods to improve the reliability of spectral density estimates.

a) Averaging over realisations

This is the most computationally economical method. Determine the power spectra of several different realisations, $g_1(t)$, $g_2(t)$, etc., of the process, and average the resultant spectral density estimates, $P_1(n)$, $P_2(n)$ etc. at each frequency.

b) Averaging over frequency

This is a means of trading off frequency resolution for improved realiability of estimates. Since $P(m)$ and $P(n)$ are nearly independent variables if $m \neq n$, we may average adjacent estimates. (This of course will only work if $E\{P(n)\}$ is reasonably constant over frequency intervals of size $m - n$.) One procedure which comes into this category is termed Hanning. Using a prime to denote the more reliable estimate

$$P^1(n) = \tfrac{1}{4} P(n-1) + \tfrac{1}{2} P(n) + \tfrac{1}{4} P(n+1)$$

This procedure frequently introduces a much greater reliability improvement than would be expected, for quite a small trade-off in resolution. This is because a time series selected at random is likely to end up at a value significantly different from its starting value. The assumption of periodicity in the data means that this abrupt signal jump gives rise to high frequency fluctuations in the spectral density so that $P(n)$ and $P(n-1)$ are negatively correlated for a given realisation. Such negative correlations did not show up in the preceding examples because the expected values were averages over all realisations.

With either method of improving reliability, the averaging of "k" independent variables reduces the scatter as $1/\sqrt{k}$. To obtain 95% confidence bands (approx. 2 standard deviations) within 10% of the mean (the standard figure for unthinking engineers to pull out of the hat) will require the averaging of 400 independent estimates!

## 4.7 Linear Systems

The introductory part of this section is taken in abbreviated form from Solodovnikov's book (see ref.10) where further details may be obtained.

Consider a linear system with k degrees of freedom. Here "k" independent co-ordinates are needed to specify the state of the system at any instant, and "k" independent excitations may be applied to the system. However because of the principle of superposition we may consider only one of these excitations at a time and set all other excitations to zero. Say the one non-zero excitation is $g_1(t)$, and one of the co-ordinates giving the resultant state of the system is $g_2(t)$. The two functions $g_1$ and $g_2$ are related by a linear differential equation

$$(b_q D^q + b_{q-1} D^{q-1} + \ldots + b_o)\, g_2 = (a_r D^r + a_{r-1} D^{r-1} + \ldots + a_o)\, g_1 \qquad (4.7.1)$$

where $D = d/dt$ and (for a second order system) $q \leq 2k$, $r \leq 2(k-1)$. Bearing in mind that the Fourier transform of $dg/dt$ is $2\pi i f G(f)$, it follows that on taking the Fourier transform of both sides of equation (4.7.1), and ignoring the initial conditions of the system (which is equivalent to ignoring the transient oscillations) the result is

$$(b_q s^q + \ldots + b_o)\, G_2(f) = (a_r s^r + \ldots + a_o)\, G_1(f) \qquad (4.7.2)$$

where

$$s = 2\pi i f$$

The transfer function of the system is given by

$$H(f) = G_2(f) / G_1(f) \qquad (4.7.3)$$

$$= A(s) / B(s) \qquad (4.7.4)$$

where the polynomials A and B are given by

$$A(s) = \sum_{t=o}^{r} a_t s^t$$

$$B(s) = \sum_{t=o}^{q} b_t s^t$$

The transfer function, H(f), may be calculated if the parameters of the system are known, or experimentally observed by measuring the output, $g_2$, caused by a known input $g_1$. The transfer function is usually presented as two graphs showing its modulus and phase.

Examples

(a) If the input $g_1(t)$, is white noise, then $G_1(f)$ is a constant, and the Fourier transform of the output is (apart from a constant multiplier) equal to the transfer function.

(b) If the input, $g_1(t)$, is an impulse (Dirac Delta), then the output $g_2(t)$, is termed the impulse response. The Fourier transform of an impulse is also a constant, so again the Fourier transform of the output is equal to the transfer function.

(c) If the input, $g_1(t)$, is a unit sine wave of frequency f, the output is also a sine wave of frequency f, with magnitude equal to the amplitude of the transfer function at frequency f, and phase (with respect to the input wave) equal to the phase of H(f).

(d) If the input, $g_1(t)$, is a step function

$$g_1(t) = \begin{matrix} 0 & t < 0 \\ 1 & t > 0 \end{matrix}$$

then the resultant output is termed the step response. The Dirac Delta is the differential of the step function, so the Fourier transform of the Dirac Delta (known to be a constant) is $2\pi if$ times the Fourier transform of a step function. Therefore the impulse response is $2\pi if$ times the step response.

## 4.8 Two Time Series

### 4.8.1 Cross Spectra

We frequently meet the situation wherein we have two or more time series which may be somewhat related, though they may be affected by random factors. In some cases there may be correlations between the instantaneous values of the variables, but no correlation between one variable at some time t and another variable at some other time $s \neq t$. If this is so, then time series analysis is inappropriate and we should use other tools such as "principal components" or "canonical correlations". (See, Kendall and Stuart Vol.3.)

If, on the other hand, the value of the variable $g_1(t)$ is affected by the values of other variables at different time instants, then we should use tools such as cross-spectral analysis. For signals $g_1(t)$, $g_2(t)$, we define the cross power spectral density as

$$P_{12}(n) = G_1^*(n)\, G_2(n) \tag{4.8.1}$$

which may be written in real and imaginary parts as

$$P_{12}(n) = N_{12}(n) + i\, Q_{12}(n) \tag{4.8.2}$$

where $N_{12}(n)$ is the co-spectrum,

$Q_{12}(n)$ is the quadrature spectrum,

$\theta_{12}(n)$ = artan (quad spectrum/co-spectrum) is the phase angle.

We also have a cross co-variance

$$C_{12}(t) = \int_{-\infty}^{\infty} g_1^*(s)\, g_2(s + t)\, ds \tag{4.8.3}$$

or

$$C_{12}(t) = (1/N) \sum_{s=0}^{N-1} g_1^*(s)\, g_2(s + t) \tag{4.8.4}$$

As previously we may show that

THE CROSS POWER SPECTRUM IS THE FOURIER TRANSFORM OF THE CROSS CO-VARIANCE.

Note $$P_{12}(n) = P_{21}^*(n) \qquad (4.8.5)$$

Examples

(a) In the case when $g_1(t)$ is the input to a linear system, and $g_2(t)$ is the output we have

$$\text{Transfer Function} = G_2(f) / G_1(f)$$

$$= G_1^* G_2 / G_1^* G_1$$

$$= P_{12}(f) / P_{11}(f) \qquad (4.8.6)$$

$$= \text{Cross spectrum/Input spectrum}$$

(b) Suppose $g_1$ and $g_2$ are both complex oscillations of the same frequency but different phases.

$$g_1(t) = \exp(2\pi i f_1 t + i\xi_1)$$

$$g_2(t) = \exp(2\pi i f_1 t + i\xi_2)$$

Then

$$G_1(f) = \exp(i\xi_1)\ \delta(f_1 - f)$$

$$G_2(f) = \exp(i\xi_2)\ \delta(f_1 - f)$$

$$G_1^*(f)\ G_2(f) = \exp\left[i(\xi_2 - \xi_1)\right]\ \delta^2(f_1 - f)$$

And this has phase angle

$$\theta_{12}(f_1) = \xi_2 - \xi_1 \qquad (4.8.7)$$

equal to the difference in phases of the two sine waves.

### 4.8.2 Coherence Function

Consider two time series $g_1(t)$, $g_2(t)$, for which we postulate $g_2(t)$ is made up of a linear function of $g_1(t)$ and some other independent signal

$$g_2(t) = g_{2L}\left[g_1(t^1)\right] + g_{2e}(t)$$

Thus

$$G_2(f) = G_{2L}(f) + G_{2e}(f) = H(f)\, G_1(f) + G_{2e}(f)$$

This is now a simple linear relationship, so to determine the relative importance of the two (randomly varying) components we measure the correlation between $G_1(f)$ and $G_2(f)$. This is called the coherence function.

$$\gamma(f) = E\{|G_1^*(f)\, G_2(f)|\} \,/\sqrt{\left[E\{|G_1|^2\} \cdot E\{|G_2|^2\}\right]}$$

$$= E\,|P_{12}(f)|/\sqrt{\left[E\{P_{11}(f)\} \cdot E\{P_{22}(f)\}\right]}$$

At frequencies where $G_{2L}$ is much greater than $G_{2e}$, $\gamma \to 1$; when the converse is true $\gamma \to 0$

## References


1 HALSTEAD,H.J. An Introduction to Statistical Methods. Macmillan, London, 1960.

2 FELLER,W. An Introduction to Probability Theory and Its Applications, Vol.1 (2nd ed.) Wiley, New York, 1957.

3 KENDALL,M.G. and STUART,A. The Advanced Theory of Statistics (3 vols.) Griffin, London, 1958-1966.

4 BENDAT,J.S. and PIERSOL,A.G. Random Data : Analysis and Measurement Procedures. Wiley, New York, 1971.

5 BLACKMAN,R.B. and TUKEY,J.W. The Measurement of Power Spectra. Dover, New York, 1959.

6 BOX,G.E.P. and JENKINS,G.M. Time Series Analysis : Forecasting and Control. Holden Day, San Francisco 1970.

7 BRIGHAM,E.O. The Fast Fourier Transform. Prentice-Hall, Englewood Cliffs, 1974.

8 HANNAN,E.J. Time Series Analysis. Methuen Monograph, London, 1960.

9 LEDOLTER and BOX,G.E.P. Topics in Time Series Analysis. (Four parts) Dept. of Statistics, Wisconsin University, Madison, (Microfiche Nos. ADA 026309 - ADA 026312) 1975-76.

10 SOLODOVNIKOV,V. Introduction to the Statistical Dynamics of Automatic Control Systems. Dover, New York, 1960.

11 YAGLOM,A.M. An Introduction to the Theory of Stationary Random Functions. Prentice-Hall, Englewood Cliffs, 1962.

# CHAPTER 5 : PRACTICAL COMPUTATIONAL QUESTIONS

## 5.1 Introduction

The purpose of this chapter is to consider some of the more practical aspects of the operation and use of Fourier transforms. The discussion will be limited to the case of equi-spaced data analysed by the Fast Fourier transform algorithm developed by Cooley and Tukey. When the term "Fourier transform" is used the discrete Fourier transform is implied. Before commencing the discussion on actual computer techniques some of the practical consequences of the concepts introduced in previous chapters will be discussed.

## 5.2 Frequency Resolution and Range

Suppose that an experiment is about to be conducted where data from one or more parameters are to be collected over a period of time (or, possibly, space) and that the data are to be analysed using Fourier techniques. After ensuring that a transducer is available to record the parameters to the desired accuracy, the next consideration is that of the recording system. The cost and complexity of the recording system depend on several factors including the sampling interval between each data value and the length of each data sampling run. These two factors, in turn, depend on the frequency range and resolution that is desired.

If N data values

$$\{ g_o, g_1, g_2 \cdots g_{N-1} \}$$

are recorded at times

$$\{ 0, \Delta t, 2\Delta t \ldots (N-1)\Delta t \}$$

i.e., at a sample interval of $\Delta t$, then the N point Fourier transform of the data may be written as

$$\{ G_o, G_1, G_2 \cdots G_{N-1} \}$$

These last correspond to values

$$\{ f_o, f_1, f_2 \cdots f_{N-1} \}$$

in the frequency domain. Here

$$f_j = j f_R / N \tag{5.2.1}$$

for $j = 0, 1, 2 \ldots N-1$, where the reading frequency $f_R$ is given by

$$f_R = 1/\Delta t \tag{5.2.2}$$

The frequency resolution, $\Delta f$, is defined as

$$\Delta f = f_j - f_{j-1} = f_R/N = 1/(N\Delta t) \tag{5.2.3}$$

Therefore, for an N point Fourier transform calculated using N data values the frequency resolution is equal to the reciprocal of the record length.

The data values

$$\{ g_o, g_1, g_2 \cdots g_{N-1} \}$$

are real and the Fourier transform of real data is Hermitian i.e.,

$$\text{real part of } G_j = \text{real part of } G_{N-j}$$

$$\text{imaginary part of } G_j = - (\text{imaginary part of } G_{N-j})$$

so that, for all practical purposes the useful range of the Fourier transform is from $G_o$ to $G_{N/2}$. Hence, the maximum frequency, $f_{max}$, able to be determined is given by

$$f_{max} = f_R/2 \tag{5.2.4}$$

Applying this to an example, assume that in order to determine a vibration in an aircraft wing it is necessary to obtain the Fourier transform of the wing tip acceleration for frequencies between 0.1 and 20 Hz in 0.05 Hz steps. Here

$$f_{max} = 20 \text{ Hz and } \Delta f = 0.05 \text{ Hz}$$

Hence,

$$f_R = 2f_{max} = 40 \text{ Hz}$$

and

$$\Delta t = 1/f_R = 1/40 \text{ second}$$

and

$$N = f_R/\Delta f = 800$$

Thus, in this example, a sample rate of at least 40 times per second and a record length of at least 20 seconds is required. These figures are minimum requirements and may have to be modified in the light of the discussion in the next sections.

## 5.3 Effects of Aliasing

The maximum frequency estimate that can be computed using a DFT is equal to half the sampling frequency. That frequency which is half the sampling frequency is generally known as the Nyquist frequency. However the data being recorded may have oscillations of a higher frequency so it is necessary to investigate the effects of these oscillations on the Fourier transform.

In Figs. 5.1(a), (b) and (c) are shown the same sinusoidal oscillation which has been sampled at three different sample rates. In the first case there is no ambiguity in the curve fitted to these data using Fourier techniques. However, in the second and third cases there are ambiguities and the computed transform will be that of the oscillation which has a frequency between 0 and the Nyquist frequency (shown as a dotted line on the Figure).

In general the DFT estimate of the true Fourier transform at the frequency f, where

$$0 < f \leq f_R/2$$

is dependent on the value of the true transform at frequencies

$$f,\ f_R - f,\ f_R + f,\ 2f_R - f,\ 2f_R + f,\ \text{etc.}$$

Therefore, to get an accurate estimate of the true transform at frequency f the amplitude of all oscillations at frequencies greater than the Nyquist frequency must be very much smaller than those at frequencies less than the Nyquist frequency. Steps must be taken to ensure that these higher frequencies are dealt with, either by increasing the sampling frequency or by filtering the data before sampling it.

Sometimes it is possible to live with aliasing if only one or two distinct known frequencies appear above the Nyquist frequency. However these frequencies will be "folded back" over other lower frequencies and may mask them out. Consider a 50 Hz noise sampled at 80 Hz. The 50 Hz noise will be folded back and will appear at 30 Hz (its alias) and this may cover another as yet undetected oscillation near 30 Hz.

The best method of overcoming the problem of aliasing is to filter the incoming data before recording it. It is not possible to design a filter with a flat response up to a cut-off frequency and then zero response above it; the complexity, size and cost of filters usually depend on the sharpness of the cut-off. In Fig. 5.2 is shown the response of some of the more well-known filters. Note that the filters may change the phasing of the signal and that for frequencies just above the cut-off frequency the energy may not be reduced by a large enough amount to stop aliasing. If the area of interest includes the frequency range near the cut-off frequency it may be necessary to correct the calculated Fourier transform using the filter's response.

A quick way to determine whether aliasing is present in the data is to make a special record of data at a higher sampling frequency than that used initially. If the transform in the region of interest is modified as compared with that for the initial sampling then aliasing is present.

## 5.4 Stability of Fourier Estimates

In Fig. 5.3(b) is shown the 256 point DFT of the data shown in Fig. 5.3(a). A glance at these results shows that it is rather difficult to determine which of the many peaks are meaningful. It is obvious that to get any useful information out of the data some averaging or smoothing techniques will have to be considered.

One method of obtaining more reliable estimates is to average the Fourier estimates over a small frequency band. This will, of course, reduce the frequency resolution but adds to the stability. Using a weighted average such as Hanning i.e.,

$$G_j^1 = (-G_{j-1} + 2\,G_j - G_{j+1})\ /4 \qquad (5.4.1)$$

has another beneficial effect in that the Hanning window reduces the leakage of high energy caused by discontinuities at the end of the data records (See Section 5.5).

The Fourier transform is a complex function and, rather than consider it as a real and imaginary part, it is sometimes convenient to consider it as a magnitude and a phase. In many cases the phase is not required and so the magnitude alone can be used. It is usual to define the Power Spectrum

$$\{ P_o, P_1, P_2 \cdots P_{N/2} \}$$

as

$$P_j = G_j\, G_j^* \qquad (5.4.2)$$

where the asterisk denotes a complex conjugate. The power spectrum is a real function and allows the use of other averaging techniques.

If there are more than 256 data values available for analysis it is possible to

(i) take blocks of 256 points and compute the DFT for each block,

(ii) compute the power spectrum,

(iii) average the power spectral estimate corresponding to each frequency.

In Fig. 5.4 is shown the result when this technique is applied to some 20 blocks of 256 points recorded during the same data run as the data in Fig. 5.3(a). The difficulties of determining meaningful information from the power spectrum of Fig. 5.3(c) are absent in Fig. 5.4.

In general, if there are N independent data values used in the calculation of m frequency estimates of the power spectrum then the 90% confidence limits can be calculated as (see ref. 1)

$$10 \{ 2/(3k - 1) \pm 1/\sqrt{(k - 1)} \} \quad \text{db} \qquad (5.4.3)$$

where the number of degrees of freedom, k, is given by

$$k = 2N/m \qquad (5.4.4)$$

Note that as N increases, k increases and the confidence bands reduce approximately as $\sqrt{N}$ for a constant number of frequency estimates, so N must be very large to get good stable estimates of the power spectrum. In Figs. 5.3(c) and 5.4 the 90% confidence limits have been shown by a dotted line to give some idea of the effect of increasing the number of data values by a factor of 20.

## 5.5 Effect of Large Oscillations

Experimental data often contain dominant oscillations which may swamp other smaller oscillations of interest. In Section 5.3 the case where these oscillations have frequencies larger than the Nyquist frequency was discussed and it was concluded that these frequencies have to be filtered out before sampling. However, the case of large oscillations at lower frequencies can be dealt with after the data are sampled.

If there is a large amount of energy in a small frequency band, the Fourier transform of the data will suffer from "leakage" and a diffraction pattern effect may be observed. The side lobes of this diffraction pattern may swamp out those details of the transform which may be required.

It is possible to overcome this problem by pre-processing the data to reduce the contribution of the dominant frequency components. Then, after taking the transform, compensation for the pre-processing may be made. For example, if it is known that there is a large amount of energy in the very low frequency end of the transform, the data could be pre-processed by forming a new time series

$$\{ g'_0, g'_1, g'_2 \cdots g'_{N-1} \}$$

according to

$$g'_j = g_j - g_{j-1} \qquad (5.5.1)$$

It can be shown that the power spectrum of this new time series

$$\{ P'_0, P'_1, P'_2 \cdots P'_{N/2} \}$$

can be corrected using

$$P_j = P'_j \; / \; \{1 - \cos (2\pi j/N)\}^2 \qquad (5.5.2)$$

This pre-whitening and post-darkening (as it is commonly known) will reduce the effect of side lobes on the high frequency side of a large oscillation but will increase the side lobes on the low frequency side. In general, any pre-processing of the data which produces an uncorrected power spectrum that is as close as possible to white noise (i.e. a flat spectrum) will optimally reduce the effect of side lobes provided, of course, that the function to correct for the pre-processing can be found.

If it is preferred not to use this type of pre-processing it is, however, advisable at least to subtract off the mean or even the straight line of best fit ("the linear trend") from the data before computing the transform. If no post-correction is applied, this will have an effect on the first few low frequency estimates of the transform but it is usually easier to live with this, than to have a larger number of estimates swamped by the side lobes of very low frequency oscillations. If no correction for low frequency oscillations is applied the transform can easily be subject to misinterpretation.

## 5.6 Computational Requirements

Using the information given in the previous sections it should be possible to come to a decision on the sampling interval, duration of data runs, filtering and pre-processing required. However, before the experiment is attempted it is useful to look at the processing requirements of the Fourier transform itself.

For all but the case of very small amounts of data, the Fast Fourier Transform algorithm is much the faster method of analysis so the discussion will be confined to it. The computer to be used must have the storage requirement of the N data values to be transformed plus extra storage for the program and data manipulation. In general, the more data manipulation space available, the faster the computation can be made.

A typical 32 point transform using the Sande modification of the Cooley-Tukey method is shown step by step below. This routine is written to "inplace" compute the transform, i.e. it puts each calculation back into the same data storage location and then sorts them out at the end of the calculation. (As there are many proven versions of FFT computer programs already available, it is generally advisable to use one of the existing programs, possibly with modifications for individual needs, rather than to attempt to write one from scratch.)

The routine shown below starts with the complex data to be transformed in locations 0 to 31. Each location contains 2 numbers - the real and imaginary part of the data. In this case the data to be transformed is real.

The total transform is

$$G(n + mC + \ell BC) = \{ \sum_{a=o}^{A-1} \exp(2\pi i a\ell/A). \exp(2\pi i am/AB). \{ \sum_{b=o}^{B-1} \exp(2\pi i bm/B). \exp(2\pi i(a+bA)/ABC). \{ \sum_{c=o}^{C-1} \exp(2\pi i c/C). g(a+bA+cAB) \}\}\} \qquad (5.6.1)$$

where N = ABC with A, B, C integers

and $0 \leq \ell \leq A-1$

$0 \leq m \leq B-1$

$0 \leq n \leq C-1$

Using a Radix 4 + 2 transform,

$C = 4$, $B = 2$ and $A = N/8$

and (5.6.1) becomes

$$G(n + 4m + 8\ell) = \{ \sum_{a=o}^{N/8-1} \exp(16\pi ia\ell/N).\exp(8\pi iam/N). \{ \sum_{b=o}^{1} \exp(2\pi in(8a + bN)/8N). \{ \sum_{c=o}^{3} \exp(2\Pi icn/4).\, g(a + Nb/8 + Nc/4)\}\}\} \qquad (5.6.2)$$

Using the fact that

$\exp(2\pi iX) = 1$ if X is integral

$= -1$ if X is 1/2, 3/2, 5/2 ...

$= +i$ if X is 1/4, 5/4, 9/4 ...

$= -i$ if X is 3/4, 7/4, 11/4 ...

this can be further simplified.

Defining

$$F_j = \cos(2\pi j/32) + i \sin(2\pi j/32) \qquad (5.6.3)$$

a step-by-step 32 point transform is shown in Figs. 5.5 to 5.10. The values of $F_j$ used in the calculation are shown in the Table below.

The first calculation (Step 1), which is of radix 4 requires factors derived from $2\pi/32$; all other steps only involve factors derived from $2\pi/16$. Hence, after Step 1, only the even number factors in the Table are used.

| j | cos(2πj/32) | sin(2πj/32) |
|---|---|---|
| 0 | 1.0000 | 0.0000 |
| 1 | 0.9808 | 0.1951 |
| 2 | 0.9239 | 0.3827 |
| 3 | 0.8315 | 0.5556 |
| 4 | 0.7071 | 0.7071 |
| 5 | 0.5556 | 0.8315 |
| 6 | 0.3827 | 0.9239 |
| 7 | 0.1951 | 0.9808 |
| 8 | 0.0000 | 1.0000 |
| | | |
| 10 | -0.3827 | 0.9239 |
| 12 | -0.7071 | 0.7071 |
| 14 | -0.9239 | 0.3827 |

Table : Factors used in 32-Point FFT

Step 6 (Fig. 5.10) is the most complicated and is usually calculated with the aid of a bit reversal routine, sometimes written in machine language to increase speed. The total routine uses approximately 1.3N storage locations and it uses the technique of dividing each calculation by 2 as the calculation proceeds. Using this technique the magnitudes of the numbers throughout the calculation remain approximately the same, minimising round-off errors and allowing fixed point variables to be used if this is a constraint posed by the computer used in the analysis.

## 5.7 Calculation of Convolutions

Before closing, brief reference will be made to the calculation of convolutions using the FFT. Here it is a question of evaluating a sum such as

$$z_m = \sum_{j=o}^{N-1} y_j \, h_{m-j} \qquad m = 0,1, \ldots N-1 \qquad (5.7.1)$$

Reference to the precautions necessary to avoid wrap-around error has already been made in Chapter 2 and this will not be repeated here. However, it is worth remarking that, because of the speed of the FFT algorithm the convolution (5.7.1) is usually calculated in an indirect manner as follows :

(i) From the data values $y_m$ and $h_m$ compute the transforms $Y_n$ and $H_n$ (using the FFT),

(ii) By virtue of the convolution theorem, the transform $Z_n$ of $z_m$ is then obtained from

$$Z_n = Y_n \, H_n \qquad (5.7.2)$$

(iii) Compute $z_m$ by applying the inverse transform to eqn (5.7.2).

This is generally a faster procedure than a direct evaluation of eqn (5.7.1).

References

1 BLACKMAN, R.B. Linear Data Smoothing and Prediction in Theory and Practice. Addison Wesley, Reading, 1965.

2 BLACKMAN, R.B. and TUKEY, J.W. The Measurement of Power Spectra. Dover, New York, 1959.

3 GENTLEMAN, W.M. and SANDE, G. Fast Fourier Transforms for Fun and Profit. 1966 Fall Joint Computer Conference, AFIPS Proc., Vol. 29, pp.563-578, 1966.

4 HANNAN, E.J. Time Series Analysis. Methuen, London, 1960

5 SOLODOVNIKOV, V.V. Introduction to Statistical Dynamics of Automatic Control Systems. Dover, New York, 1960.

## FFT PROGRAMS AVAILABLE ON THE PDP-10 COMPUTER

| NAME | LANGUAGE | DOCUMENTATION | CORE SIZE | | TIME (MSEC) |
|---|---|---|---|---|---|
| HARM | FORTRAN | A | 2504+2.5*N | 7504 | 576 (410) |
| COOL | FORTRAN | C | 2005+2.0*N | 6005 | 470 (402) |
| FFT4 | FORTRAN | A | 372+2.0*N | 4412 | 2620 |
| BITSWP | MACRO | | 20 | | |
| FFT | MACRO | B | 431+2.0*N | 4431 | 916 |
| FFTPAK | FORTRAN | C | 720+3.0*N | 6720 | 594+140 # |
| FFT2 | FORTRAN | B | 550+2.5*N | 5640 | 822 |
| REFIT | MACRO | | 70 | | |
| FFTPAS | PASCAL | A | 370+2.0*N | 4410 | 3500 |
| BITSWP | MACRO | | 20 | | |
| XFFT | FORTRAN | A | 376+2.0*N | 4416 | 3800 |
| BITSWP | MACRO | | 20 | | |
| FOURI4 | PASCAL | A | 527+2.5*N | 5547 | 1800 |
| BITSWP | MACRO | | 20 | | |

CORE SIZE IS IN OCTAL NUMBER OF 36 BIT WORDS

TIME IS THE CPU TIME FOR ONE 1024 POINT COMPLEX TRANSFORM

DOCUMENTATION A= VERY GOOD B=OK C=POOR

( ) TIMES FOR F10 OPTIMIZATION

# CALCULATED RESULT WILL NOT TRANSFORM COMPLEX DATA

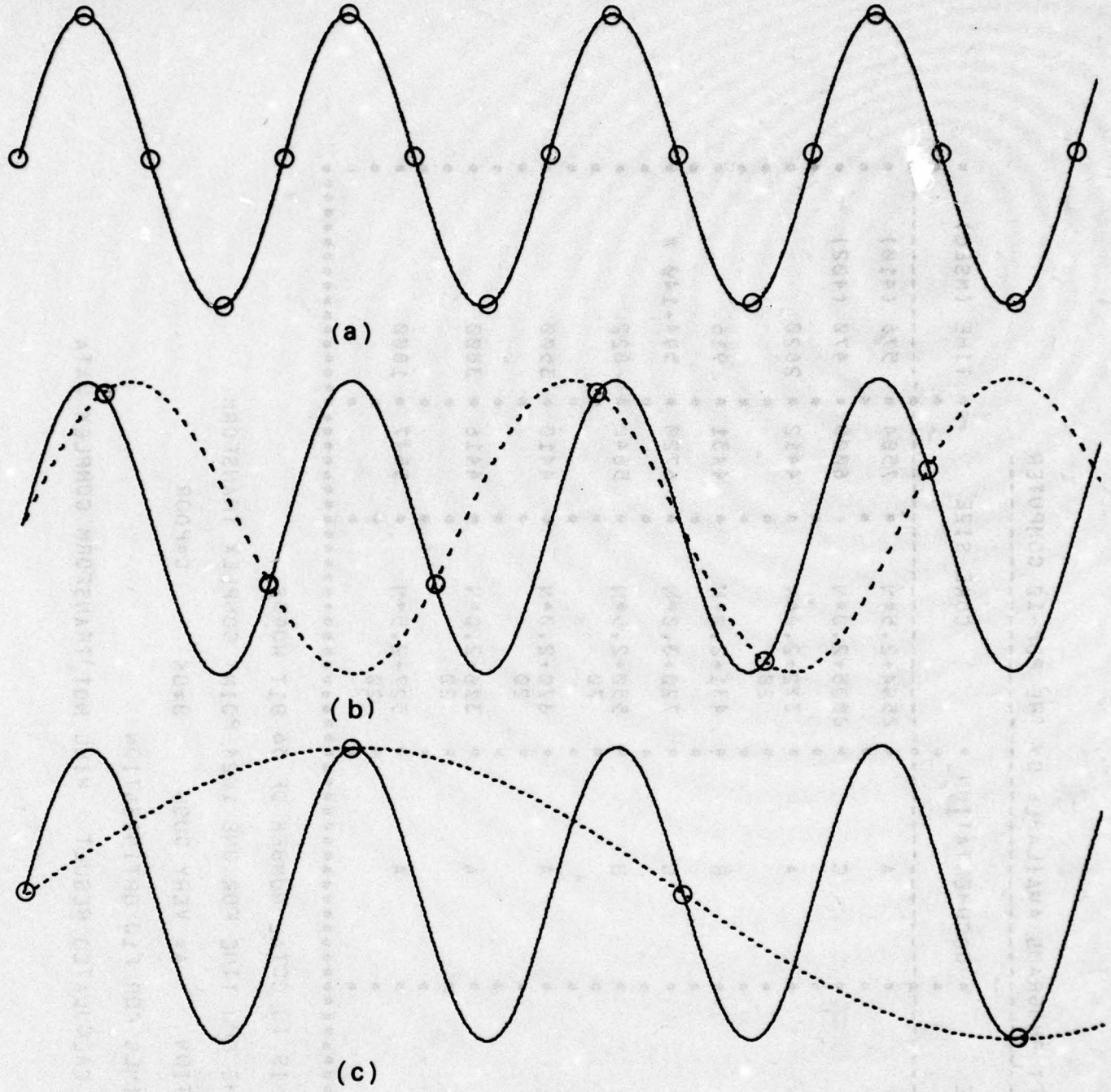


FIG. 5.1. EFFECT OF ALIASING; SINU SOIDAL WAVE SAMPLED AT 3 SAMPLING RATES (Sampling points circled)

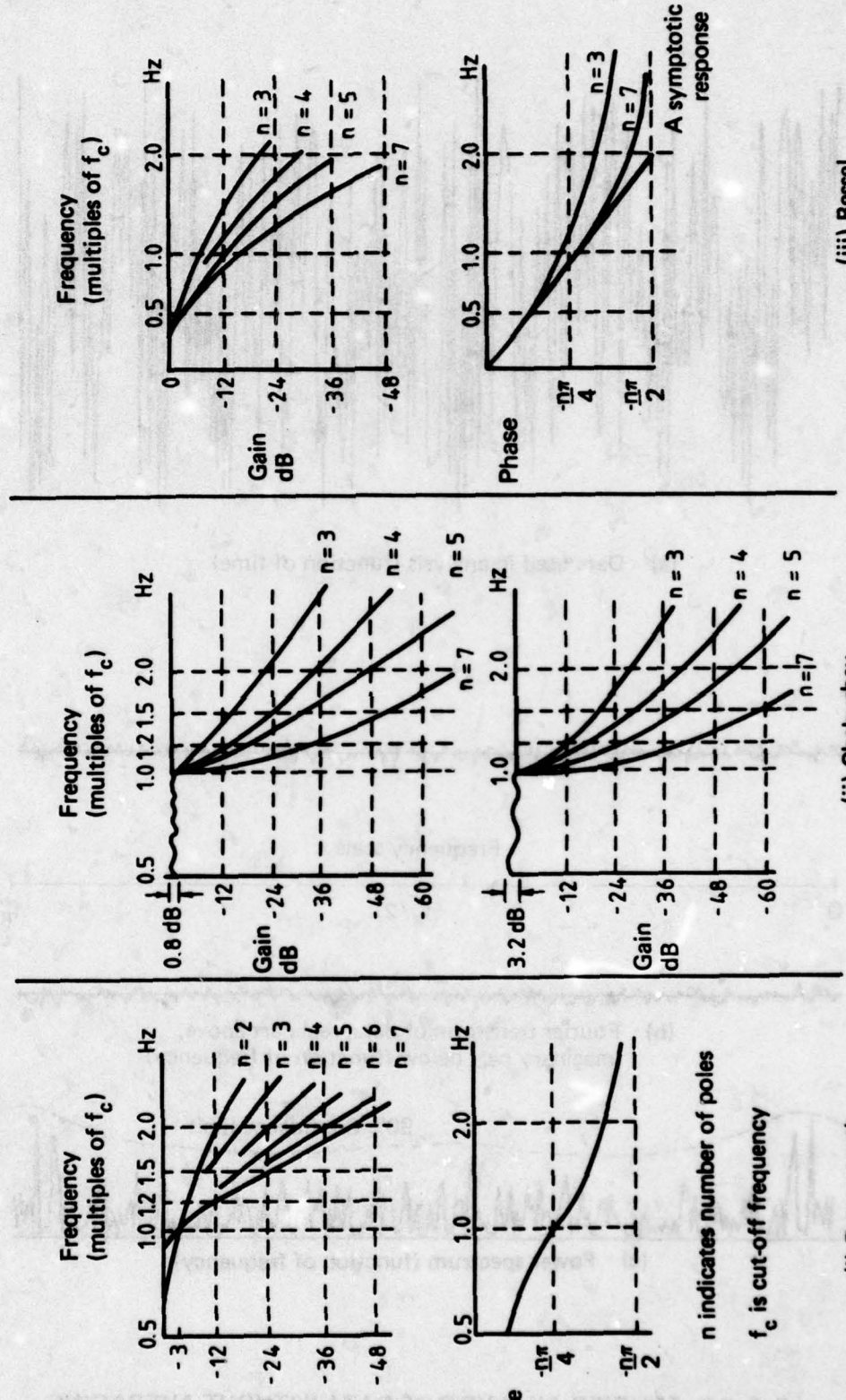


FIG. 5.2 RESPONSE OF SOME WELL KNOWN FILTERS

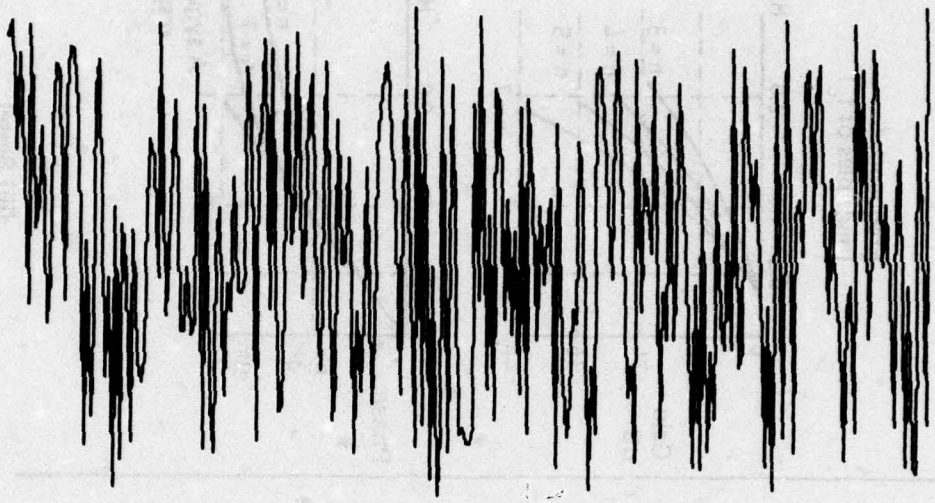

(a) Data used in analysis (function of time)

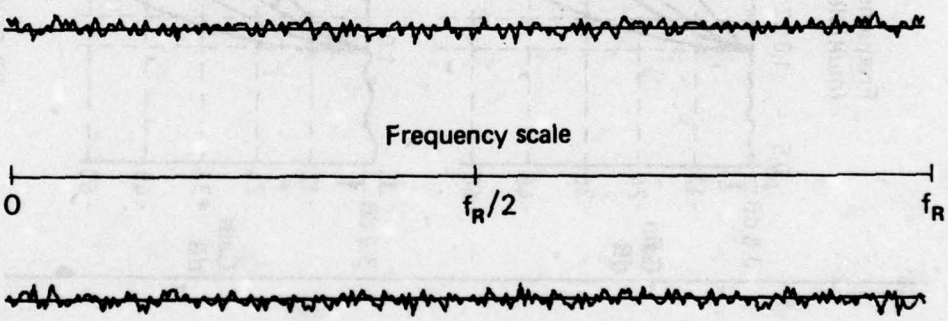


(b) Fourier transform of data; real part above, imaginary part below (function of frequency)

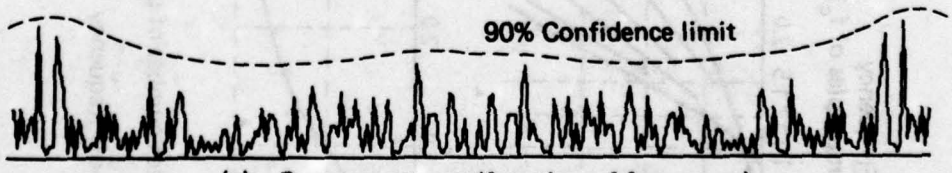


(c) Power spectrum (function of frequency)

FIG. 5.3 FOURIER ANALYSIS OF DATA WITHOUT AVERAGING

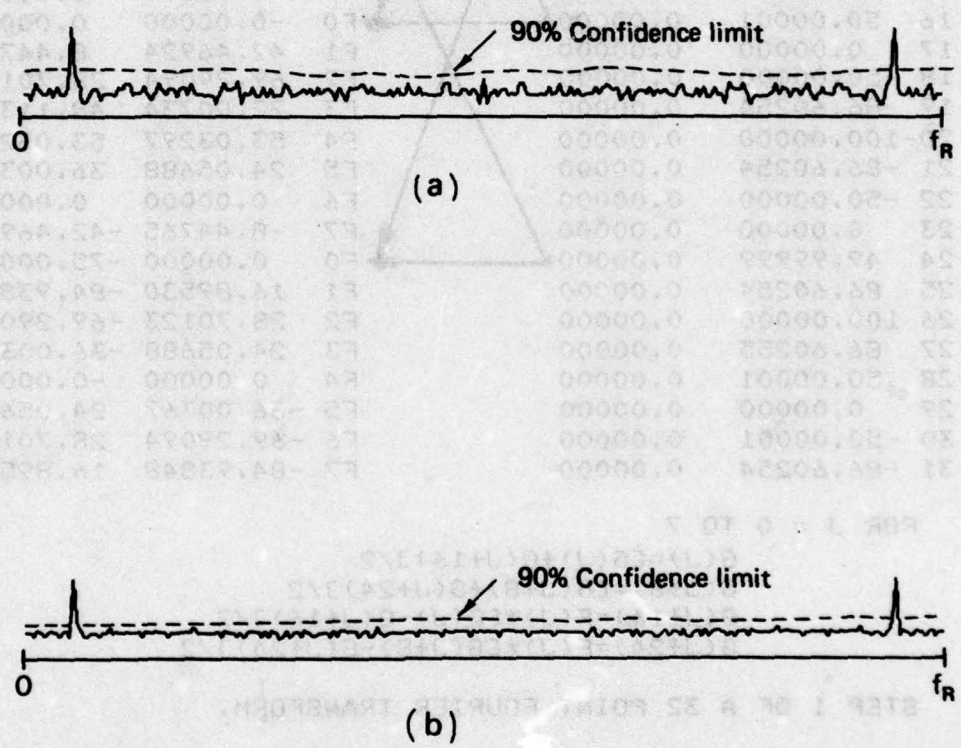


**FIG. 5.4 FOURIER ANALYSIS OF DATA WITH AVERAGING; POWER SPECTRA OBTAINED**
**(a) From 20 summations**
**(b) From 200 summations**
**OF 256 POINT FOURIER TRANSFORM**

| # | OLD ARRAY REAL | OLD ARRAY IMAG | FACTOR | NEW ARRAY REAL | NEW ARRAY IMAG |
|---|---|---|---|---|---|
| 0 | 50.00000 | 0.00000 | | 50.00000 | 0.00000 |
| 1 | 86.60254 | 0.00000 | | 43.30127 | 0.00000 |
| 2 | 100.00000 | 0.00000 | | 25.00000 | 0.00000 |
| 3 | 86.60254 | 0.00000 | | -0.00000 | 0.00000 |
| 4 | 50.00000 | 0.00000 | | -25.00000 | 0.00000 |
| 5 | 0.00000 | 0.00000 | | -43.30127 | 0.00000 |
| 6 | -50.00000 | 0.00000 | | -50.00000 | 0.00000 |
| 7 | -86.60254 | 0.00000 | | -43.30127 | 0.00000 |
| 8 | -100.00000 | 0.00000 | | -25.00001 | 0.00000 |
| 9 | -86.60254 | 0.00000 | | -0.00000 | 0.00000 |
| 10 | -50.00000 | 0.00000 | | 25.00000 | 0.00000 |
| 11 | 0.00000 | 0.00000 | | 43.30127 | 0.00000 |
| 12 | 50.00000 | 0.00000 | | 50.00000 | 0.00000 |
| 13 | 86.60254 | 0.00000 | | 43.30127 | 0.00000 |
| 14 | 100.00000 | 0.00000 | | 25.00000 | 0.00000 |
| 15 | 86.60254 | 0.00000 | | 0.00000 | 0.00000 |
| 16 | 50.00001 | 0.00000 | F0 | -0.00000 | 0.00000 |
| 17 | 0.00000 | 0.00000 | F1 | 42.46924 | 8.44765 |
| 18 | -50.00000 | 0.00000 | F2 | 69.29094 | 28.70123 |
| 19 | -86.60254 | 0.00000 | F3 | 72.00734 | 48.11376 |
| 20 | -100.00000 | 0.00000 | F4 | 53.03297 | 53.03297 |
| 21 | -86.60254 | 0.00000 | F5 | 24.05688 | 36.00367 |
| 22 | -50.00000 | 0.00000 | F6 | 0.00000 | 0.00000 |
| 23 | 0.00000 | 0.00000 | F7 | -8.44765 | -42.46924 |
| 24 | 49.99999 | 0.00000 | F0 | 0.00000 | -75.00000 |
| 25 | 86.60254 | 0.00000 | F1 | 16.89530 | -84.93847 |
| 26 | 100.00000 | 0.00000 | F2 | 28.70123 | -69.29094 |
| 27 | 86.60255 | 0.00000 | F3 | 24.05688 | -36.00367 |
| 28 | 50.00001 | 0.00000 | F4 | 0.00000 | -0.00000 |
| 29 | 0.00000 | 0.00000 | F5 | -36.00367 | 24.05688 |
| 30 | -50.00001 | 0.00000 | F6 | -69.29094 | 28.70124 |
| 31 | -86.60254 | 0.00000 | F7 | -84.93848 | 16.89530 |

```
FOR J = 0 TO 7
        G(J)=[G(J)+G(J+16)]/2
        G(J+8)=[G(J+8)+G(J+24)]/2
        G(J+16)=F(J)*[G(J)-G(J+16)]/2
        G(J+24)=F(J)*[G(J+8)-G(J+24)]/2
```

STEP 1 OF A 32 POINT FOURIER TRANSFORM.

FIGURE 5.5

| # | OLD ARRAY REAL | OLD ARRAY IMAG | FACTOR | NEW ARRAY REAL | NEW ARRAY IMAG |
|---|---|---|---|---|---|
| 0 | 50.00000 | 0.00000 | | 12.50000 | 0.00000 |
| 1 | 43.30127 | 0.00000 | | 21.65063 | 0.00000 |
| 2 | 25.00000 | 0.00000 | | 25.00000 | 0.00000 |
| 3 | -0.00000 | 0.00000 | | 21.65064 | 0.00000 |
| 4 | -25.00000 | 0.00000 | | 12.50000 | 0.00000 |
| 5 | -43.30127 | 0.00000 | | 0.00000 | 0.00000 |
| 6 | -50.00000 | 0.00000 | | -12.50000 | 0.00000 |
| 7 | -43.30127 | 0.00000 | | -21.65063 | 0.00000 |
| 8 | -25.00001 | 0.00000 | F0 | 37.50000 | 0.00000 |
| 9 | -0.00000 | 0.00000 | F2 | 20.00257 | 8.28533 |
| 10 | 25.00000 | 0.00000 | F4 | 0.00000 | 0.00000 |
| 11 | 43.30127 | 0.00000 | F6 | -8.28533 | -20.00257 |
| 12 | 50.00000 | 0.00000 | F8 | 0.00000 | -37.50000 |
| 13 | 43.30127 | 0.00000 | F10 | 16.57066 | -40.00514 |
| 14 | 25.00000 | 0.00000 | F12 | 26.51648 | -26.51648 |
| 15 | 0.00000 | 0.00000 | F14 | 20.00257 | -8.28533 |
| 16 | -0.00000 | 0.00000 | | -0.00000 | -37.50000 |
| 17 | 42.46924 | 8.44765 | | 29.68227 | -38.24541 |
| 18 | 69.29094 | 28.70123 | | 48.99609 | -20.29485 |
| 19 | 72.00734 | 48.11376 | | 48.03211 | 6.05504 |
| 20 | 53.03297 | 53.03297 | | 26.51649 | 26.51648 |
| 21 | 24.05688 | 36.00367 | | -5.97340 | 30.03027 |
| 22 | 0.00000 | 0.00000 | | -34.64547 | 14.35062 |
| 23 | -8.44765 | -42.46924 | | -46.69306 | -12.78697 |
| 24 | 0.00000 | -75.00000 | F0 | -0.00000 | 37.50000 |
| 25 | 16.89530 | -84.93847 | F2 | -6.05503 | 48.03210 |
| 26 | 28.70123 | -69.29094 | F4 | -20.29482 | 48.99606 |
| 27 | 24.05688 | -36.00367 | F6 | -29.68225 | 38.24538 |
| 28 | 0.00000 | -0.00000 | F8 | -26.51649 | 26.51648 |
| 29 | -36.00367 | 24.05688 | F10 | -17.01077 | 25.45843 |
| 30 | -69.29094 | 28.70124 | F12 | -14.35062 | 34.64544 |
| 31 | -84.93848 | 16.89530 | F14 | -23.97523 | 42.05870 |

```
FOR K = 0 , 16
        FOR J = 0 TO 7
                G(J+K)=[G(J+K)+G(J+K+8)]/2
                G(J+K+8)=F(2*J)*[G(J+K)-G(J+K+8)]/2
```

STEP 2 OF A 32 POINT FOURIER TRANSFORM.

FIGURE 5.6

| # | OLD ARRAY REAL | OLD ARRAY IMAG | FACTOR | NEW ARRAY REAL | NEW ARRAY IMAG |
|---|---|---|---|---|---|
| 0 | 12.50000 | 0.00000 | | 12.50000 | 0.00000 |
| 1 | 21.65063 | 0.00000 | | 10.82532 | 0.00000 |
| 2 | 25.00000 | 0.00000 | | 6.25000 | 0.00000 |
| 3 | 21.65064 | 0.00000 | | 0.00000 | 0.00000 |
| 4 | 12.50000 | 0.00000 | F0 | -0.00000 | 0.00000 |
| 5 | 0.00000 | 0.00000 | F4 | 7.65465 | 7.65465 |
| 6 | -12.50000 | 0.00000 | F8 | 0.00000 | 18.75000 |
| 7 | -21.65063 | 0.00000 | F12 | -15.30930 | 15.30930 |
| 8 | 37.50000 | 0.00000 | | 18.75000 | -18.75000 |
| 9 | 20.00257 | 8.28533 | | 18.28662 | -15.85990 |
| 10 | 0.00000 | 0.00000 | | 13.25824 | -13.25824 |
| 11 | -8.28533 | -20.00257 | | 5.85862 | -14.14395 |
| 12 | 0.00000 | -37.50000 | F0 | 18.75000 | 18.75000 |
| 13 | 16.57066 | -40.00514 | F4 | -15.85989 | 18.28661 |
| 14 | 26.51648 | -26.51648 | F8 | -13.25824 | -13.25824 |
| 15 | 20.00257 | -8.28533 | F12 | 14.14394 | -5.85861 |
| 16 | -0.00000 | -37.50000 | | 13.25824 | -5.49176 |
| 17 | 29.68227 | -38.24541 | | 11.85444 | -4.10757 |
| 18 | 48.99609 | -20.29485 | | 7.17531 | -2.97212 |
| 19 | 48.03211 | 6.05504 | | 0.66952 | -3.36596 |
| 20 | 26.51649 | 26.51648 | F0 | -13.25824 | -32.00824 |
| 21 | -5.97340 | 30.03027 | F4 | 36.74526 | -11.53291 |
| 22 | -34.64547 | 14.35062 | F8 | 17.32273 | 41.82078 |
| 23 | -46.69306 | -12.78697 | F12 | -40.15204 | 26.82873 |
| 24 | -0.00000 | 37.50000 | | -13.25824 | 32.00824 |
| 25 | -6.05503 | 48.03210 | | -11.53290 | 36.74527 |
| 26 | -20.29482 | 48.99606 | | -17.32272 | 41.82075 |
| 27 | -29.68225 | 38.24538 | | -26.82874 | 40.15204 |
| 28 | -26.51649 | 26.51648 | F0 | 13.25824 | 5.49176 |
| 29 | -17.01077 | 25.45843 | F4 | -4.10756 | 11.85443 |
| 30 | -14.35062 | 34.64544 | F8 | -7.17531 | -2.97210 |
| 31 | -23.97523 | 42.05870 | F12 | 3.36595 | -0.66952 |

```
FOR K = 0 , 8 , 16 , 24
        FOR J = 0 TO 3
                G(J+K)=[G(J+K)+G(J+K+4)]/2
                G(J+K+4)=F(4*J)*[G(J+K)-G(J+K+4)]/2
```

STEP 3 OF A 32 POINT FOURIER TRANSFORM

FIGURE 5.7

| # | OLD ARRAY REAL | OLD ARRAY IMAG | FACTOR | NEW ARRAY REAL | NEW ARRAY IMAG |
|---|---|---|---|---|---|
| 0 | 12.50000 | 0.00000 | | 9.37500 | 0.00000 |
| 1 | 10.82532 | 0.00000 | | 5.41266 | 0.00000 |
| 2 | 6.25000 | 0.00000 | F0 | 3.12500 | 0.00000 |
| 3 | 0.00000 | 0.00000 | F8 | 0.00000 | 5.41266 |
| 4 | -0.00000 | 0.00000 | | -0.00000 | 9.37500 |
| 5 | 7.65465 | 7.65465 | | -3.82733 | 11.48198 |
| 6 | 0.00000 | 18.75000 | F0 | -0.00000 | -9.37500 |
| 7 | -15.30930 | 15.30930 | F8 | 3.82733 | 11.48198 |
| 8 | 18.75000 | -18.75000 | | 16.00412 | -16.00412 |
| 9 | 18.28662 | -15.85990 | ETC. | 12.07262 | -15.00193 |
| 10 | 13.25824 | -13.25824 | F0 | 2.74588 | -2.74588 |
| 11 | 5.85862 | -14.14395 | F8 | 0.85798 | 6.21400 |
| 12 | 18.75000 | 18.75000 | | 2.74588 | 2.74588 |
| 13 | -15.85989 | 18.28661 | | -0.85797 | 6.21400 |
| 14 | -13.25824 | -13.25824 | F0 | 16.00412 | 16.00412 |
| 15 | 14.14394 | -5.85861 | F8 | -12.07261 | -15.00192 |
| 16 | 13.25824 | -5.49176 | | 10.21678 | -4.23194 |
| 17 | 11.85444 | -4.10757 | | 6.26198 | -3.73677 |
| 18 | 7.17531 | -2.97212 | F0 | 3.04147 | -1.25982 |
| 19 | 0.66952 | -3.36596 | F8 | 0.37080 | 5.59246 |
| 20 | -13.25824 | -32.00824 | | 2.03224 | 4.90627 |
| 21 | 36.74526 | -11.53291 | | -1.70339 | 7.64791 |
| 22 | 17.32273 | 41.82078 | F0 | -15.29049 | -36.91451 |
| 23 | -40.15204 | 26.82873 | F8 | 19.18082 | 38.44865 |
| 24 | -13.25824 | 32.00824 | | -15.29048 | 36.91450 |
| 25 | -11.53290 | 36.74527 | | -19.18082 | 38.44865 |
| 26 | -17.32272 | 41.82075 | F0 | 2.03224 | -4.90625 |
| 27 | -26.82874 | 40.15204 | F8 | 1.70339 | 7.64792 |
| 28 | 13.25824 | 5.49176 | | 3.04147 | 1.25983 |
| 29 | -4.10756 | 11.85443 | | -0.37080 | 5.59246 |
| 30 | -7.17531 | -2.97210 | F0 | 10.21678 | 4.23193 |
| 31 | 3.36595 | -0.66952 | F8 | -6.26198 | -3.73675 |

```
FOR K = 0 , 4 , 8 , ..... , 24 , 28
        FOR J = 0 , 1
                G(J+K)=[G(J+K)+G(J+K+2)]/2
                G(J+K+2)=F(8*J)*[G(J+K)-G(J+K+2)]/2
```

STEP 4 OF A 32 POINT FOURIER TRANSFORM

FIGURE 5.8

| # | OLD ARRAY REAL | OLD ARRAY IMAG | | FACTOR | NEW ARRAY REAL | NEW ARRAY IMAG |
|---|---|---|---|---|---|---|
| 0 | 9.37500 | 0.00000 | → | | 7.39383 | 0.00000 |
| 1 | 5.41266 | 0.00000 | → | F0 | 1.98117 | 0.00000 |
| 2 | 3.12500 | 0.00000 | → | | 1.56250 | 2.70633 |
| 3 | 0.00000 | 5.41266 | → | F0 | 1.56250 | -2.70633 |
| 4 | -0.00000 | 9.37500 | | | -1.91366 | 10.42849 |
| 5 | -3.82733 | 11.48198 | ETC. | F0 | 1.91366 | -1.05349 |
| 6 | -0.00000 | -9.37500 | | | 1.91366 | 1.05349 |
| 7 | 3.82733 | 11.48198 | | F0 | -1.91366 | -10.42849 |
| 8 | 16.00412 | -16.00412 | | | 14.03837 | -15.50302 |
| 9 | 12.07262 | -15.00193 | | F0 | 1.96575 | -0.50110 |
| 10 | 2.74588 | -2.74588 | | | 1.80193 | 1.73406 |
| 11 | 0.85798 | 6.21400 | | F0 | 0.94395 | -4.47994 |
| 12 | 2.74588 | 2.74588 | | | 0.94395 | 4.47994 |
| 13 | -0.85797 | 6.21400 | | F0 | 1.80193 | -1.73406 |
| 14 | 16.00412 | 16.00412 | | | 1.96576 | 0.50110 |
| 15 | -12.07261 | -15.00192 | | F0 | 14.03837 | 15.50302 |
| 16 | 10.21678 | -4.23194 | | | 8.23938 | -3.98435 |
| 17 | 6.26198 | -3.73677 | | F0 | 1.97740 | -0.24759 |
| 18 | 3.04147 | -1.25982 | | | 1.70614 | 2.16632 |
| 19 | 0.37080 | 5.59246 | | F0 | 1.33533 | -3.42614 |
| 20 | 2.03224 | 4.90627 | | | 0.16443 | 6.27709 |
| 21 | -1.70339 | 7.64791 | | F0 | 1.86782 | -1.37082 |
| 22 | -15.29049 | -36.91451 | | | 1.94517 | 0.76707 |
| 23 | 19.18082 | 38.44865 | | F0 | -17.23566 | -37.68158 |
| 24 | -15.29048 | 36.91450 | | | -17.23565 | 37.68157 |
| 25 | -19.18082 | 38.44865 | | F0 | 1.94517 | -0.76708 |
| 26 | 2.03224 | -4.90625 | | | 1.86781 | 1.37083 |
| 27 | 1.70339 | 7.64792 | | F0 | 0.16443 | -6.27709 |
| 28 | 3.04147 | 1.25983 | | | 1.33533 | 3.42614 |
| 29 | -0.37080 | 5.59246 | | F0 | 1.70614 | -2.16631 |
| 30 | 10.21678 | 4.23193 | | | 1.97740 | 0.24759 |
| 31 | -6.26198 | -3.73675 | | F0 | 8.23938 | 3.98434 |

FOR K = 0 , 2 , 4 , ..... , 28 , 30

G(K)=[G(K)+G(K+1)]/2

G(K+1)=F(0)*[G(K)-G(K+1)]/2

STEP 5 OF A 32 POINT FOURIER TRANSFORM

FIGURE 5.9

| # | OLD ARRAY REAL | OLD ARRAY IMAG | FACTOR | NEW ARRAY REAL | NEW ARRAY IMAG |
|---|---|---|---|---|---|
| 0 | 7.39383 | 0.00000 | | 7.39383 | 0.00000 |
| 1 | 1.98117 | 0.00000 | | 8.23938 | -3.98435 |
| 2 | 1.56250 | 2.70633 | | 14.03837 | -15.50302 |
| 3 | 1.56250 | -2.70633 | | -17.23565 | 37.68157 |
| 4 | -1.91366 | 10.42849 | | -1.91366 | 10.42849 |
| 5 | 1.91366 | -1.05349 | | 0.16443 | 6.27709 |
| 6 | 1.91366 | 1.05349 | | 0.94395 | 4.47994 |
| 7 | -1.91366 | -10.42849 | | 1.33533 | 3.42614 |
| 8 | 14.03837 | -15.50302 | | 1.56250 | 2.70633 |
| 9 | 1.96575 | -0.50110 | | 1.70614 | 2.16632 |
| 10 | 1.80193 | 1.73406 | | 1.80193 | 1.73406 |
| 11 | 0.94395 | -4.47994 | | 1.86781 | 1.37083 |
| 12 | 0.94395 | 4.47994 | | 1.91366 | 1.05349 |
| 13 | 1.80193 | -1.73406 | | 1.94517 | 0.76707 |
| 14 | 1.96576 | 0.50110 | | 1.96576 | 0.50110 |
| 15 | 14.03837 | 15.50302 | | 1.97740 | 0.24759 |
| 16 | 8.23938 | -3.98435 | | 1.98117 | 0.00000 |
| 17 | 1.97740 | -0.24759 | | 1.97740 | -0.24759 |
| 18 | 1.70614 | 2.16632 | | 1.96575 | -0.50110 |
| 19 | 1.33533 | -3.42614 | | 1.94517 | -0.76708 |
| 20 | 0.16443 | 6.27709 | | 1.91366 | -1.05349 |
| 21 | 1.86782 | -1.37082 | | 1.86782 | -1.37082 |
| 22 | 1.94517 | 0.76707 | | 1.80193 | -1.73406 |
| 23 | -17.23566 | -37.68158 | | 1.70614 | -2.16631 |
| 24 | -17.23565 | 37.68157 | | 1.56250 | -2.70633 |
| 25 | 1.94517 | -0.76708 | | 1.33533 | -3.42614 |
| 26 | 1.86781 | 1.37083 | | 0.94395 | -4.47994 |
| 27 | 0.16443 | -6.27709 | | 0.16443 | -6.27709 |
| 28 | 1.33533 | 3.42614 | | -1.91366 | -10.42849 |
| 29 | 1.70614 | -2.16631 | | -17.23566 | -37.68158 |
| 30 | 1.97740 | 0.24759 | | 14.03837 | 15.50302 |
| 31 | 8.23938 | 3.98434 | | 8.23938 | 3.98434 |

BIT REVERSAL STEP
G(J) IS INTERCHANGED WITH G(K)
IF J IS BIT REVERSED K

I.E. IF J = 2 = 00010 BINARY
32 BIT REVERSE J = 01000 = 8 DECIMAL
THEREFORE G(2) IS INTERCHANGED WITH G(8)

STEP 6 OF A 32 POINT FOURIER TRANSFORM

FIGURE 5.10

# CHAPTER 6 : THE RETRIEVAL OF SIGNALS FROM NOISE

## 6.1 Introduction

In many practical measurement situations, the signal under observation is accompanied by significant amounts of "noise" i.e., other signals unrelated to the signal under observation and adding no additional information to it. This noise may be wide band (e.g. Gaussian or thermal noise), narrow band (e.g. 50 Hz electrical mains interference) or a mixture of both. The amplitude of the noise can be sufficient to swamp the signal completely. In many instances, signal retrieval techniques can considerably improve the signal to noise ratio (SNR).

Techniques such as coherence functions can aid in the estimation of the occurrence time of a signal, i.e. the response to a known stimulus, but where the signal waveform is required other techniques must be employed. This chapter contains a discussion of some signal retrieval techniques and their application. Further information can be obtained from the references listed at the end of the chapter.

## 6.2 The Retrieval Process

It will be evident from the Introduction that any noise retrieval process when viewed in the frequency domain must amount, explicitly or otherwise, to a filtering operation. Where the dominant components of the power spectra of signal and noise are significantly different, use of appropriate high pass, low pass, band pass or band stop filtering can provide an adequate means of retrieving the signal. The realisation and use of such filters will be discussed later in this Section. However in many practical measurements, the signal and noise spectra overlap and, where the signal is a response to a repetitive stimulus, other techniques can prove useful; some of these will now be discussed.

### 6.2.1 Coherent Averaging

A time-limited signal that is buried in noise time-locked to an external stimulus can often be retrieved by coherent averaging. By synchronized additive combinations of repeated sweeps of the noisy signal, a selective enhancement of the signal waveform can be achieved at the expense of the associated noise and it can be shown that this technique produces a non-linear filter, i.e. one that acts on the noise leaving the

signal unaffected, even when the two share dominant Fourier components.

The averaging process is achieved by synchronising each recorded sweep of data with a trigger waveform having a constant time relationship to the signal. Successive sweeps are averaged, so that, if the signal repeats identically in form every time it appears, the averaged waveform contains a constant amount of signal. If the noise is uncorrelated with the signal, the summation of the different noise samples will reduce the noise by partial cancellation because the contribution of the noise is sometimes positive, sometimes negative. Thus, as will be discussed further below, the noise is, in effect, reduced and filtered. The effect is shown in Fig. 6.1.

(a) Calculation of signal enhancement: Averaging can be performed using either a digital computer or a special-purpose digital averager. When writing a computer programme, it is convenient to store and display a running average of the stored sweeps of data. In calculating the effect of averaging it will be assumed that the signal and noise are uncorrelated, that the noise is ergodic and that each sample of it is independent and that the signal is stationary and time invariant.

If the noisy signal is $x(t)$, then

$$x(t) = s(t) + n(t) \qquad (6.2.1)$$

where $s(t)$ is the signal and $n(t)$ is the noise. A convenient measure of the relative signal strength is the "signal-to-noise ratio", SNR(t) given by

$$SNR(t) = s(t) \; / \sqrt{(\bar{n}^2)} \qquad (6.2.2)$$

where the denominator in eqn (6.2.2) is the root mean square (RMS) value of the noise. (Note that the signal-to-noise ratio is sometimes defined as the ratio of signal and noise power.) It can be shown that, after $K$ sweeps of data have been accumulated and the results averaged the SNR becomes

$$SNR(K,t) = Ks(t) \; / \sqrt{\{KR_{nn}(o) + 2 \sum_{j=1}^{K-1} (K-j) \, R_{nn}(j,t)\}} \qquad (6.2.3)$$

when $R_{nn}(t)$ is the auto-correlation function of the noise. If this last is known the SNR is completely specified. For the case of Gaussian noise,

$$R_{nn}(0) = \bar{n}^2$$
$$R_{nn}(t) = 0 \qquad (t \neq 0) \tag{6.2.4}$$

and (6.2.3) reduces to

$$SNR\ (K,t) = \sqrt{K}\ \ s(t)\ /\ \sqrt{(\bar{n}^2)} \tag{6.2.5}$$

(If $n(t)$ is violently asymmetrical, then the average value will contain a DC shift that has been ignored here).

When $n(t)$ is not Gaussian, the averaging can lead to an enhancement either much better or much worse than $\sqrt{k}$ depending on the form of the second term in the denominator of eqn (6.2.3).

There are two important points to note here :

(i) If $n(t)$ contains a significant oscillatory term then SNR(K,t) may itself be an oscillating function, making the use of averaging somewhat hazardous.

(ii) For a $\sqrt{K}$ improvement, it is necessary only that

$$\sum_{j=1}^{K-1} (K-j)\ R_{nn}(j,t) = 0 \tag{6.2.6}$$

In addition to Gaussian noise, this condition can be shown to be satisfied for any noise having a power spectral density of the form $|\omega|^{-\alpha}$ where $0 < \alpha \leq 1$ (e.g. "flicker" noise in semi-conductors).

The RMS noise figures calculated above are the mean or "expected" values of a stochastic process. Thus, in practice, as the average is being built up, the RMS noise will oscillate about its expected value

causing the signal to rise out of the noise somewhat erratically. If $R_{nn}(t)$ is known, it is possible to estimate the likely magnitude of variability of the noise fluctuations in the output. It is thus possible to estimate confidence limits on any signal component thought to have arisen through the averaging process and to separate stimulus-locked fluctuations of the averaged noise.

Where these fluctuations are Gaussian or near Gaussian applications of Student's t-test at the 95% level may be sufficient. Where the form of the distribution is unknown confidence limits can be estimated using the Chebyshev inequality or by the use of non-parametric statistics.

(b) Practical limitations of averaging: In practice the assumptions made in (a) above regarding the characteristics of the signal and noise will not all be valid. In particular,

(i) any latency "jitter" in the signal relative to its stimulus will smear the averaged signal,

(ii) the signal and noise will never be entirely uncorrelated since the "window" involved in the sampling process ensures that both have frequency components in common and, hence, a finite cross-correlation. In most, but not all, instances this will not be a significant factor.

In the absence of statistical checks the validity of any averaged response must always be a subject of some concern.

(c) Non-linear filtering: Since the averaging process adds successive signal components in phase, the frequency spectrum of the signal remains unaltered. The effect on the noise spectrum, however, will often be quite considerable. As an example, consider the case where sweeps of the signal are taken at intervals of $T_o$ seconds. Then after $K$ sweeps the total recorded noise at any time $t$ after the commencement of a sweep will be

$$n_{tot}(t) = n(t) + n(t + T_o) + n(t + 2T_o) + \cdots + n(t + (K-1)T_o) \qquad (6.2.7)$$

On taking the Fourier transform of this last, employing the shift theorem, and summing the resultant series it will be found that

$$N_{tot}(f) = N(f) \sin \{K\pi fT_o\} / \sin \{\pi fT_o\} \qquad (6.2.8)$$

i.e. the transform $N(f)$ has been low-pass filtered. Thus, in this instance, the averaging process acts as a non-linear filter, filtering the noise but not the signal.

(d) Phase domain averaging: Averaging in the phase domain can be used to extract a signal whose shape remains constant but whose latency is subject to considerable jitter. The basis of the technique is illustrated diagrammatically in Fig. 6.2. It will be seen that the signal shape is preserved.

Phase domain techniques are particularly effective in processing noisy signals because most of the information determining the shape of the signal is contained in the phase spectrum. The additions of small amounts of signal to noise will lead to a significant degree of organisation in the phase spectrum of the noise.

(e) A word of warning: In the practical realisation of data acquisition and averaging, due consideration should be given to the choice of word length. If, for example, the signal of interest is immersed in 40 db of noise, the 6 most significant bits of the word will contain noise only and it will be seen that the use of 10-bit A-to-D conversion will considerably degrade the signal-to-noise ratio of the acquired signal and prolong the averaging process.

The effects of rounding and truncation errors on the addition and division operations needed to compute the averaged signal can be quite significant if double precision arithmetic is not used.

## 6.3 Digital Filtering

### 6.3.1 General

In many instances, averaging or other non-linear signal processing techniques are either inapplicable or yield unsatisfactory

results. Where the residual signal and noise have significantly different frequency spectra, linear filtering may effect a significant improvement in the signal-to-noise ratio. Although the specification of a suitable filter clearly implies some "a priori" knowledge of signal and noise spectra, in most cases enough information is available to allow a reasonable specification to be drawn up initially even if later changes have to be made.

Where the signals are already stored in a digital computer the use of digital techniques enables extremely precise filter characteristics to be realised, as well as saving the costs involved in the construction of complex analogue filters. In addition digital filters can provide characteristics unrealisable in analogue form (without the use of delay times).

Digital filtering can be produced by time or frequency domain manipulations of data and these two approaches will now be considered in detail.

### 6.3.2 Time Domain Filters

Time domain averages are realised using moving average techniques analogous to the moving average series discussed in Chapter 4. The sampling process converts the signal time series $\{x(t)\}$ to the stored data array $\{x(n)\}$ by sampling it at intervals of $\Delta t$ sec (where the interval is sufficiently small to avoid aliasing problems).

(a) Non-recursive filters: A non-recursive filter merely replaces $x(n)$ with a weighted sum $y(n)$ made up from $x(n)$ and neighbouring points in the data array. This may be expressed in terms of a difference equation

$$y(n) = \sum_{j=-m}^{r-1} a_j \, x(n-j) \qquad (6.3.1)$$

where $m, r = 0, 1, 2 \ldots$

Such a filter's operation may be illustrated by the symmetrical three point filter series

$$y(n) = (1/4)\, x(n-1) + (1/2)\, x(n) + (1/4)\, x(n+1) \qquad (6.3.2)$$

(Note that this filter will be physically unrealisable since $x(n+1)$ is ahead of $x(n)$ in time. This is of no concern where [illegible] is already stored.)

Since the sampling rate is $1/(\Delta t)$ the filter transfer function

$$H(\omega) = Y(\omega) / X(\omega) \qquad (6.3.3)$$

(where $\omega = 2\pi f$ and $X$ and $Y$ are the Fourier transforms of $x$ and $y$) may be found by noting that, from the shift theorem, the transform of $x(n-j)$ is

$$X(\omega) \exp(-ij\omega(\Delta t))$$

and, hence, the filter becomes

$$Y(\omega) = (1/2)\, X(\omega) + (1/4)\{\exp(i\omega(\Delta t)) + \exp(-i\omega(\Delta t))\}X(\omega) \qquad (6.3.4)$$

Hence,

$$H(\omega) = \{1 + \cos(\omega\Delta t)\}/2 \qquad (6.3.5)$$

This transfer function is shown in Fig. 6.3. Note that the data band width is limited by the sampling rate to

$$\omega_{max} = \pi/2(\Delta t) \text{ rad/sec} \qquad (6.3.6)$$

so that only the first "quadrant" of the filter expression is of significance. Note also that the low pass filter introduces zero phase shift. This is a result of the symmetrical filter algorithm and is a useful property where measurement of the latency of components in the filtered signal is important. The effect of a filter containing a pair of critically damped conjugate poles is included for comparison.

The corresponding high-pass filter

$$H(\omega) = (1 - \cos \omega t) /2 \qquad (6.3.7)$$

is obtained using the series

$$y(n) = -(1/4)\, x(n-1) + (1/2)\, x(n) - (1/4)\, x(n+1) \qquad (6.3.8)$$

These filters can be shown to have 3 db cut-off points of

$$f_o = 0.183 / (\Delta t) \text{ Hz} \qquad (6.3.9)$$

The filtering operation may be repeated as many times as desired. This has the effect of lowering $f_o$ in the low-pass case, or raising $f_o$ in the high pass case by a factor

$$0.875 \arccos \{2^{(1-1/2k)} - 1\} \qquad (6.3.10)$$

after $k$ operations.

The design of digital filters having given transfer functions can be carried out in the $z$ plane using the conformal transformation

$$z = \exp (i\omega t) \qquad (6.3.11)$$

This permits the reduction of the difference euqation to a transfer function e.g. for the above filter (6.3.2) use of (6.3.11) gives

$$Y(z) = (1/4)\, (1/z + 2 + z)\, X(z) \qquad (6.3.12)$$

$$\text{i.e.,} \quad H(z) = \{1 + (z + 1/z) /2\} /2 \qquad (6.3.13)$$

Discussion of $z$ plane design techniques can be found in various texts.

(b) Recursive (auto-regressive) filters: While the non-recursive filter is extremely simple the algorithms become large and unwieldy where high performance filters are required. In these situations, recursive

algorithms (analogous to the autoregressive series of Chapter 4) may be of use. These include previously filtered data points in each moving average calculation. This leads to a drastic reduction in the number of multiplications required.

The general difference equation may be written as

$$y(n) = \sum_{j=-m}^{r-1} a_j x(n-j) + \sum_{j=1-m}^{s-1} b_j y(n-j) \qquad (6.3.14)$$

The power of recursive filters is best illustrated by a simple example. Consider the non-recursive series

$$y(n) = \sum_{j=-p}^{p} x(n+j) \qquad (6.3.15)$$

comprising (2p+1) unit samples, or transforming into the z plane

$$H(z) = Y(z) \,/\, X(z) = (z^{-p} + \cdots + 1 + \cdots + z^{p}) \qquad (6.3.16)$$

$$\text{i.e.,} \quad H(z) = \{z^{p} - z^{-(p+1)}\} \,/\, \{1 - z^{-1}\} \qquad (6.3.17)$$

On applying the inverse transformation, the result is

$$y(n) - y(n-1) = x(n+p) - x(n-(p+1)) \qquad (6.3.18)$$

$$\text{i.e.,} \quad y(n) = y(n-1) + x(n+p) - x(n-(p+1)) \qquad (6.3.19)$$

This recursive difference equation contains three points only. Note that this filter algorithm is equivalent to a non-recursive algorithm containing <u>any</u> number of points.

Recursive filters may need some additional non-recursive filters to remove considerable side lobes. Coefficient rounding and truncation can lead to instability and oscillation. With these qualifications recursive filters can provide a useful tool in signal processing. They are particularly attractive for the design of real time digital filters utilising shift registers and digital multipliers.

Although only high and low pass filters have been discussed above, it will be evident that band-pass and band-stop filters can be realised using the same techniques.

### 6.3.3 Fourier Transform Filters

Transformed data may be manipulated in the frequency domain by multiplying the real and imaginary components by the appropriate weighting function. The modified data may then be returned to the time domain. Very high performance filters can be produced using this technique which is, in theory, capable of producing "brick wall filters" having an infinite asymptotic slope at the cut-off frequencies.

In practice, the complete removal of one or two spectral components as a means of removing a single interfering signal can lead to unacceptable "ringing" in the filtered signal. This effect can be reduced by tapering the spectral components each side of the components being removed. Where only simple filters are required time domain filtering will in general be simpler and more convenient.

### 6.3.4 Selection of Filter Characteristics - Optimal Filtering

Choice of a filter to separate signal and noise is normally approached on a somewhat empirical basis. Where there is a priori knowledge of the spectral characteristics of signal and noise it is possible to arrive at an optimal filter characteristic for signal recovery.

Filter characteristics generated by this technique are often physically unrealisable but this is unimportant where digital filters are used. The filters discussed here will be assumed time-invariant, but the same approach may be extended to signal-dependent (e.g. Kalman) filters. Consider a signal $s(t)$, having a power spectral density $P_s(f)$, immersed in noise $n(t)$, having a power spectral density $P_n(f)$. After signal and noise are passed through a filter $H(f)$ (the inverse of which is $h(t)$), the signal-to-noise ratio is

$$SNR(t) = \{\int_{-\infty}^{\infty} s(t-\lambda)\ h^2(\lambda)\ d\lambda\} \ / \ \{\int_{-\infty}^{\infty} n^2(t-\lambda)\ h^2(\lambda)\ d\lambda\} \quad (6.3.20)$$

Choosing $H(f)$ to maximise SNR leads to the result

$$H(f) = S(f) \quad (6.3.21)$$

i.e., the optimal filter should follow the a priori estimate of the signal spectrum $S$ (the transform of $s$).

Another approach is to find the filter that makes the output $s + n$, the best least squares estimate of the signal. This leads to the result

$$H(f) \simeq P_s(f) \ / \ P_n(f) \quad (6.3.22)$$

This operation will practically always lead to a physically unrealisable filter. In most cases the simple result (6.3.21) will be adequate.

## 6.4 Spectral Analysis

### 6.4.1 General

In many instances the signal being measured is continuous (e.g. mechanical vibration in response to an applied force). In such cases the signal is best characterised by its frequency spectrum. This normally takes the form of a power spectrum, indicating the distribution of energy with frequency. (This has the advantage of being easier to interpret and use than the magnitude spectrum in many engineering situations.)

Any finite data sample can supply only an estimate of the true power spectrum; thus spectral computation is meaningless without an assessment of the relevant confidence limits.

### 6.4.2 Power Spectrum Estimation

Once the spectral resolution and confidence limits required, and the number of data points in each FFT are known, it is possible to

specify the experimental protocol. This has already been discussed in Chapter 5 but, for completeness, will be outlined again here.

The sampling interval, $\Delta t$, is of course governed by the Nyquist criterion

$$\Delta t \leqslant 1/2\, f_{max} \qquad (6.4.1)$$

where $f_{max}$ is the highest frequency component in the signal. The number of points, N, in each data block is linked to the frequency resolution, $\Delta f$ by

$$\Delta f = 1/(N\, \Delta t) \qquad (6.4.2)$$

It thus pays to use as large a value of N as possible. The total length of signal required is determined by the amplitude uncertainty that can be tolerated in the computed spectrum. Provided that the spectrum is reasonably flat or has been "pre-whitened" by the use of a suitable filter then adjacent spectral harmonics will be essentially uncorrelated and will follow a chi-squared distribution having 2 degrees of freedom per harmonic (since each contains a real and an imaginary contribution). The chi-squared distribution having k degrees of freedom has a mean k and a variance 2k. Hence, the coefficient of variation, CV, is

$$CV = \text{standard deviation / mean} = \sqrt{(2/k)} \qquad (6.4.3)$$

In particular, if $k = 2$, $CV = 1$, and, however long the data run, the computed spectra will be unreliable. The problem can be overcome either by the use of frequency smoothing or segment averaging to increase the effective number of degrees of freedom.

(a) Frequency smoothing: If m neighbouring values of the computed spectrum are averaged then the resolution $\Delta f$ will be degraded to $m(\Delta f)$ but each point of the new spectrum will have 2m degrees of freedom. The spectrum will therefore have a CV given by

$$CV = 1/\sqrt{m} \qquad (6.4.3)$$

Note that, using this method, a total data length

$$T_r = mN(\Delta t) \tag{6.4.4}$$

will be required to maintain the original resolution.

(b) Segment averaging: An alternative approach is to average corresponding values from $q$ separate spectra. This will lead to a CV given by

$$CV = 1/\sqrt{q} \tag{6.4.5}$$

and a total data run $T_t$ of

$$T_t = qN(\Delta t) \tag{6.4.6}$$

The above two techniques may be combined if desired. Thus for a given value of CV, it is possible to specify completely a procedure for the calculation of power spectra. Tables of the chi-squared distribution for $k$ degrees of freedom are readily available, but many of these do not include the large values of $k$ often required for data processing. For $k > 50$, the relationship

$$\chi_p^2 \simeq \{z_p + \sqrt{(2k - 1)}\}^2/2 \tag{6.4.7}$$

where $z_p$ is the corresponding percentile deviation for a normal distribution will often be found useful.

(c) Effective degrees of freedom: The final spectrum can be used to calculate the number of effective degrees of freedom, $k_e$. This last will be less than $k$ since, in general, the assumption of independence of adjacent spectral values will not be entirely valid. The equivalent bandwidth $B_E$ of the power spectrum $P(f)$ is given by

$$B_E = \{\int_0^\infty P(f)\, df\}^2 / \int_0^\infty \{P(f)\}^2\, df \tag{6.4.8}$$

In terms of this,

$$k_e = 2 B_E T_r - 1 \qquad (6.4.9)$$

This result may be used to correct the confidence limits of the computed spectrum.

(d) Bias in power spectral estimation: Any estimate of a process based on a finite amount of information will generally display some bias, however small. This may be defined by

$$b = G_e - G \qquad (6.4.10)$$

where $b$ is the bias

$G$ is the true value of the function

$G_e$ is its estimated value.

In ref.1 it is shown that the normalised mean square error of a power spectrum is

$$t^2 \simeq (1/bT_r) + (b^4/576)\ (P^{11}/P)^2 \qquad (6.4.11)$$

The second term represents a bias which becomes important for a spectrum having significant dips or peaks. It will thus be evident that an extremely careful choice of $b$ must be made when computing such spectra. It can be shown that the effect of this bias error is to compress the dynamic range of the spectrum, minimising the amplitudes of peaks or troughs.

References

1 BENDAT, J.S. and PIERSOL, A.G. Random Data. Wiley, New York, 1971.

2 BLACKMAN, R.B. and TUKEY, J.W. The Measurement of Power Spectra. Dover, New York, 1959.

3 ERNST, R.R. Sensitivity Enhancement in Magnetic Resonance. Rev. Sci. Insts. vol. 36, p.1689, 1965.

4 JENKINS, G.M. and WAHS, D.G. Spectral Analysis and its Applications. Holden-Day, San Francisco, 1968.

5 LYNN, P.A. An Introduction to the Analysis and Processing of Signals. Macmillan, London, 1973.

6 RADER, C.M. and GOLD, B. Digital Filter Design Techniques in the Frequency Domain. Proc. IEEE. vol. 55, p. 149, 1967.

7 SCHWARTZ, M. and SHAW, L. Signal Processing. McGraw-Hill, New York, 1975.

8 WILCOCK, A.H. and KIRSNER, R.L.G. A Digital Filter for Biological Data. Med. and Biol. Eng., vol. 7, p. 653, 1969.

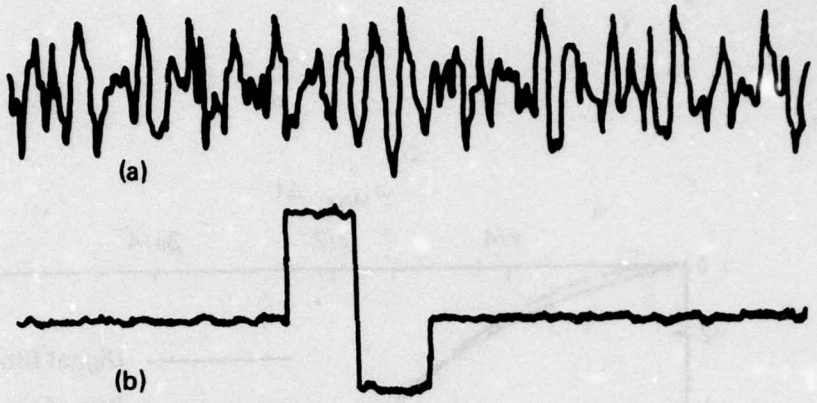


(a) Single sweep of noisy signal

(b) Average of 1024 sweeps

FIG. 6.1 RETRIEVAL OF SIGNAL BY AVERAGING

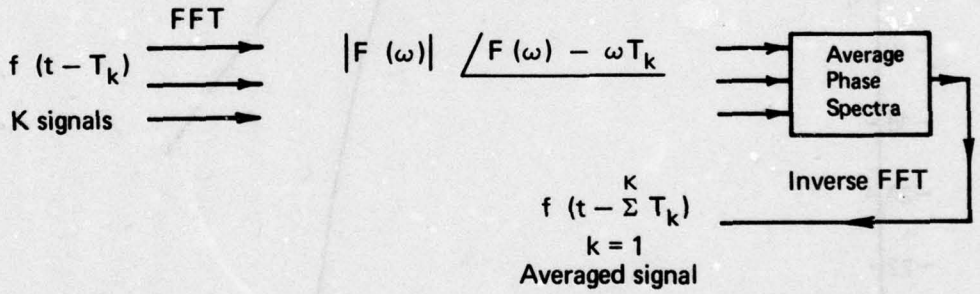


FIG. 6.2 PHASE DOMAIN AVERAGING

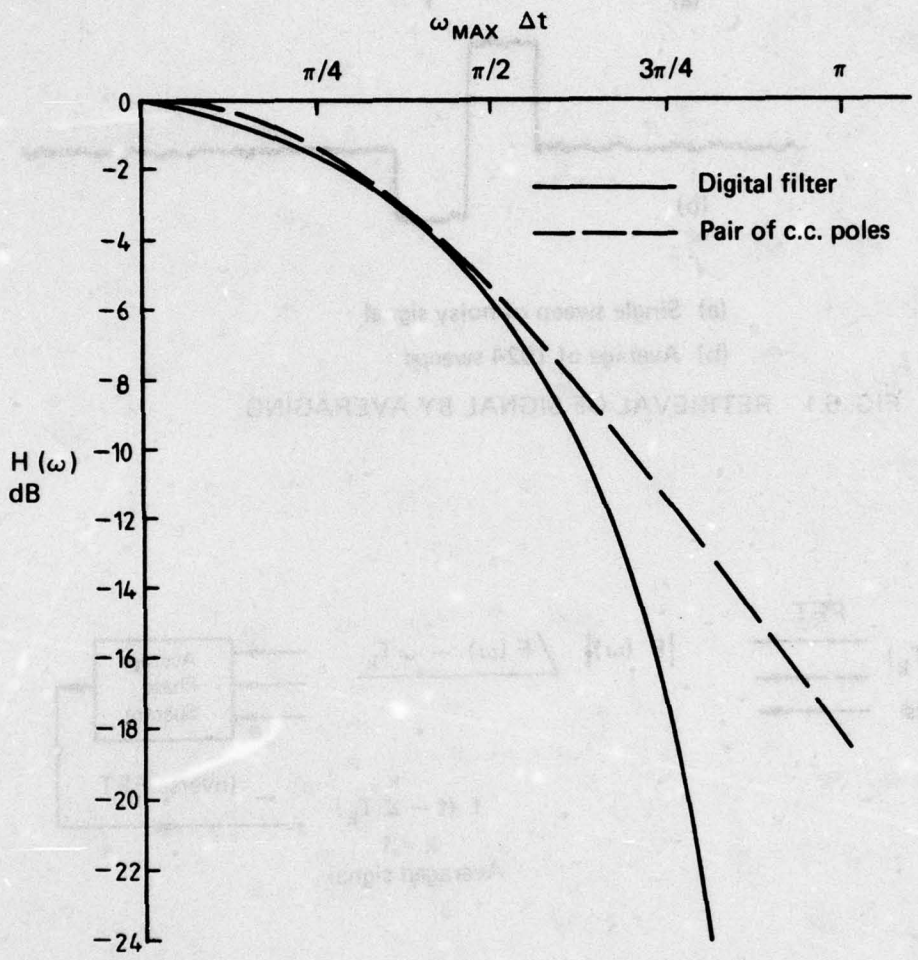


FIG. 6.3 NON-RECURSIVE FILTER TRANSFER FUNCTION

# CHAPTER 7 : APPLICATION OF FOURIER TRANSFORMS TO VIBRATION PROBLEMS

## 7.1 Introduction

Fourier transforms are a powerful tool for solving many vibration problems and their use is finding more and more acceptance each day. Their use allows a more rapid determination of the natural modes and frequencies of a structure without a consequent loss of accuracy. This forms the basis of the so-called "chirp" test wherein the structure is excited by rapid frequency sweeps and the transient response measured at various locations on the structure. The required natural modes and frequencies are then calculated from the measured data, contrasting with the so-called "steady-state" test in which each of the modes is excited in turn and individually measured.

The most important concept in this approach to vibration analysis is that of a transfer function of a system. This function is a mathematical description of the system and describes the way in which it responds to an input. If the system is a mechanical one, i.e. if it consists of masses, springs and dampers then the transfer function describes the relationship between an exciting force and the resulting vibration. Similarly the transfer function of an electrical system may relate a current at some point in the circuit to an applied voltage.

To help illustrate the properties of a transfer function the equations of motion of a simple, single-degree-of-freedom, mechanical system will be developed in Section 7.2. The extension to a multi-degree-of-freedom system will be indicated but not rigorously performed. The following Sections then describe some of the experimental methods used to determine the transfer function.

## 7.2 Linear System Theory

Consider the simple mass-spring-damper system shown in Fig.7.1. If the mass is excited by a force f(t), it responds such that its amplitude of vibration is given by x(t). This simple system possesses two important properties which are fundamental to the application of Fourier transform theory. Firstly it is linear. That is, if a force $f_1(t)$ produces a response $x_1(t)$, and another force $f_2(t)$ produces a

different response $x_2(t)$, then a combined force $f_1(t) + f_2(t)$ will produce a response $x_1(t) + x_2(t)$. This implies that a complicated forcing function may be considered in terms of simpler constituent functions, the response to each determined, and then these responses combined to give the response to the original force. The second important property is that of shift invariance. This implies that if a force is shifted in time (i.e., delayed or advanced) the only effect is that the response is shifted by the same amount.

The second-order, linear differential equation relating the response $x(t)$ to the applied force $f(t)$ is

$$m \ddot{x}(t) + b \dot{x}(t) + k x(t) = f(t) \qquad (7.2.1)$$

where $m$ is the mass

$b$ is the viscous damping coefficient

and $k$ is the stiffness.

Given a particular $f(t)$, this eqn (7.2.1) may then be solved for $x(t)$ by the standard mathematical techniques.

For our purposes here we will consider the special case of a simple harmonic forcing function. This may be written a number of ways but it is easiest to use the complex exponential notation :

$$f(t) = F.\exp(i\omega t) = F.(\cos\omega t + i \sin \omega t) \qquad (7.2.2)$$

where, as is usual, only the real or the imaginary part represents the relevant physical quantity. Here $F$ is the peak amplitude of the force which oscillates at a circular frequency of $\omega$ radians/second. Since the system is linear the steady (non-transient) response $x(t)$ will also be simple harmonic of frequency $\omega$ but with a phase lag of $\phi$. This response function may also be written in a number of ways, such as

$$x(t) = A \exp(i\omega t + i\phi) = (Y + i Z) \exp(i\omega t) = X \exp(i\omega t) \qquad (7.2.3)$$

where A, Y and Z are real but X is complex. We will use the last form, i.e.

$$x(t) = X \exp(i\omega t) \tag{7.2.4}$$

Substituting eqns (7.2.2) and (7.2.4) into eqn (7.2.1) gives

$$(-\omega^2 m + i\omega b + k)\, X \exp(i\omega t) = F.\exp(i\omega t) \tag{7.2.5}$$

i.e.,

$$X = F \,/\, (-\omega^2 m + i\omega b + k)$$

$$= F \;\; H(\omega) \tag{7.2.6}$$

$H(\omega)$ is, of course, complex and its modulus and argument (or phase) are given by

$$|H| = 1/\sqrt{((-\omega^2 m + k)^2 + \omega^2 b^2)} \tag{7.2.7}$$

and

$$\arg(H) = \arctan((-\omega b)/(-\omega^2 m + k)) \tag{7.2.8}$$

The relationships given in eqns (7.2.7) and (7.2.8) are illustrated as functions of $\omega$ in Figs. 7.2a and 7.2b. The two figures may be combined to give a single vector plot or Argand diagram as shown in Fig. 7.2c.

It may be worth noting here that since F is real the argument of H is the same phase lag $\phi$ as given in eqn (7.2.3). The natural frequency of the system is defined to be that frequency for which this phase is $-\Pi/2$ radians and Fig. 7.2b shows that this frequency is $\sqrt{(k/m)}$ radians/second. The peak of the modulus curve shown in Fig. 7.2a occurs at a lower frequency, $\sqrt{((k/m) - (b^2/2m^2))}$. The height of the peak in Fig.7.2a is given by

$$|H|_M = 2m/(b\sqrt{(4mk - b^2)}) \tag{7.2.9}$$

and the so-called "static deflection" (i.e., $|H|$ at zero frequency) is

$$|H(o)| = 1/k \tag{7.2.10}$$

Then the magnification at resonance is given by

$$R = |H|_M \; / \; |H(o)| = 2m\,k \; / \; ( b \sqrt{(4m\,k - b^2)}) \qquad (7.2.11)$$

The resonant frequency (or peak amplitude frequency) is given by

$$\omega_M = \sqrt{(k/m - b^2/(2m^2))} \qquad (7.2.12)$$

If the values of $R$ and $\omega_M$ are known the two parameters

$$\bar{\omega} = \sqrt{(k/m)} = \text{natural frequency} \qquad (7.2.13)$$

and $$\gamma = b/(2\sqrt{(mk)}) = \text{ratio of damping to critical} \qquad (7.2.14)$$

may be evaluated exactly.

If the damping is small ($\gamma \lesssim 0.05$, i.e. $\lesssim$ 5% of critical damping) it can be shown that the following approximate relations may be used :

$$\bar{\omega} \approx (1 + 1 \; / \; (4\,R^2))\; \omega_M \qquad (7.2.15)$$

and $$\gamma \approx 1/(2R) \qquad (7.2.16)$$

These two important parameters which characterise the system may also be obtained from the vector plot illustrated in Fig.7.2c. Again if the damping is small ($\gamma \lesssim 0.05$) this plot is almost circular with the negative imaginary axis as a diameter. The natural frequency, $\bar{\omega}$, is the frequency at which this diameter intersects the circle. Then if a second diameter drawn normal to the first intersects the circle at frequencies $\omega_A$ and $\omega_B$

$$\gamma \approx (\omega_B - \omega_A) \; / \; (2\,\bar{\omega}) \qquad (7.2.17)$$

Whilst this derivation of the form of $H(\omega)$ is for a single degree-of-freedom system, the extension to many degrees-of-freedom is straight-forward.

Eqn (7.2.5) then becomes a set of simultaneous equations, usually written in matrix form. The exact form of $H(\omega)$ is then more difficult to write down but the plot of its modulus will be similar to that for the single degree-of-freedom system (Fig. 7.2a) except that there will, in general, be more peaks (Fig. 7.3). Each peak indicates a resonance, and there is a natural frequency $\bar{\omega}$, and damping ratio $\gamma$, associated with each resonance. If the peaks are well separated, each may be considered in isolation, and the single-degree-of-freedom eqns (7.2.15) and (7.2.16) may be applied. If however, some of the peaks are grouped closely together, more sophisticated techniques must be used.

## 7.3 Transfer Function

The function $H(\omega)$ which relates the simple harmonic response $X$, to the simple harmonic applied force $F$, is the transfer function of the system. This transfer function is rarely known explicitly but must be determined experimentally, usually as a table of complex values at discrete frequencies over some range of interest. It may be determined directly by applying a simple harmonic force of some frequency $\omega$ to the system and, after all the transients have decayed, measuring the simple harmonic response. This gives the value of $H$ at the one frequency $\omega$. The frequency is then altered and the process repeated until the whole of Fig. 7.3 is built up. This is a very slow process and it is far quicker, theoretically at least, to use Fourier transforms.

Consider any arbitrary forcing function $f(t)$. This may be expressed in terms of its Fourier integral as

$$f(t) = (1/2\pi) \int_{-\infty}^{\infty} F(\omega) \exp(i\omega t)\, d\omega \qquad (7.3.1)$$

This implies that the arbitrary function $f(t)$ may be broken down into an integral sum of simple harmonic components over a continuous range of frequencies. Then each component produces a response given by eqn (7.2.6) as

$$X(\omega) = H(\omega)\, F(\omega) \qquad (7.3.2)$$

Due to the linearity and shift-invariance of our system the total response $x(t)$ is the integrated sum of the component responses, viz

$$x(t) = (1/2\pi) \int_{-\infty}^{\infty} X(\omega) \exp(i\omega t)\, d\omega \qquad (7.3.3)$$

Then from eqn (7.3.2) the transfer function is given by

$$H(\omega) = X(\omega) / F(\omega) \qquad (7.3.4)$$

where, as shown in the first lecture, the frequency domain functions are given by

$$X(\omega) = \int_{-\infty}^{\infty} x(t) \exp(-i\omega t)\, dt \qquad (7.3.5)$$

and

$$F(\omega) = \int_{-\infty}^{\infty} f(t) \exp(-i\omega t)\, dt \qquad (7.3.6)$$

The eqn (7.3.4) may be considered as the definition of the transfer function $H(\omega)$.

Referring again to eqn (7.3.2) it can be seen that this is in the form of a product and so, from the convolution theorem,

$$x(t) = h(t) * f(t) \qquad (7.3.7)$$

where * indicates convolution and where $h(t)$ is the Fourier transform of $H(\omega)$. Consider the special case of $f(t) = \delta(t)$ where $\delta(t)$ is the delta function, i.e. an impulse. Then the associated response $x_I(t)$ is given by

$$\begin{aligned} x_I(t) &= h(t) * \delta(t) \\ &= h(t) \end{aligned} \qquad (7.3.8)$$

Thus $h(t)$, the Fourier transform of the transfer function, is the impulse response of the system and is given by

$$h(t) = (1/2\pi) \int_{-\infty}^{\infty} H(\omega) \exp(i\omega t)\, d\omega \qquad (7.3.9)$$

For the single degree-of-freedom system described earlier this gives

$$h(t) = A \exp(-\lambda t) \sin(\omega_D t) \qquad (7.3.10)$$

where A is an amplitude factor = $\omega_D/m$

$\omega_D$ is the circular decay frequency = $\bar{\omega}\sqrt{(1-\gamma^2)}$ and $\lambda$ is the decay rate = $\gamma\bar{\omega}$. A typical plot of h(t) is shown in Fig. 7.4. For a multi-degree-of-freedom system the form of the impulse response involves combinations of terms like the one in eqn (7.3.10).

The physical interpretation of eqn (7.3.2) is straightforward. The forcing function f(t) is considered to be the sum of a number of harmonic oscillations, the amplitudes of which are specified by F(ω). The transfer function H(ω) indicates how the system responds to each frequency, giving the responses as X(ω). The equivalent equation in the time domain is eqn (7.3.7). The physical significance of this equation is as follows. The forcing function f(t) is considered to be a train of impulses of the appropriate amplitude and time delay. The response of the system to each of these impulses is obtained and the convolution integral sums them to give the final response.

(Whilst in the above the Fourier transform has always been written in the integral form, in practical calculations it generally proves necessary to approximate this by a DFT which, of course, is evaluated using the FFT algorithm. This should be borne in mind throughout.)

## 7.4 Determination of the Transfer Function

It was shown in eqn (7.3.4) that the transfer function could be determined from the Fourier transforms of the input force and of the resulting response of the system. This is true for any forcing function and we will first consider the special case of the impulsive force.

Eqn (7.3.9) shows that the impulse response of the system is the Fourier transform of the transfer function. This then indicates an apparently easy method of determining the transfer function - i.e., by applying an impulse and then taking the Fourier transform of the response. The difficulty in this approach is in generating the impulsive force. It must be of infinite amplitude and zero duration, a pair of conditions impossible to meet. Even an approximation to this, e.g. a hammer blow for mechanical systems or a voltage pulse for electrical systems, is not always successful as it requires a high energy concentration (i.e. large

amplitude) in order to generate sufficient length of time-history response for accurate analysis, especially if the damping (b) is high. This application of a high energy-concentration pulse is not always acceptable as it may damage the system under investigation. It is better if the input energy is applied at a lower level to the system but for a longer time.

In this latter approach the determination of the transfer function is achieved using eqn (7.3.4) directly with a convenient form of input force. The calculation is more accurate if the applied force has nearly equal energy at all frequencies over the range of interest and there are three common forcing functions with this property. The first is white noise which is defined as a random signal which has equal energy at all frequencies, provided that the noise is of sufficiently long duration. Usually it cannot be obtained in the real world so a pseudo-white noise is used. This signal has nearly equal energies over some limited range of interest. This forcing function and its power spectrum are shown in Fig. 7.5a.

A more common forcing function is the fast frequency sweep. If the transfer function is required over some range $\omega_1$ to $\omega_2$, then the frequency of the force is increased rapidly from $\omega_1$ to $\omega_2$ whilst exciting the system. This force and its power spectrum are shown in Fig. 7.5b. This is perhaps the most commonly used force input.

The third forcing function is called the "impulse sine" and is the same as the sinc function described in the first lecture. It is of the form

$$f(t) = \sin(\omega_1(t-T)) \;/\; (t-T) \qquad (7.4.1)$$

This function and its power spectrum are shown in Fig. 7.5c. The power spectrum is essentially flat up to the cut-off frequency $\omega_1$ and in the limit as $\omega_1$ approaches infinity, the impulse sine becomes the delta function. However, it is easier to generate than a true impulse and it has a lower energy concentration. Moreover it applies energy to the system over a relatively wide frequency range much more quickly than a frequency sweep. For these reasons it is a very useful forcing function especially when test conditions cannot be maintained for more than a brief period.

The foregoing method of determining the transfer function involved dividing the Fourier transform of the response by that of the input force. However the transfer function may also be calculated from a knowledge of the cross- , and auto-power spectra of the response and input.

The auto-power spectrum of the response $X(\omega)$ was defined in earlier lectures as

$$G_{XX}(\omega) = X(\omega)\ X^*(\omega) \tag{7.4.2}$$

where * indicates the complex conjugate. Then substituting from eqn (7.3.2) gives

$$G_{XX}(\omega) = (H(\omega).F(\omega)).(H(\omega).F(\omega))^*$$

$$= |H(\omega)|^2 . G_{FF}(\omega) \tag{7.4.3}$$

where $G_{FF}(\omega)$ is the auto-power spectrum of the exciting force. Thus

$$|H(\omega)|^2 = G_{XX}(\omega) / G_{FF}(\omega) \tag{7.4.4}$$

Eqn (7.4.4) allows the calculation of only the modulus of the transfer function with no phase information. However this is often sufficient to determine many of the properties (e.g., natural frequencies and dampings) of the system. Eqn (7.4.4) may also be used when the exact form of the input is unknown but where its power spectrum is known as would be the case if the excitation were electrical noise. For this case the energy spectrum of the input is frequently assumed to be flat over the frequency range of interest.

In order to obtain the phase content of the transfer function from the power spectra, the cross-power spectrum must be used. This is defined as

$$G_{XF}(\omega) = X(\omega).\ F^*(\omega)$$

$$= (H(\omega).\ F(\omega)).\ F^*(\omega)$$

$$= H(\omega).\ G_{FF}(\omega) \tag{7.4.5}$$

whence

$$H(\omega) = G_{XF}(\omega) \; / \; G_{FF}(\omega) \qquad (7.4.6)$$

Note that eqn (7.4.6) may only be applied if the forcing function f(t) is known. The cross-power spectrum may then be determined from the cross-correlation function or from the Fourier transforms of the input and response.

## 7.5 Effect of Noise

In the preceding Sections it was assumed that the Fourier transform of both the input force and of the response were obtainable and also that they were both precise and accurate. If, as usually occurs in the real world, the signals are contaminated with noise then ways to overcome this must be found.

Consider now the case where the response $X(\omega)$ is partially due to the input force $F(\omega)$, and partially due to some random noise $N(\omega)$.

i.e.,

$$X(\omega) = H(\omega).\ F(\omega) + N(\omega) \qquad (7.5.1)$$

Then if eqn (7.3.4) is used to determine the noise contaminated transfer function $H_N(\omega)$, we get

$$H_N(\omega) = X(\omega) \; / \; F(\omega)$$

$$= H(\omega) + N(\omega) \; / \; F(\omega) \qquad (7.5.2)$$

The last term is an error which must be removed or at least minimised. Here advantage may be taken of the randomness of the noise which implies that its mean is zero. Hence if many estimates of the "noisy" transfer function $H_N(\omega)$ are taken and then averaged, the mean result is a better estimate of the true transfer function $H(\omega)$ as the error term should average to zero. This of course requires the noise to be truly random and that a sufficiently large number of estimates be taken.

Next consider the effect of this noise on the power spectrum of the response. From eqn (7.4.2)

$$G_{XX}(\omega) = (H(\omega).\ F(\omega) + N(\omega)).\ (H(\omega).\ F(\omega) + N(\omega))^*$$

$$= |H(\omega)|^2\ G_{FF}(\omega) + H(\omega)\ G_{FN}(\omega) + H^*(\omega)\ G_{NF}(\omega) + G_{NN}(\omega) \qquad (7.5.3)$$

where the last three terms represent the error due to the noise. The two cross-power spectra $G_{FN}(\omega)$ and $G_{NF}(\omega)$ are measures of the relationship between the input force $F(\omega)$ and the noise $N(\omega)$ (they are in fact the Fourier transforms of the cross-correlations of these two signals). Since there is no such relationship these two spectra have random values and will average to zero if sufficient estimates of $G_{XX}(\omega)$ are taken and averaged. The last term $G_{NN}(\omega)$ is a measure of the energy of the noise at each frequency and so will not average to zero but will always remain as an error term. If we denote this mean value of $G_{XX}(\omega)$ by $\bar{G}_{XX}(\omega)$ we get

$$\bar{G}_{XX}(\omega) = |H(\omega)|^2\ G_{FF}(\omega) + \bar{G}_{NN}(\omega) \qquad (7.5.4)$$

Applying eqn (7.4.4) to obtain the modulus of the transfer function we get

$$|H_N(\omega)|^2 = \bar{G}_{XX}(\omega)\ /\ G_{FF}(\omega)$$

$$= |H(\omega)|^2 + \bar{G}_{NN}(\omega)\ /\ G_{FF}\ (\omega) \qquad (7.5.5)$$

The error term here is always positive so that the estimated transfer function is always larger than the true one. However, if the noise and input force have roughly constant energy over the frequency range, then the function $|H_N(\omega)|^2$ may still have most of the essential characteristics of the true function $|H(\omega)|^2$. That is, the peaks representing resonances may still be apparent, especially if the damping is low and qualitative estimates of this damping may be made from the "sharpness" of the peaks. If, however, either $G_{NN}(\omega)$ or $G_{FF}(\omega)$ varies greatly over the frequency range, $|H_N(\omega)|^2$ must be treated carefully.

Eqn (7.4.5) gives the expression for the cross-spectrum as

$$G_{XF}(\omega) = (H(\omega).\ F(\omega) + N(\omega)).\ F^*(\omega)$$

$$= H(\omega).\ G_{FF}(\omega) + G_{NF}(\omega) \qquad (7.5.6)$$

Again this quantity $G_{NF}(\omega)$ should have random values and average to zero, so the mean cross-spectrum $\bar{G}_{XF}(\omega)$ is

$$\bar{G}_{XF}(\omega) = H(\omega).\ G_{FF}(\omega) \qquad (7.5.7)$$

whence

$$H_N(\omega) = \bar{G}_{XF}(\omega)\ /\ G_{FF}(\omega)$$

$$= H(\omega) \qquad (7.5.8)$$

Hence this estimate of the transfer function is unaffected by uncorrelated noise, provided only that a sufficiently large number of averages has been taken.

This then leads to the coherence function which is a means of determining both the amount of noise present and also whether sufficient averages have been taken. The coherence function $\Gamma^2(\omega)$ is defined as

$$\Gamma^2(\omega) = |G_{XF}(\omega)|^2\ /\ (G_{XX}(\omega).\ G_{FF}(\omega)) \qquad (7.5.9)$$

Making use of eqn (7.4.5) we get

$$|G_{XF}(\omega)|^2 = G_{XF}(\omega).\ G^*_{XF}(\omega)$$

$$= X(\omega).\ F^*(\omega).\ X^*(\omega).\ F(\omega)$$

$$= G_{XX}(\omega).\ G_{FF}(\omega) \qquad (7.5.10)$$

Hence $\Gamma^2(\omega) = 1$ for all $\omega$ irrespective of the noise content of the signals. If however, the averaged values of the power spectra as given by eqns (7.5.4) and (7.5.7) are used then the coherence function becomes

$$\Gamma^2(\omega) = |\bar{G}_{XF}(\omega)|^2 \;/\; (\bar{G}_{XX}(\omega) \cdot G_{FF}(\omega))$$

$$= \{|H(\omega)|^2 \cdot G_{FF}^2(\omega)\} \;/\; \{(|H(\omega)|^2 \cdot G_{FF}(\omega) + G_{NN}(\omega)) \cdot G_{FF}(\omega)\}$$

$$= \{|H(\omega)|^2 \cdot G_{FF}(\omega)\} \;/\; \{|H(\omega)|^2 \cdot G_{FF}(\omega) + G_{NN}(\omega)\}$$

$\leq 1$ since $G_{NN}(\omega)$ must be positive for all values of $\omega$.

Thus, as the number of averages increase the value of the coherence function $\Gamma^2(\omega)$ decreases from unity until a minimum value is reached. The smaller this minimum value, the greater the level of noise contaminating the system at that frequency.

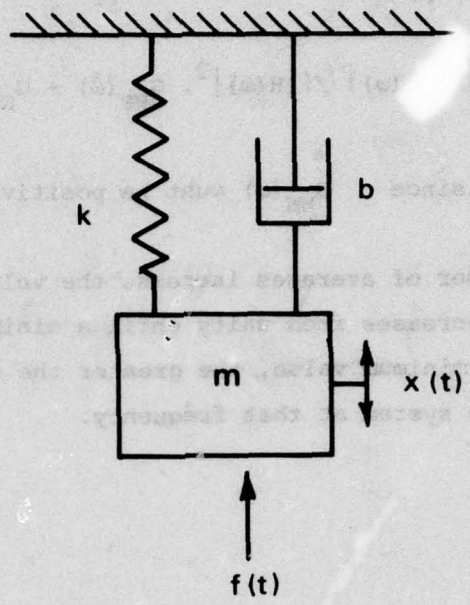


FIG. 7.1 SINGLE DEGREE-OF-FREEDOM SYSTEM

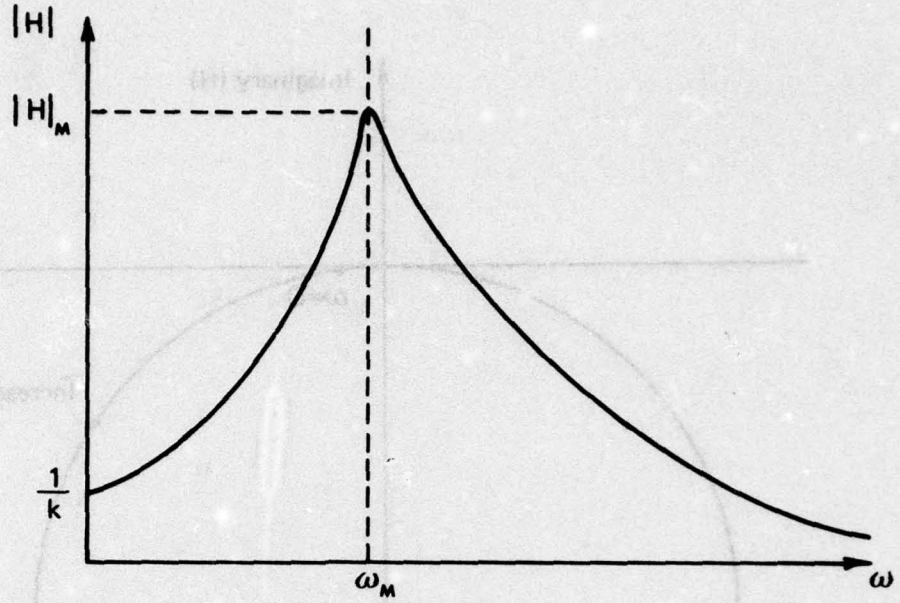


FIG. 7.2a MODULUS OF TRANSFER FUNCTION

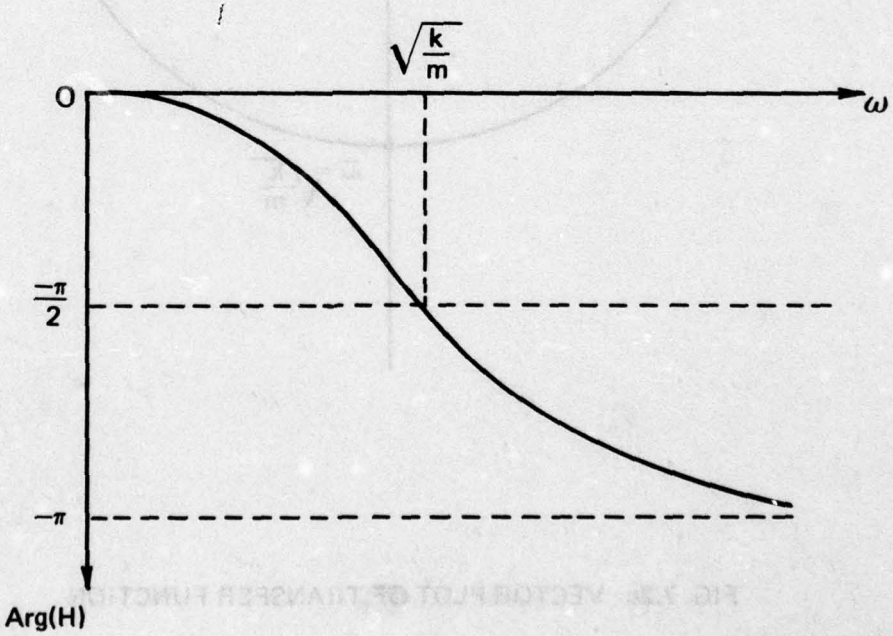


FIG. 7.2b ARGUMENT OF TRANSFER FUNCTION

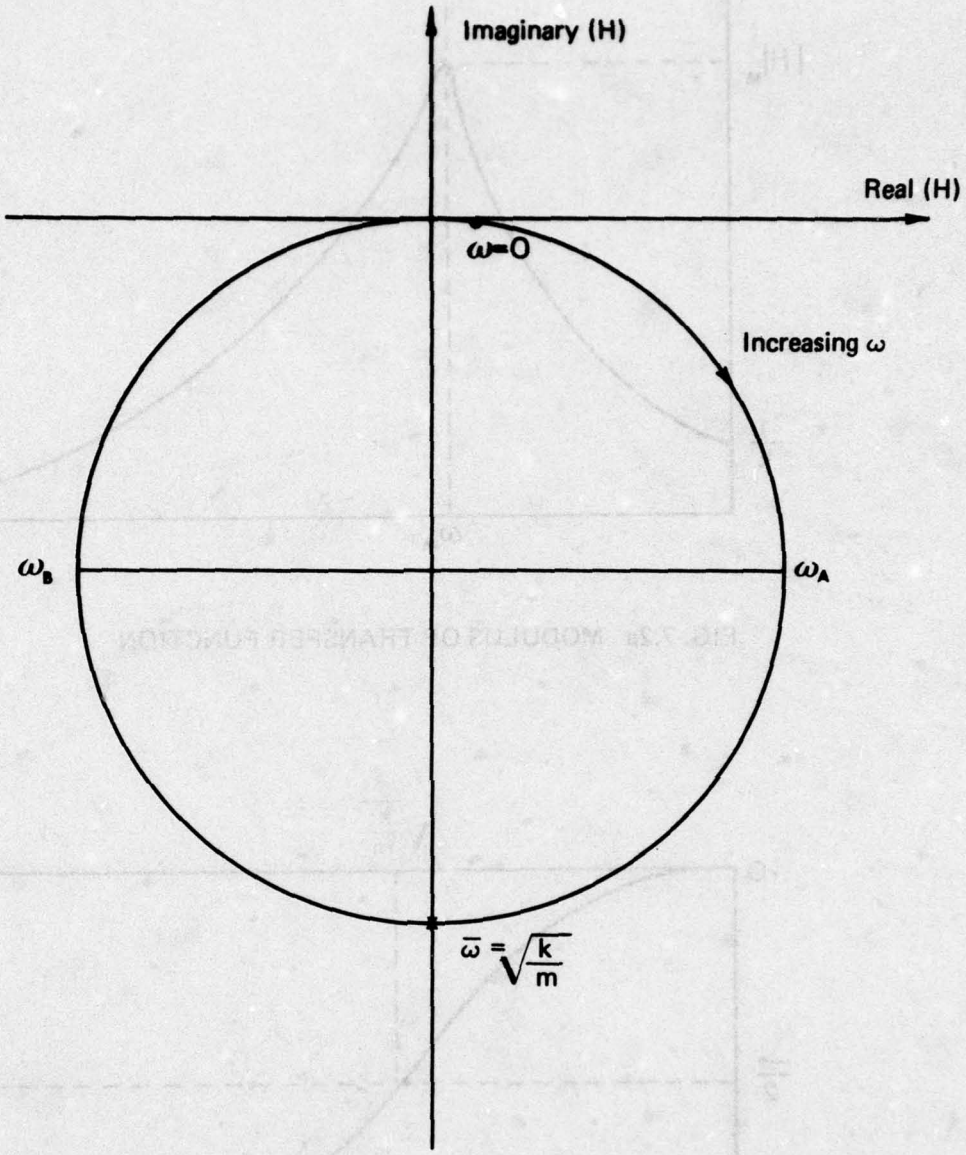


FIG. 7.2c VECTOR PLOT OF TRANSFER FUNCTION

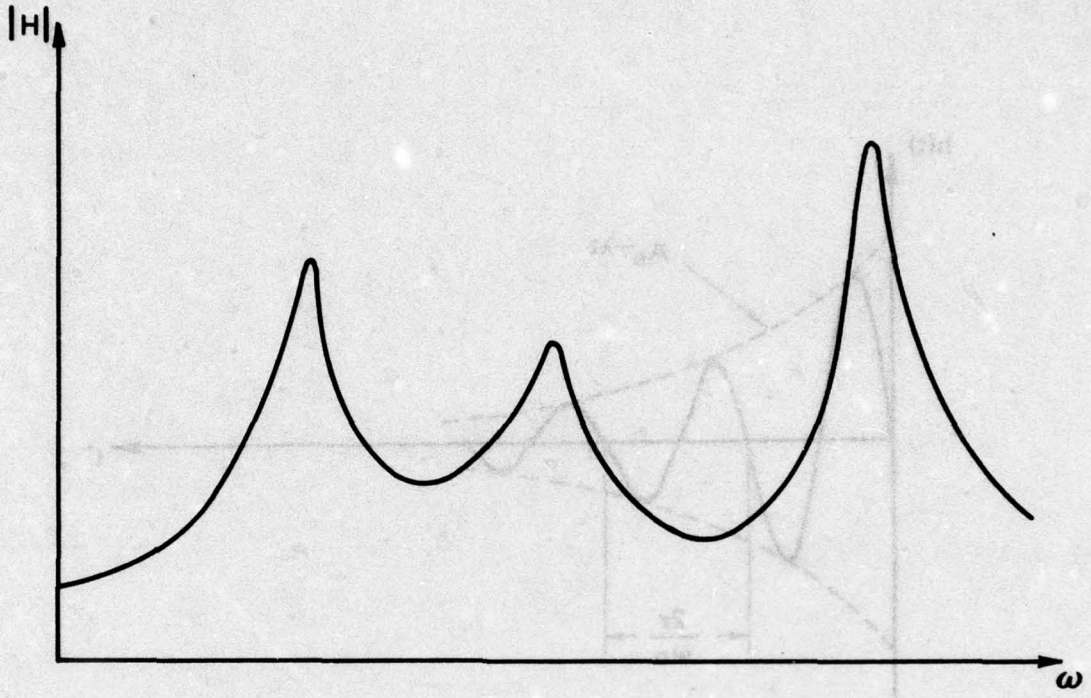


FIG. 7.3 MODULUS OF TRANSFER FUNCTION FOR MULTI-DEGREE-OF-FREEDOM SYSTEM

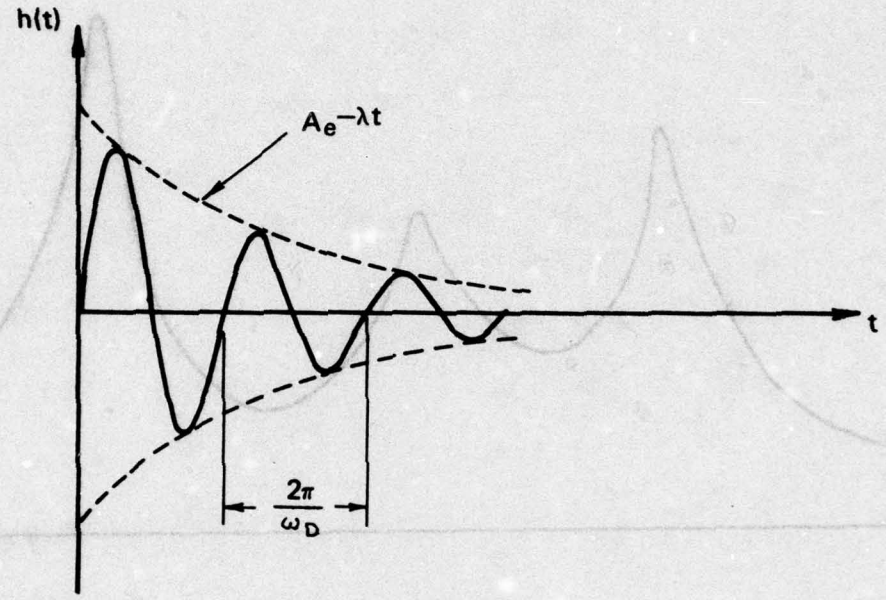


FIG. 7.4 IMPULSE RESPONSE OF A SINGLE D.O.F. SYSTEM

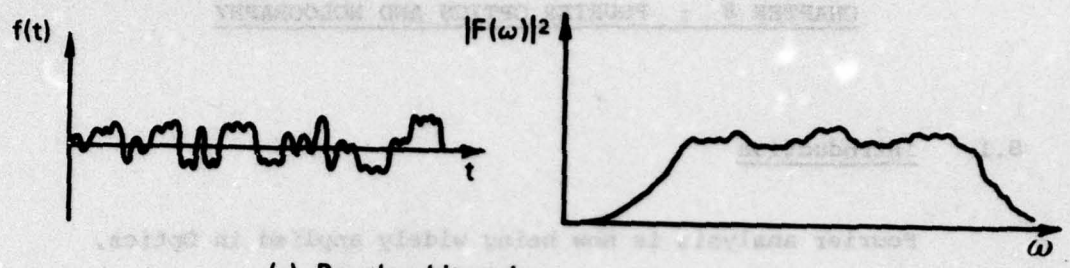


(a) Pseudo-white noise

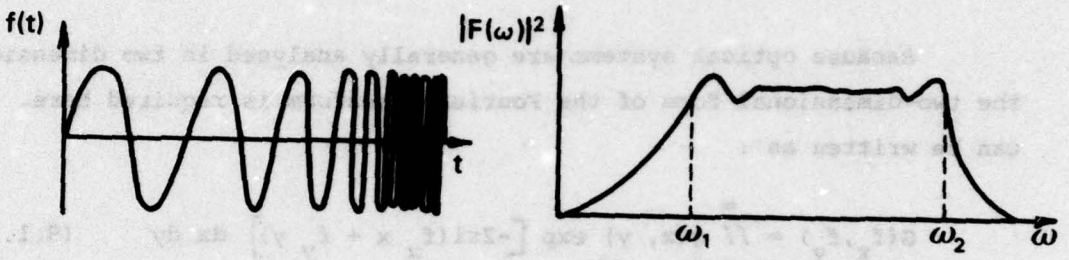


(b) Fast frequency sweep

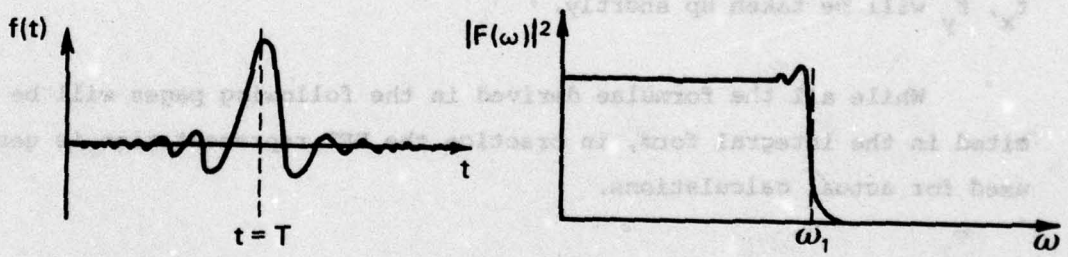


(c) Impulse sine

FIG. 7.5 FORCING FUNCTIONS AND POWER SPECTRA

# CHAPTER 8 : FOURIER OPTICS AND HOLOGRAPHY

## 8.1 Introduction

Fourier analysis is now being widely applied in Optics, especially in connection with the theory of image formation, optical data processing and holography. In the following pages, a necessarily rather brief account is given of some of these applications. The key idea throughout is the use of the Fourier transform in handling diffraction or wave-front interference effects.

Because optical systems are generally analysed in two dimensions, the two-dimensional form of the Fourier transform is required here. This can be written as :

$$G(f_x, f_y) = \int\int_{-\infty}^{\infty} g(x, y) \exp\left[-2\pi i(f_x x + f_y y)\right] dx\, dy \qquad (8.1.1)$$

with the inverse relation

$$g(x, y) = \int\int_{-\infty}^{\infty} G(f_x, f_y) \exp\left[2\pi i(f_x x + f_y y)\right] df_x\, df_y \qquad (8.1.2)$$

The physical significance of the transform (or frequency) parameters $f_x$, $f_y$ will be taken up shortly.

While all the formulae derived in the following pages will be cited in the integral form, in practice the DFT representation is generally used for actual calculations.

It will be necessary throughout to assume several results from Optics theory with relatively little discussion. Details of these may be found in standard texts e.g. those of Goodman (1), Shulman (2) and Fowles (3).

## 8.2 Frequency Analysis of Optical Systems

In this discussion only coherent optical systems will be considered i.e. those systems illuminated by light which has the property of being able to form interference fringes.

The term "frequency" used in the following sections does not refer to the phase variations with time of the light itself, but refers to the spatial or angular frequency at a particular plane. The various spatial frequency components in a light beam may be considered as plane waves propagating at different angles.

From the one-dimensional view in Fig. 8.1(a), a plane monochromatic wave strikes a flat surface at an angle $\theta$ to the perpendicular to the surface. The lines of zero phase are $\lambda$ apart along the direction of propagation, and $L$ apart along the plane. The spatial frequency along the plane is given by :

$$f_x = 1/L = \sin \theta/\lambda \tag{8.2.1}$$

Considering the two-dimensional case, (Fig. 8.1(b)), if the plane wave strikes the flat surface obliquely, such that the direction of wave propagation makes angles with the perpendicular to the surface of $\theta$ in the $x$ direction and $\alpha$ in the $y$ direction, then the spatial frequency components are given by

$$f_x = \sin \theta/\lambda = 1/L_x \tag{8.2.2}$$

and

$$f_y = \sin \alpha/\lambda = 1/L_y \tag{8.2.3}$$

## 8.3 Diffraction in Terms of the Spatial Frequency Spectrum

Consider a monochromatic, but otherwise unspecified complex light wave propagating in the positive $z$ direction, as defined in Fig. 8.2 At the x, y plane, the light field $g(x, y, o)$ has a spectrum

$$G(f_x, f_y) = \int_{-\infty}^{\infty} \int g(x, y, o) \exp \left[-2\pi i (f_x x + f_y y)\right] dxdy \tag{8.3.1}$$

A unit amplitude plane wave, propagating with direction cosines $(\alpha, \beta, \gamma)$ is described (1) by

$$B(x, y, z) = \exp\left[2\pi i(\alpha x + \beta y + \gamma z)/\lambda\right] \qquad (8.3.2)$$

where

$$\gamma = \sqrt{1 - \alpha^2 - \beta^2}$$

Comparing the exponential terms of (8.3.1) and (8.3.2) it might seem reasonable that the light field g(x, y, o) could be regarded as a plane wave with direction cosines

$$\alpha = \lambda f_x, \quad \beta = \lambda f_y$$

and

$$\gamma = \sqrt{\{1 - (\lambda f_x)^2 - (\lambda f y)^2\}}$$

This is indeed borne out by a more exact analysis which takes as its starting point the Kirchhoff diffraction formula (4).

Eqn (8.2.1) may then be re-written as

$$G(\alpha/\lambda, \beta/\lambda) = \int_{-\infty}^{\infty}\int g(x, y, o) \exp\left[-2\pi i(\alpha x/\lambda + \beta y/\lambda)\right]. \; dxdy \qquad (8.3.3)$$

This is known as the angular or spatial frequency spectrum of g(x, y, o).

Now assume an opaque screen in the x, y plane with an aperture $\Sigma$ (Fig. 8.2) which is large compared with $\lambda$. The transmittance of $\Sigma$ is defined as

$t(x, y) = 1$ within $\Sigma$

$t(x, y) = 0$ elsewhere.

Applying the classical Kirchhoff boundary conditions (4)

(i) Within $\Sigma$, the incident beam is the same as it would be without the screen being present.

(ii) In the geometric shadow of the screen, the incident beam is zero.

The beam immediately behind the screen is given by

$$g_t(x,y,o) = g_i(x,y,o)\ t(x,y) \tag{8.3.4}$$

where $g_t$ is the transmitted beam and $g_i$ is the incident beam.

Since a product in the space $(x,y)$ domain becomes a convolution in the spatial frequency domain, (8.3.4) may be written in terms of spatial frequency

$$G_t(\alpha/\lambda,\beta/\lambda) = G_i(\alpha/\lambda,\ \beta/\lambda) * T\ (\alpha/\lambda,\ \beta/\lambda) \tag{8.3.5}$$

where

$$T(\alpha/\lambda,\ \beta/\lambda) = \int\int_{-\infty}^{\infty} t(x,y)\exp\{-2\pi i(\alpha x/\lambda + \beta y/\lambda)\}\ dxdy \tag{8.3.6}$$

The diffracted spectrum is thus found by convolving the incident spectrum with the aperture "spectrum". The diffracted beam is found by transforming the result back into the space domain.

## 8.4 Image Formation

A thin bi-convex lens may be considered to perform a phase transformation on an input light wave. The form of this transformation may be readily calculated from the thickness variations of the lens. Using this phase function, it can be shown that a normally incident plane wave is mapped by a bi-convex lens into a converging spherical wave, provided the paraxial approximation is valid. Using this result, it can be further shown, e.g. ref.(1), that if an object of transmittance $t_o(x_o,y_o)$, placed at the front focal plane of a bi-convex lens, is illuminated by a normally incident monochromatic plane wave (Fig. 8.3), then the lens output converges to a distribution at the focal plane of the lens which is described by

$$G(x_i,y_i) = \int\int_{-\infty}^{\infty} t_o(x_o,y_o)\exp\left[-2\pi i(x_o x_i + y_o y_i)/\lambda f\right]dx_o dy_o \qquad (8.4.1)$$

where f is the focal length of the lens and the Fresnel (near-field) approximation is assumed. Note that the linear co-ordinates are used for the transform, as these are generally more meaningful to the user.

A generalized optical imaging system may be characterized by the relation (1)

$$G_i(x_i,y_i) = \int\int_{-\infty}^{\infty} h(x_i,y_i;\, x_o,y_o)\; g_o\,(x_o,y_o)\; dx_o\; dy_o \qquad (8.4.2)$$

where i and o are the image and object subscripts and h is the so-called "impulse response" (also known as the point response or imaging kernel), i.e. the response of the system at the image plane to a point source at the object plane.

A system may be completely characterized by knowledge of the function h. As an example, to determine the value of h for the simple imaging system illustrated in Fig. 8.3 let the object be a point source, i.e. a three dimensional $\delta$-function . The object produces a spherical wave, which, after passing through the lens, is described by

$$g_L(x,y) = g_o(x,y)\; P(x,y)\exp\left[-2\pi i(x^2 + y^2)/2\lambda f\right] \qquad (8.4.3)$$

where P(x,y) is the lens pupil function, defined as

$P(x,y) = 1$ within the lens aperture

$P(x,y) = 0$ outside " " "

and with the paraxial approximation for the spherical wave. The quantity $g_L(x,y)$ becomes the function h at the image plane.

The complete expression for h at the image plane is cumbersome, but with the assumption that the image is recorded on photographic film, which time averages amplitude to record light intensity and thus eliminates phase terms, and defining $M = d_i/d_o$, the expression

simplifies (1) to

$$h(x_i,y_i;x_o,y_o) \simeq (1/\lambda^2 d_o d_i) \iint_{-\infty}^{\infty} P(x,y) \cdot$$

$$\exp\{-2\pi i \left[(x_i + Mx_o)x + (y_i + My_o)y\right]/\lambda d_i\}\, dxdy \quad (8.4.4)$$

where $M$ is the system magnification.

This expression is the Fraunhofer diffraction of the lens aperture, centred on the image co-ordinates

$$x_i = -Mx_o;\ y_i = -My_o$$

To relate this result back to the effect on the image quality, it is convenient to make the following change of variables

$$\bar{x}_o = -Mx_o;\ \bar{y}_o = -My_o;\ \bar{x} = x/\lambda d_i;\ \bar{y} = y/\lambda d_i;\ \bar{h} = h/M$$

and define

$$g_g(x_i,y_i) = g_o(-x_i/M, -y_i/M)/M \quad (8.4.5)$$

as the geometric (no diffraction) image prediction. The imaging process is then described by the convolution

$$g_i(x_i,y_i) = \bar{h}(x_i,y_i) * g_g(x_i,y_i) \quad (8.4.6)$$

where

$$\bar{h}(x_i,y_i) = \iint_{-\infty}^{\infty} P(\lambda d_i\bar{x}, \lambda d_i\bar{y}) \exp\left[-2\pi i(x_i\bar{x} + y_i\bar{y})\right]\, d\bar{x}\, d\bar{y}$$

Because the function $\bar{h}(x_i,y_i)$ does not have zero width, as would be the case for a perfect impulse response, the image tends to be smoothed out, resulting in a loss of fine image detail.

## 8.5 Optical Filters

The general principles of optical filtering were independently demonstrated about the turn of the century by Abbé and Porter in the following manner (5) :

A mesh is Fourier transformed at the focal plane of a lens to give a pattern of dots (Fig. 8.4). With all the dots, the inverse Fourier transform yields an image of the complete mesh (Fig. 8.5(a) and (b)). If only one row of dots is passed through a slit, only one axis of the mesh is imaged (Fig. 8.5(c), (d), (e) and (f) ).

Little progress was then made until the 1950's when Marechal, in Paris, devised a technique for de-blurring photographs using special optical filters (6).

In the 1960's, when good quality coherent sources became readily available, real progress began to be made. From this work came the coherent processor (Fig. 8.6). The input to be filtered is placed at $P_1$ and illuminated by a plane wave. At $P_2$, the input, of transmittance $g(x,y)$, is Fourier transformed to give

$$k_1 G(x_2/\lambda f_1, y_2/\lambda f_1) \tag{8.5.1}$$

where $\lambda$ is the wavelength, $f_1$ is focal length of the lens and $k_1$ is a complex constant. At $P_2$ is placed a filter of transmittance

$$t(x_2,y_2) = k_2 H(x_2/\lambda f_1, y_2/\lambda f_1) \tag{8.5.2}$$

where $k_2$ is a complex constant. The output of the filter is proportional to $GH$, and after Fourier transformation by $L_2$, and photographic recording, the output at $P_3$ (with rotated $x,y$ axes to eliminate negative signs) is given by

$$I(x_3,y_3) = K\left|\int_{-\infty}^{\infty}\int g(\xi,\eta)\ h\ (x_3-\xi,\ y_3-\xi)\ d\xi\ \ d\eta\right|^2 \tag{8.5.3}$$

An example of a filter which could be placed at $P_2$ is the Vander Lugt" filter (6), dating from 1963. From Fig. 8.7, the response

to be filtered, h, is placed at the back focal plane of a lens and Fourier transformed in monochromatic light onto high resolution film (spectroscopic plate or similar). At the same time part of the illuminating beam is directed onto the film at an angle $\theta$. Interference fringes are produced, which, after film development, gives a transmittance

$$t(x_2,y_2) = A_o^2 + |H|^2/\lambda^2 f^2 + (A_o/\lambda f)\, H \exp(2\pi i \alpha y_2) + (A_o/\lambda f)\, H^* \exp(-2\pi i \alpha y_2) \qquad (8.5.4)$$

where $\alpha = \text{Sin}\ \theta/\lambda$, $A_o$ is the amplitude of the angled beam, and the asterisk denotes the conjugate.

If the filter is placed at $P_2$ in the coherent processor (Fig. 8.6), the output is of the form shown in Fig. 8.8.

The spatial separation of the convolution and cross-correlation terms is proportional to the angle $\theta$. The filter, sometimes referred to as a "mask" because it consists only of density variations, may be considered as the function H modulating in phase and amplitude the relatively high spatial frequency "carrier" provided by the angled beam.

## 8.6 Synthetic Aperture Radar and Sonar

An aircraft radar system has a range resolution as a function of time, and an azimuth or lateral resolution which is given by Cutrona et al. (8) to be of the order of $\lambda R/d$, where R is the distance to the target, $\lambda$ is the wavelength and D is the antenna diameter. For a 1000 metre range and a wavelength of 0.1 metre, the resolution is 100/D metres. Thus to give photographic resolution a very long antenna would be required. The solution is to use the movement of the aircraft to synthesize an apparent antenna of a length sufficient to realize the required resolution (8).

Consider an aircraft moving at a fixed velocity $v_a$ along a level path x, with a point scatterer on the ground at $x_1$ at right angles to the flight path a distance $d_1$ away (Fig. 8.9). Bursts of signal, approximately described by $A_o \exp(2\pi i f_R t)$, where $f_R$ is the radar

AD-A062 156 AERONAUTICAL RESEARCH LABS MELBOURNE (AUSTRALIA) F/G 12/1
LECTURES ON MODERN FOURIER TRANSFORM METHODS.(U)
FEB 78 B C HOSKIN

UNCLASSIFIED ARL/STRUC-TM-276 NL

3 OF 3
AD A062156

END
DATE FILMED
3-79
DDC

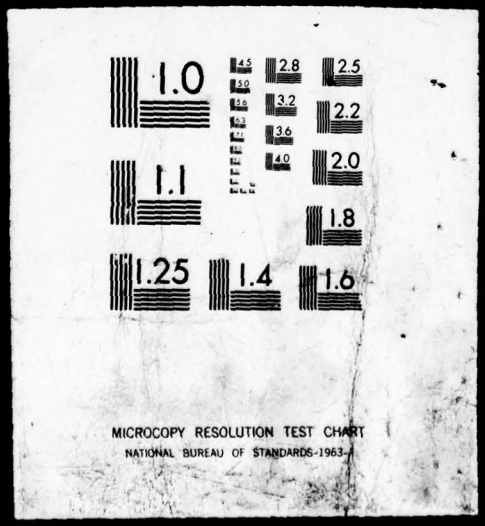

signal frequency, are being transmitted at a rapid rate. At $x_2$, the received signal reflected from the scatterer is

$$S_2(t) = B_1 \exp\{2\pi i f_R(t-2d/c)\} \qquad (8.6.1)$$

where $B_1$ is an amplitude factor for the scatterer at $x_1$,

$$d = \sqrt{\{d_1^2 + (x_2 - x_1)^2\}} \approx d_1 + (x_2 - x_1)^2/2d_1$$

and c is the velocity of light.

With $(x_2 - x_1) = v_a t$ and $c = f_R\lambda_R$, the return from N scatterers at position $x_1$ on the ground to the aircraft at $x_2$ is given by

$$S_2(t) = \sum_N B_N \exp\{2\pi i f_R(t-2d_1/\lambda_R f_R - v_a t/d_1\lambda_R f_R)\} \qquad (8.6.2)$$

This signal is synchronously demodulated and the result used to modulate a CRT trace to give the range record. The recording film is drawn past the CRT face to give the azimuth record (Fig. 8.10). The developed film is read out by being illuminated with a plane coherent wave with corrective optics to compensate for the slanted view of the antenna and the different foci in range and azimuth. The fact that the film record in the azimuth direction is a phase and amplitude record formed by comparing the reflected signal with a mutually coherent reference oscillator on the aircraft means that synthetic aperture radar is closely related to holography, to be discussed in the next section.

All of the principles discussed above apply equally well to the case of synthetic aperture sonar imaging.

## 8.7 Holography

### 8.7.1 Offset Reference Holography

Holography is a method of imaging in which the coherent light scattered by an object is recorded interferometrically on film. Illumination of the developed film by coherent light yields an image of the object.

The most common technique of formation is the offset reference method (9), in which a reference beam (Fig. 8.11) is directed onto a photographic plate at an angle, while the light scattered (by reflection from, or transmission through) the object also falls on the plate. A photographic record of the interference fringes formed by the two beams is the hologram.

Reconstruction is achieved by illuminating the developed hologram with the constructing beam. Two images, one real and one virtual, are obtained (Fig. 8.12).

The parallel between the offset reference hologram and Vander Lugt filter formation (Fig. 8.7) is evident. The two concepts originated from the same laboratory at about the same time.

In the spatial frequency domain, if the object spectrum (Fig.8.13(a)) is of width $w$, then the condition for separation of the images from the central order beam (Fig. 8.13(b)) is that

$$\alpha > 3w \tag{8.7.1}$$

where the spatial frequency of the reference, $\alpha = \sin\theta/\lambda$, where $\theta$ is the reference beam angle, and $\lambda$ is the wavelength.

The offset reference may be considered an analogue of the carrier in a radio transmitter, with the twin images being equivalent to the two side bands.

### 8.7.2 Fourier Transform Holography

In this method of formation, (10), an object, which may be considered as a collection of point scatterers, is illuminated by a coherent source (Fig. 8.14). A mutually coherent point source, R, is located a short distance, $\xi_o$, away from the centre of the object, and coplanar with it. The spherical wave at the recording film due to the reference source is approximated by

$$A_R(x) = A_1 \exp(2\pi i\, x^2/2\lambda f) \tag{8.7.2}$$

The wave at the film plane from an object point at $\xi_o$ is given by

$$A_o(x) = A(\xi_o) \exp\left[2\pi i (x - \xi_o)^2 / 2\lambda f\right] \qquad (8.7.3)$$

If $\xi_o$ is small so $\xi_o^2 << x$, then the whole object wave is described by

$$A_{obj}(x) = \int_{\xi_1}^{\xi_N} A(\xi) \exp\left[2\pi i\, x^2/2\lambda f\right] \exp\left[-2\pi i\, x\xi/f\lambda\right] d\xi \qquad (8.7.4)$$

The intensity recorded by the film is

$$\begin{aligned} I(x) &= (A_R + A_{obj})\,(A_R + A_{obj})^* \\ &= |A_1|^2 + |A_{obj}|^2 + A_1 \int_{\xi_1}^{\xi_N} A(\xi) \exp(-2\pi i\, x\xi/f\lambda) d\xi \\ &\quad + A_1 \int_{\xi_1}^{\xi_N} A(\xi)^* \exp(+2\pi i\, x\xi/\lambda f) d\xi \end{aligned} \qquad (8.7.5)$$

where the asterisk denotes the conjugate. The last two terms of (8.7.5) are the Fourier transform of the object and its conjugate; hence the name Fourier Transform holography.

Reconstruction is achieved by illuminating the hologram with the coherent source and converging the output with a lens (Fig. 8.15) to produce twin offset images.

The Fourier transform holography is restricted to two-dimensional objects, but has a relatively low spatial frequency content, especially if $\xi_o$ is small, enabling normal film to be used. The offset reference type of hologram, in contrast, can produce three-dimensional images but the high spatial frequency content requires spectroscopic plate for recording.

## References


1 GOODMAN, J.W. Introduction to Fourier Optics. McGraw-Hill, New York, 1968.

2 SHULMAN, A.R. Optical Data Processing. Wiley, New York, 1970.

3 FOWLES, G.R. Introduction to Modern Optics. Holt, Rinehart and Winston, New York, 1968.

4 KIRCHHOFF, G. Zur Theorie der Lichtstrahlen, Wiedemann Ann. (2) vol. 18, p. 663, 1883

5 PORTER, A.B. On the Diffraction Theory of Microscope Vision. Phil. Mag., (6) vol. 11, p. 154, 1906.

6 Referenced in (1) above, pp. 146-147.

7 VANDER LUGT, A.B. Signal Detection by Complex Spatial Filters. IEEE Trans. Inform. Theory, IT-10, No. 2, 1964.

8 CUTRONA, L.J. On the application of Coherent Optical Processing Techniques to Synthetic Aperture Radar. Proc. IEEE, vol. 54, p. 1026, 1966.

9 DE VELIS, J.B., and REYNOLDS, G.O. Theory and Applications of Holography. Addison-Wesley, Reading 1967.

10 STROKE, G.W. An Introduction to Coherent Optics and Holography. Academic Press, New York, 1969.

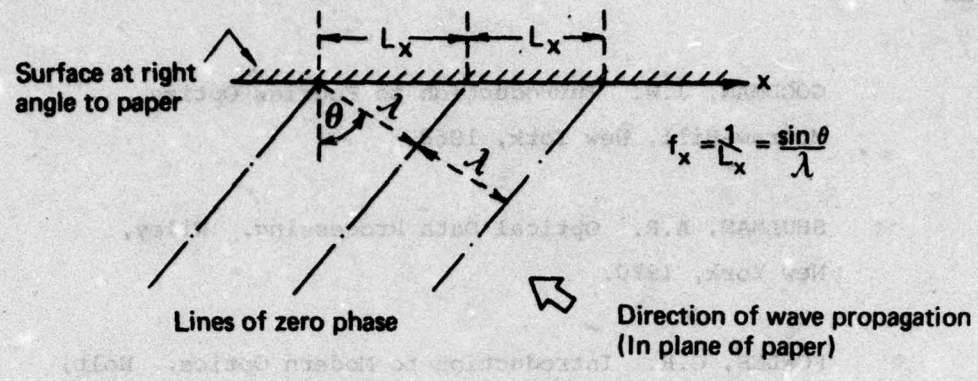


(a)

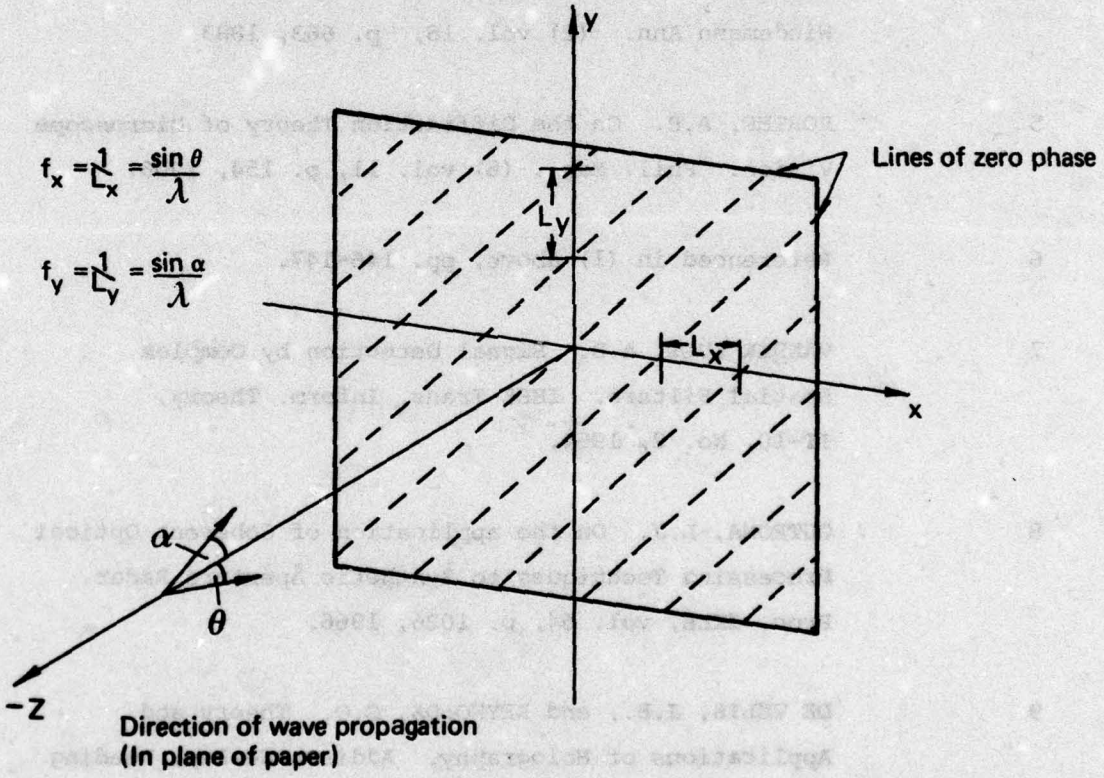


(b)

FIG. 8.1 THE CONCEPT OF SPATIAL FREQUENCY
(a) At right angles to the receiving plane
(b) In the receiving plane

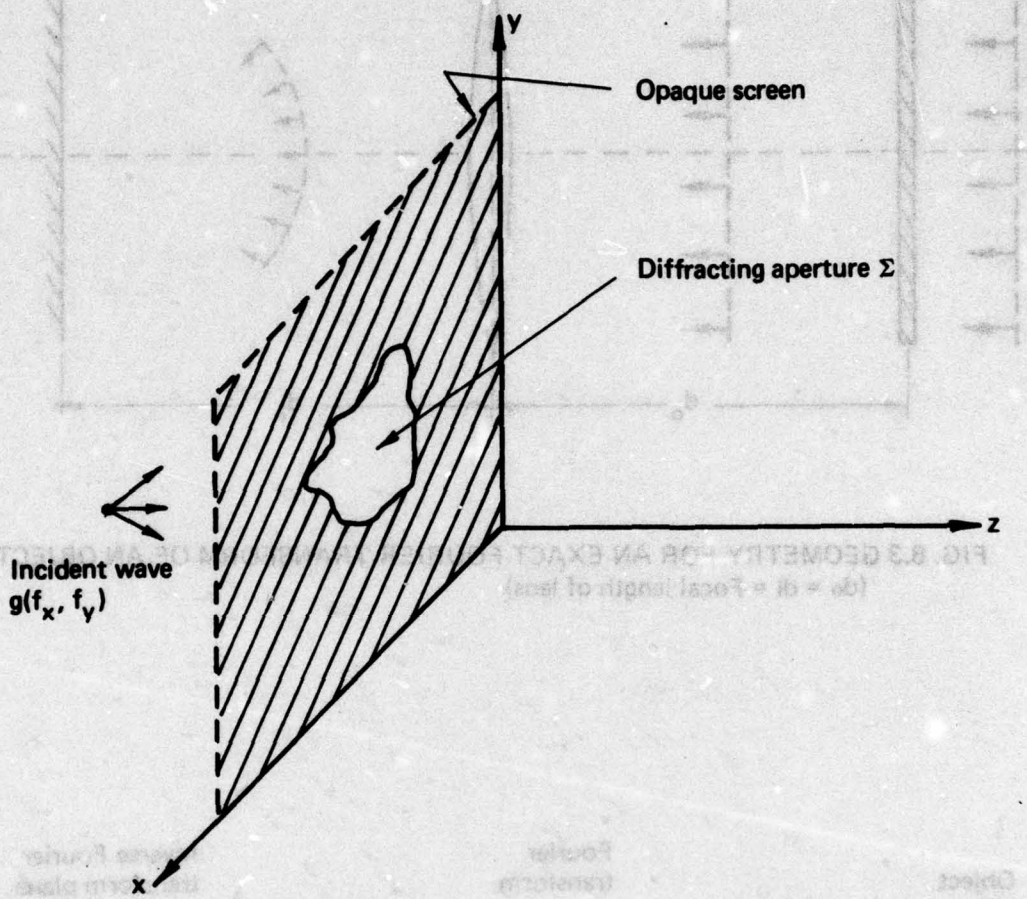


FIG. 8.2 DIFFRACTING APERTURE Σ IN AN OPAQUE SCREEN IN THE x, y PLANE

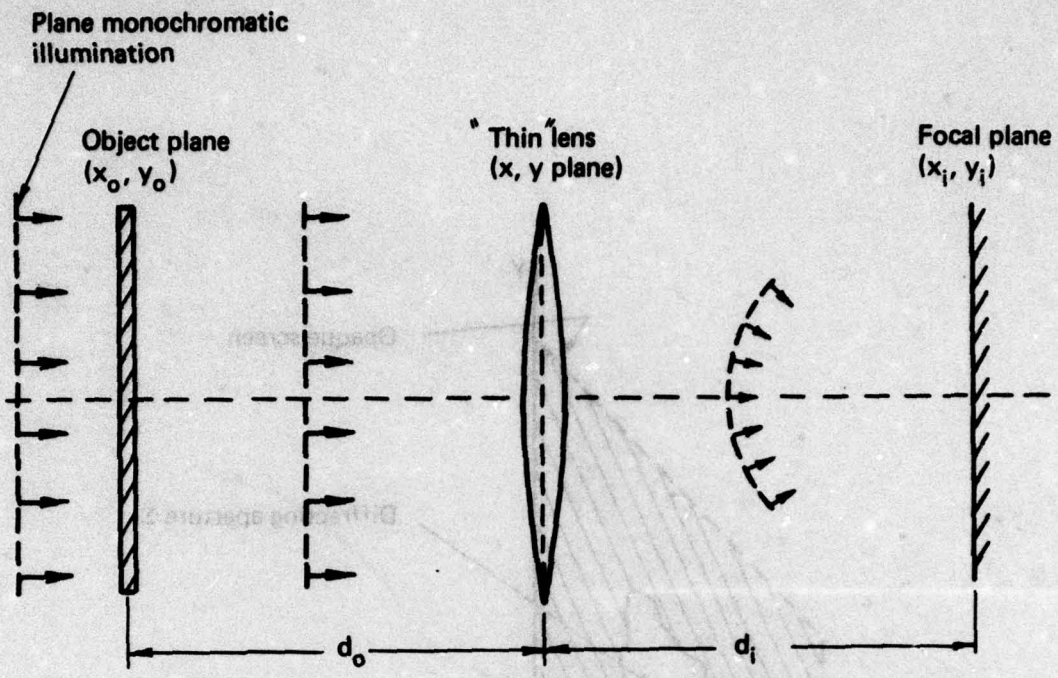


FIG. 8.3 GEOMETRY FOR AN EXACT FOURIER TRANSFORM OF AN OBJECT
($d_o = d_i$ = Focal length of lens)

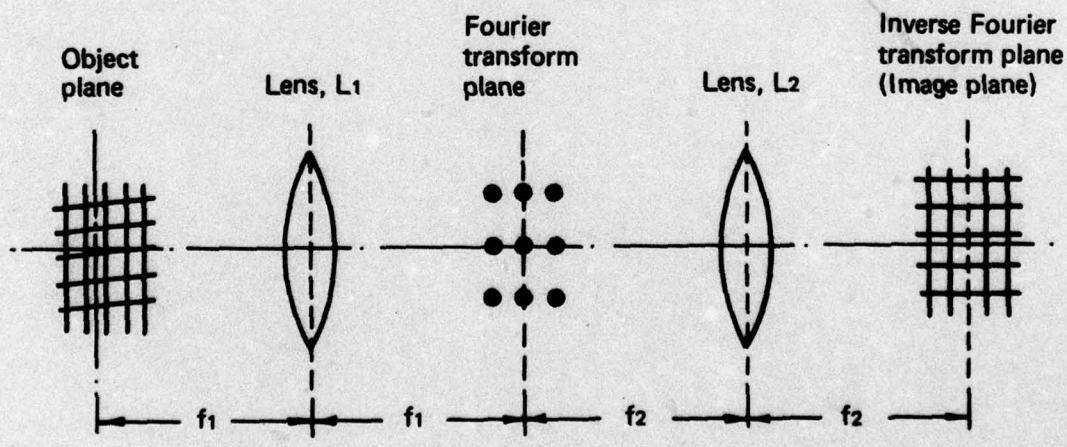


FIG. 8.4 GEOMETRY TO FOURIER TRANSFORM MESH AND INVERSE FOURIER TRANSFORM ITS SPECTRUM

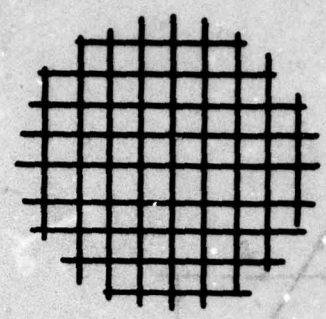

(a) Object mesh

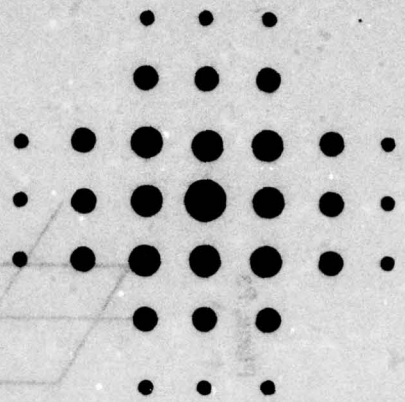

(b) Spectrum of (a)

(c) Vertical component only of (a)

(d) Image due to (c)

(e) Horizontal component only of (a)

(f) Image due to (e)

FIG. 8.5 FOURIER TRANSFORM OF MESH

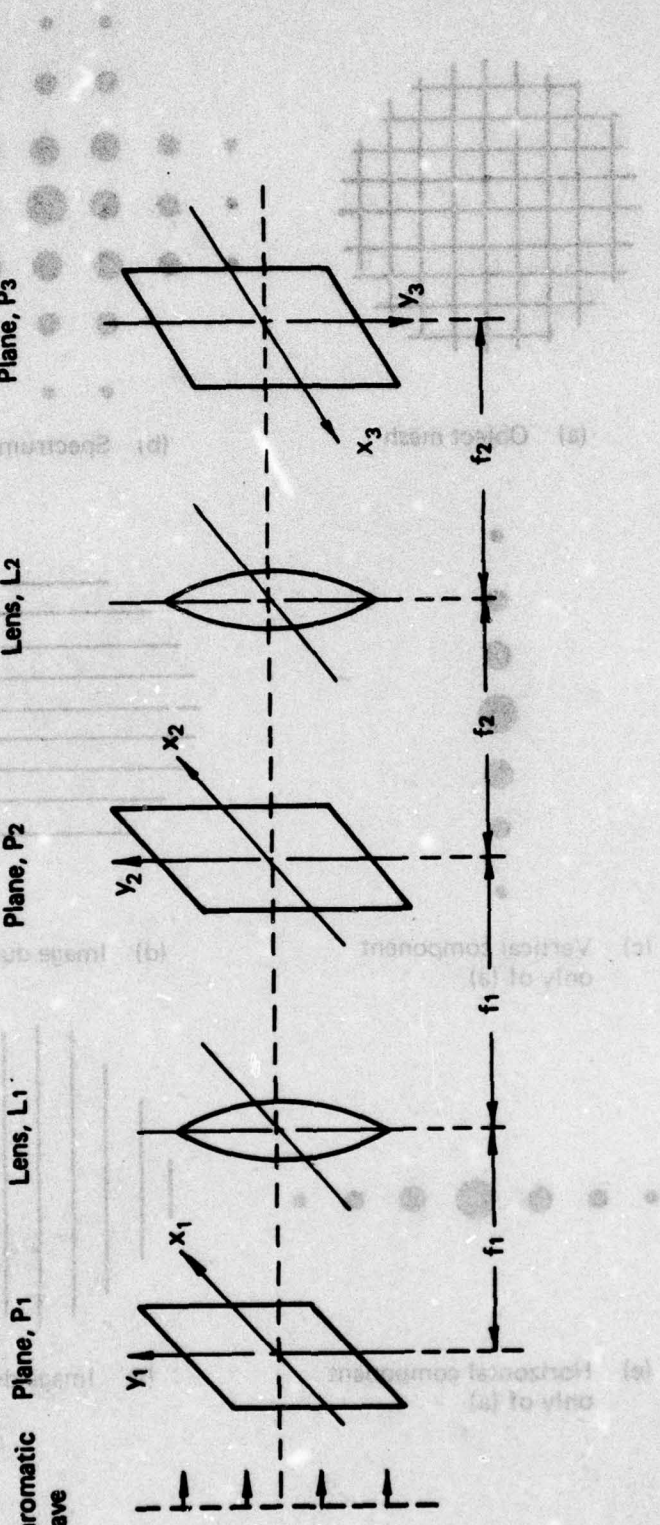


FIG. 8.6 COHERENT PROCESSOR GEOMETRY

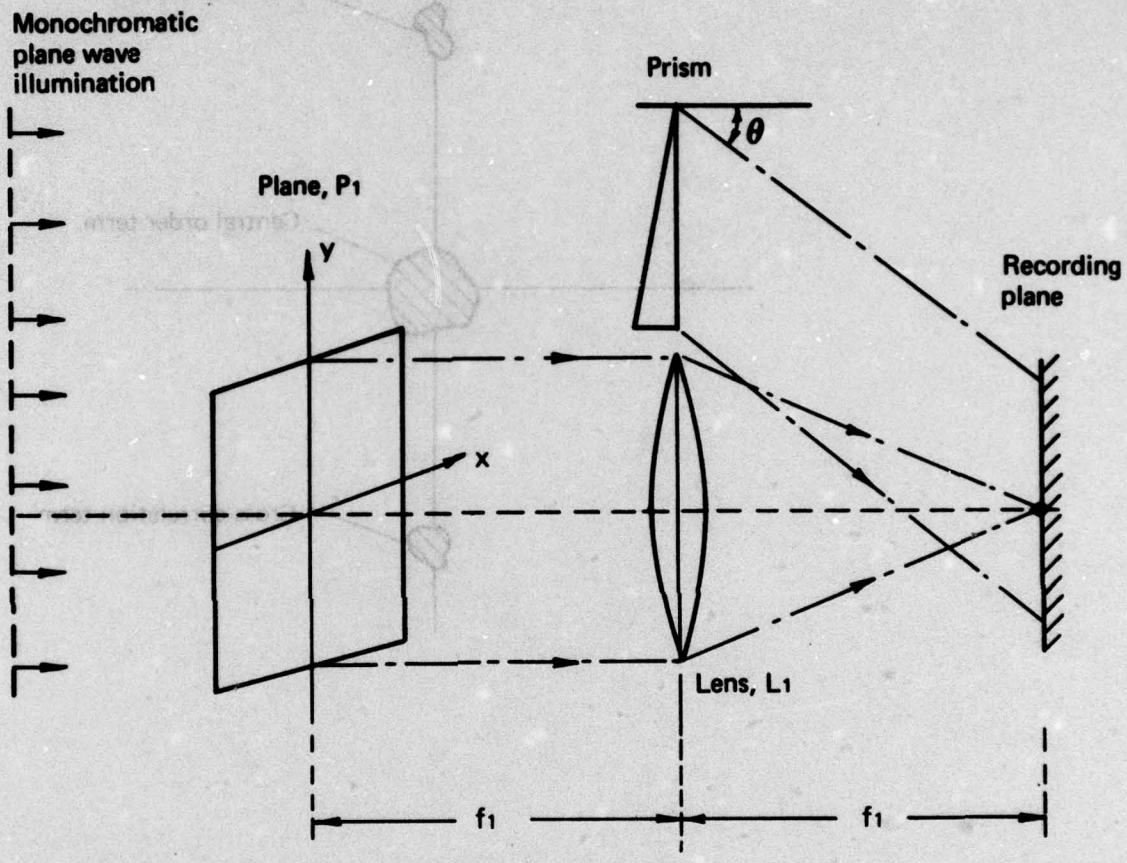


FIG. 8.7 VANDER LUGT FILTER FORMATION GEOMETRY

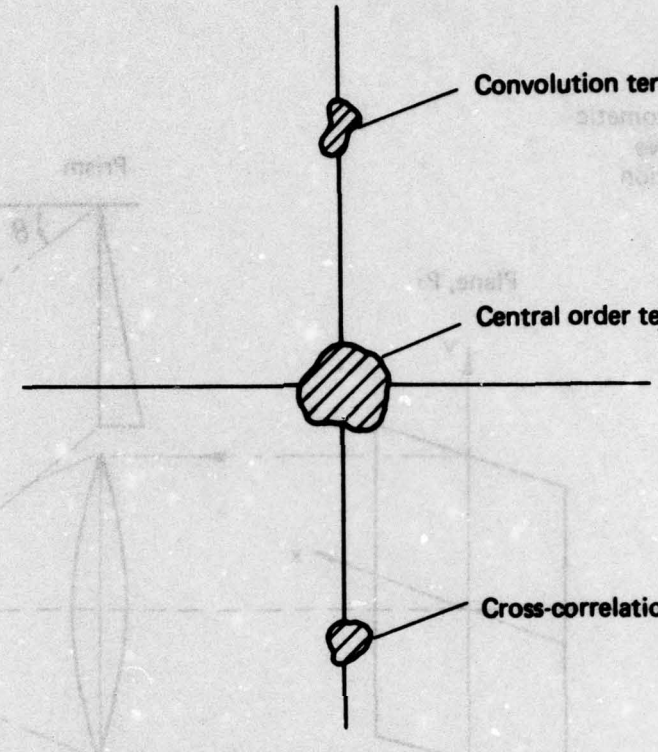


FIG. 8.8 OUTPUT PLANE INTENSITY OF THE COHERENT PROCESSOR WITH VANDER LUGT FILTER

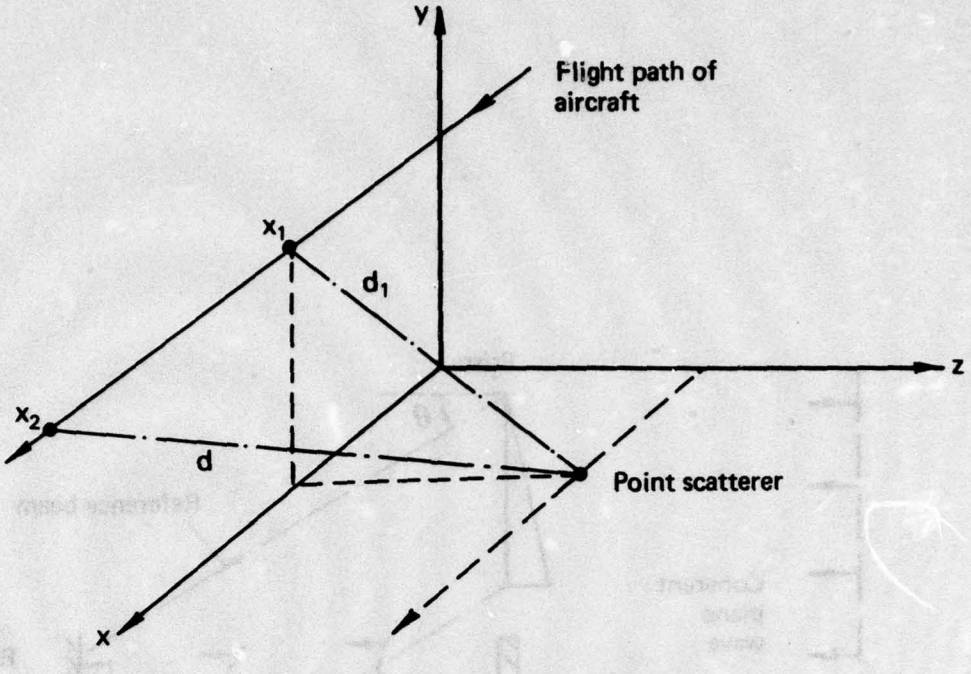


FIG. 8.9 SYNTHETIC APERTURE RADAR GEOMETRY

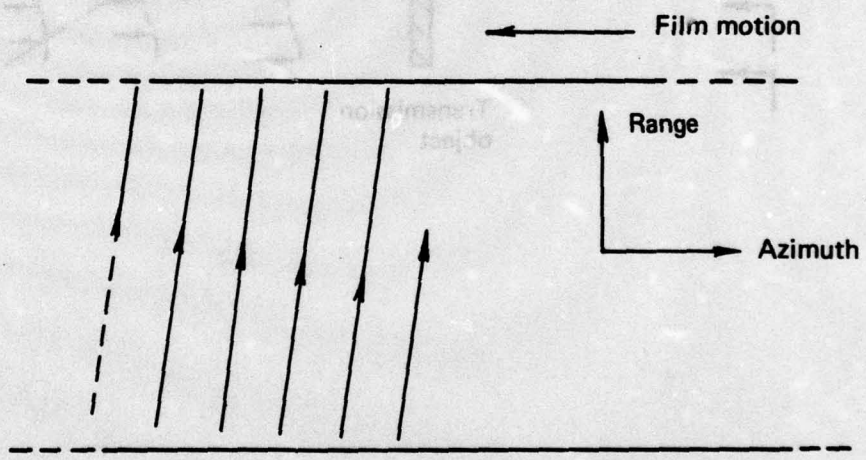


FIG. 8.10 SYNETHETIC APERTURE RADAR RECORDING

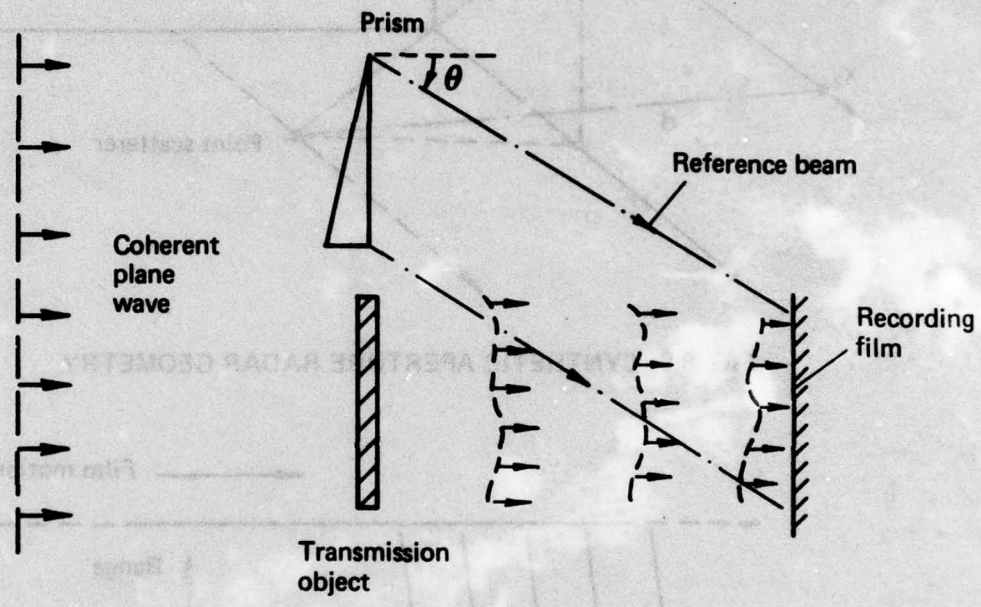


FIG. 8.11 OFFSET REFERENCE HOLOGRAPHY RECORDING GEOMETRY

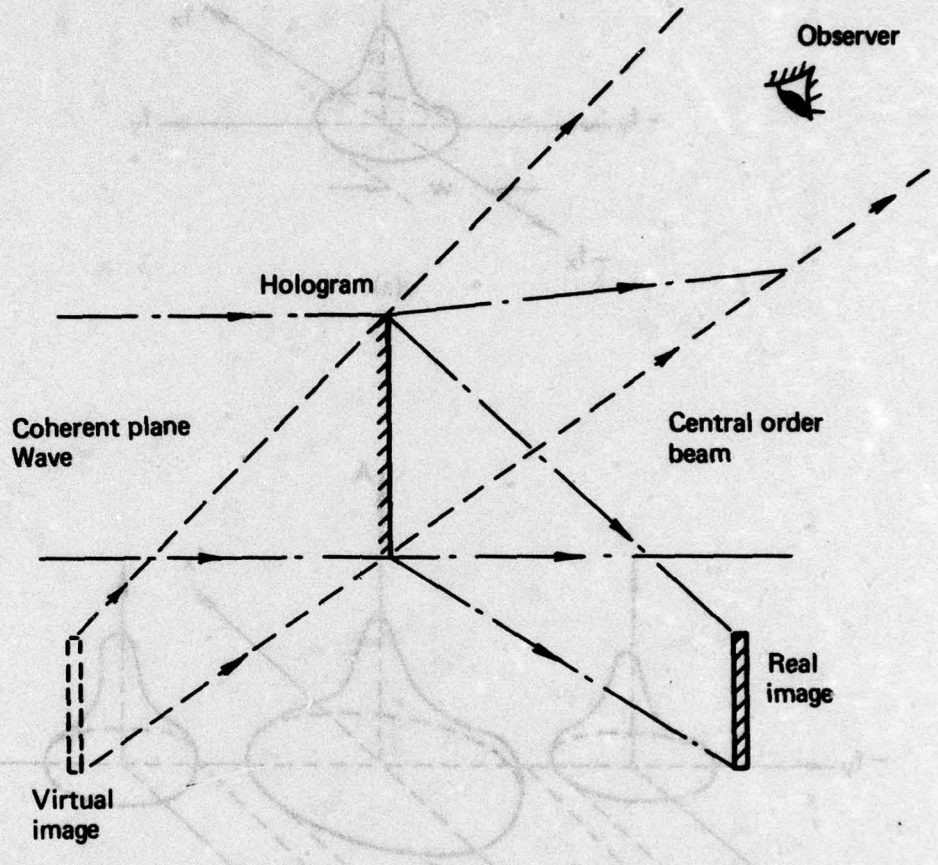


**FIG. 8.12 OFFSET REFERENCE HOLOGRAM RECONSTRUCTION**

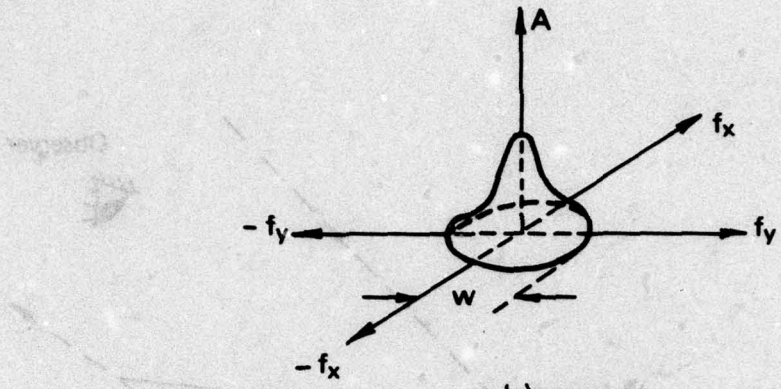


(a)

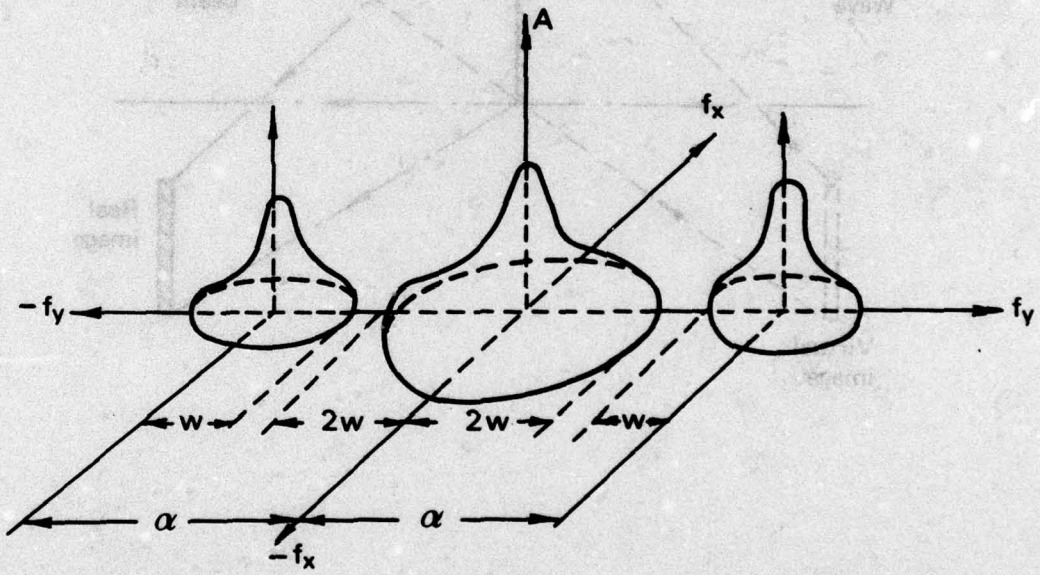


(b)

**FIG. 8.13 CONDITION FOR IMAGE SEPARATION IN OFFSET REFERENCE HOLOGRAMS**

**(a) Spectrum of object, 2w wide**

**(b) Spectrum of hologram output, with separation if $\alpha > 3w$**

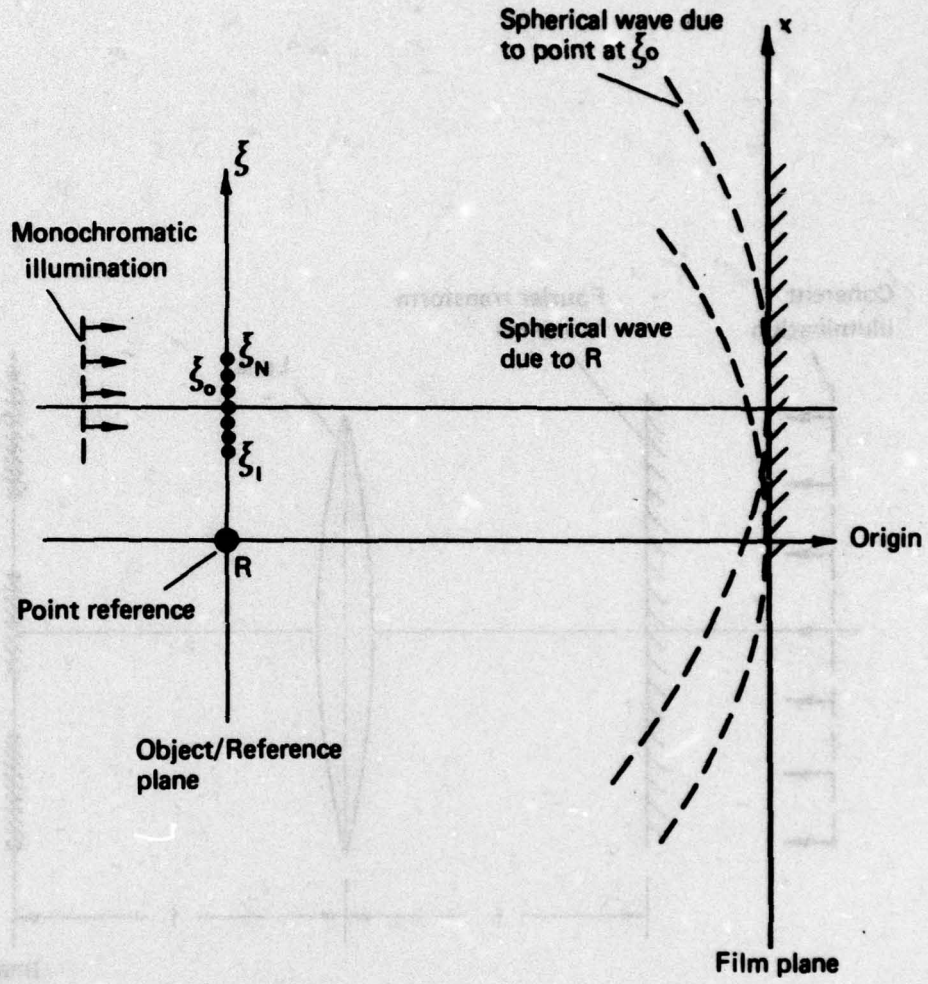


FIG. 8.14 FOURIER TRANSFORM HOLOGRAM FORMATION GEOMETRY

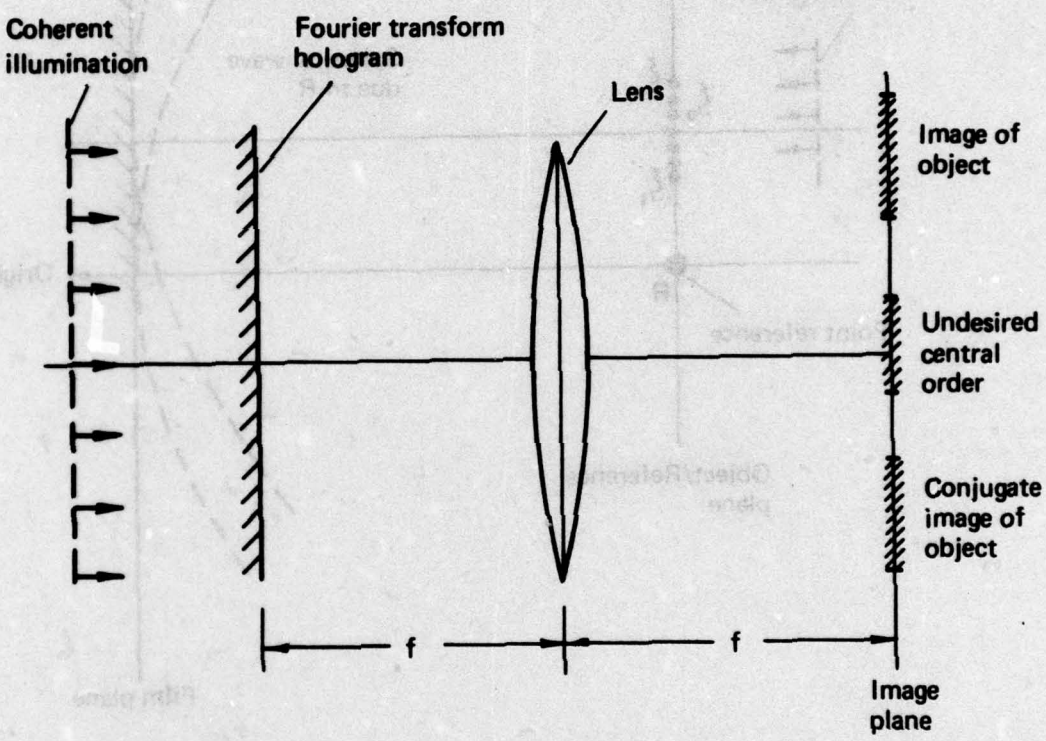


**FIG. 8.15 RECONSTRUCTION OF FOURIER TRANSFORM HOLOGRAM**

DOCUMENT CONTROL DATA SHEET

Security classification of this page UNCLASSIFIED

| | |
|---|---|
| 1. DOCUMENT NUMBERS | 2. SECURITY CLASSIFICATION |
| a. AR Number: AR-001-271 | a. Complete document: UNCLASSIFIED |
| b. Document Series and Number: Structures Technical Memorandum 276 | b. Title in isolation: UNCLASSIFIED |
| c. Report Number: ARL-STRUC-TECH-MEMO-276 | c. Summary in isolation: UNCLASSIFIED |

3. TITLE:

LECTURES ON MODERN FOURIER TRANSFORM METHODS.

| | |
|---|---|
| 4. PERSONAL AUTHOR(S): Edited by HOSKIN, Brian C. | 5. DOCUMENT DATE: February, 1978 |
| | 6. TYPE OF REPORT AND PERIOD COVERED: |
| 7. CORPORATE AUTHOR(S): Aeronautical Research Laboratories | 8. REFERENCE NUMBERS |
| | a. Task: DST 76/152 |
| 9. COST CODE: 21 6901 | b. Sponsoring Agency: Dept. of Defence (DST) |
| 10. IMPRINT: Aeronautical Research Laboratories, Melbourne | 11. COMPUTER PROGRAM(S) (Title(s) and Language(s)): |

12. RELEASE LIMITATIONS (of the document)

Approved for Public Release.

| 12-0 OVERSEAS: | NO | P.R. | A | B | C | D | E |
|---|---|---|---|---|---|---|---|

13. ANNOUNCEMENT LIMITATIONS (of the information on this page):

No limitations.

| 14. DESCRIPTORS: | | 15. COSATI CODES: |
|---|---|---|
| Fourier Transformation. | Fourier Analysis. | 1201 |
| Fourier Series. | Time Series Analysis. | |
| Fourier Integrals. | Computation. | |

16. ABSTRACT:

This memorandum is a compilation of notes prepared in connection with a series of lectures on Modern Fourier Transform Methods given at the Aeronautical Research Laboratories. The topics covered include Classical Fourier Methods, the Discrete Fourier Transform, the Fast Fourier Transform Algorithm, Time Series Analysis, Practical Computational Questions, The Retrieval of Signals from Noise, Application of Fourier Transforms to Vibration Problems, and Fourier Optics and Holography.

## DISTRIBUTION

| | Copy No. |
|---|---|
| **AUSTRALIA** | |
| **DEPARTMENT OF DEFENCE** | |
| **Central Office** | |
| Chief Defence Scientist | 1 |
| Executive Controller, ADSS | 2 |
| Superintendent, Defence Science Administration | 3 |
| Defence Library | 4 |
| JIO | 5 |
| Assistant Secretary, DISB | 6-21 |
| **Aeronautical Research Laboratories** | |
| Chief Superintendent | 22 |
| Superintendent, Structures Division | 23 |
| Divisional file, Structures Division | 24 |
| Author(s): B.C. Hoskin | 25 |
| P. Gottlieb | 26 |
| D.J. Sherman | 27 |
| M. Thomson | 28 |
| P.A. Farrell | 29 |
| A.J. Farrell | 30 |
| R. Kirsner - St. Vincent's Hospital, Melbourne | 31 |
| Library | 32 |
| R. Callinan | 33 |
| R. Jones | 34 |
| B. Emslie | 35 |
| B. Green | 36 |
| T. Ryall | 37 |
| **Materials Research Laboratories** | |
| Library | 38 |
| **Defence Research Centre** | |
| Library | 39 |
| **Central Studies Establishment** | |
| Library | 40 |
| **Engineering Development Establishment** | |
| Library | 41 |
| **RAN Research Laboratory** | |
| Library | 42 |

| | Copy No. |
|---|---|
| **Air Office** | |
| Aircraft Research & Development Unit | 43 |
| Air Force Scientific Adviser | 44 |
| **Army Office** | |
| Army Scientific Adviser | 45 |
| **Royal Military College** | |
| Library | 46 |
| **Navy Office** | |
| Naval Scientific Adviser | 47 |
| **DEPARTMENT OF PRODUCTIVITY** | |
| **Government Aircraft Factories** | |
| Library | 48 |
| **DEPARTMENT OF TRANSPORT** | |
| Director-General/Library | 49 |
| **STATUTORY, STATE AUTHORITIES AND INDUSTRY** | |
| Qantas, Library | 50 |
| Trans Australia Airlines, Library | 51 |
| Ansett Airlines of Australia, Library | 52 |
| Commonwealth Aircraft Corporation (Manager) | 53 |
| Hawker de Havilland Pty. Ltd. (Librarian) Bankstown | 54 |
| **SPARES** | 55-74 |